

UNIVERSITY OF SOUTHAMPTON

VARIATION OF PFK ACTIVITY IN MODEL MEMBRANE SYSTEMS

CHENG JI

THESIS SUBMITTED FOR THE DEGREE OF MASTER OF PHILOSOPHY

DEPARTMENT OF CHEMISTRY

DECEMBER 2004

UNIVERSITY OF SOUTHAMPTON

ABSTRACT

FACULTY OF SCIENCE

CHEMISTRY

Master of Philosophy

VARIATION OF PFK ACTIVITY IN MODEL MEMBRANE SYSTEMS

by Cheng Ji

PFK (phosphofructokinase or fructose-6-phosphate-1 kinase) is a key enzyme in the glycolysis pathway. It catalyses the transfer of the terminal phosphate from adenosine triphosphate to fructose 6-phosphate and sets the overall rate of glycolysis.

Cellular membrane is one of the most complex yet important structures in cells. Many essential cell events have been found relative to membrane conformations and other properties such as membrane surface charge and stored curvature energy. Several glycolytic enzymes including PFK have been reported to interact with cell membrane components and their functions are thus regulated by a complicated mechanism. It has been proposed that the membrane—enzyme interaction is essential for cell's biological functions.

The aim of the research described in this thesis was to investigate whether PFK activity could be regulated by membrane lipid composition in a way that is consistent with stored elastic energy playing a dominant role in the regulation. Using large unilamellar vesicles as model system of biological membranes, activities of PFK from *Bacillus stearothermophilus* were tested in five vesicles systems, which were chosen so as to give particular changes in membrane stored elastic energy. The experimental methodology for the enzyme assays were studied and optimized first before the final PFK assays were tested. The experimental results showed a slight enhancement of enzyme activity.

Contents

Abstract	II	
Contents	III	
List of Figures	IV	
List of Tables	V	
Acknowledgements	VI	
Chapter 1	Introduction to Cellular Membrane & Membrane-enzyme Interaction	1
Chapter 2	Introduction of Phosphofructokinase	20
Chapter 3	PFK from <i>Bacillus stearothermophilus</i>	39
Chapter 4	Experimental Methods	51
Chapter 5	Optimization of TLC Separation and Assay Conditions	67
Chapter 6	BsPFK Activity in Five Vesicle Systems	83
References		94
Appendix 1	Glossary and Abbreviation	102
Appendix 2	Lipid vesicles composition and preparation	103
Appendix 3	Specific activity in vesicle systems	104
Appendix 4	Amino acid sequence of EcPFK and RM-PFK	109
Appendix 5	Scintillation counting results and data processing	111

List of Figures

Figure 1.1	A schematic diagram of a membrane bilayer	3
Figure 1.2	Schematic diagram of the erythrocyte membrane structure	4
Figure 1.3	An example of phosphoglyceride structure	8
Figure 1.4	Schematic diagrams of lateral stress distribution within a bilayer	12
Figure 1.5	Main properties of primary and secondary protein structures	15
Figure 1.6	Protein-membrane association patterns	16
Figure 1.7	Functional domain of CCT & amino acids sequence of domain C	17
Figure 2.1	A schematic drawing of PFK tetrameric structure	23
Figure 2.2	The flow of glycolytic pathway	24
Figure 2.3	A schematic plot of PFK allosteric inhibition by ATP	27
Figure 2.4	A schematic drawing of PFK regulation mechanisms	31
Figure 2.5	A&B A schematic drawing of concerted model of PFK tetramer	32
Figure 3.1	Schematic diagram of reaction flux and ATP-inhibition	41
Figure 3.2	A schematic representation of BsPFK three dimensional structure	48
Figure 3.3	Helix wheel plots of exposed helices from BsPFK	49
Figure 4.1	Coupled assays of PFK by linking FBP or ADP to the oxidation of NADH	52
Figure 5.1	Termination of PFK assay by EDTA solution	69
Figure 5.2	Termination of PFK assay by CuCl ₂ or HCl solution	70
Figure 5.3	Autoradiography of separation result using charcoal-TLC method	72
Figure 5.4	Autoradiography to check the TLC separation on cellulose plates	74
Figure 5.5	Autoradiography to check the TLC separation on silica gel plates	75
Figure 5.6	Autoradiography of TLC separation using a number of EDTA solvents	76
Figure 5.7	Optimization of PFK assay conditions	78
Figure 5.8	PFK activity tested for different assay incubation time	79
Figure 5.9	A&B PFK assay error range study	80
Figure 6.1—Figure 6.10	PFK activity in five vesicles systems	85

List of Tables

Table 1.1	Formulas of lipid structure units and some common lipid species	6
Table 1.2	Common fatty acids in membrane lipid tail domain	7
Table 1.3	Factors affecting membrane phase behaviour and their function tendency	10
Table 1.4	Lipid molecule shape model & curvature in a frustrated bilayer	11
Table 2.1	Glycolytic enzymes and free energy of each enzymic reaction	25
Table 3.1	Hydrophobicity analyses of BsPFK amino acids	44
Table 3.2	Amino acids of BsPFK	45
Table 4.1	Buffer pH at different temperature	54
Table 4.2	Lipid composition of DOPC/DOPE vesicles	55
Table 4.3	Tested spray reagents to visualize spots on TLC plates	61
Table 4.4	Solvent systems used in TLC on DEAE cellulose plates	62
Table 4.5	Solvent systems used in TLC on normal cellulose plates	63
Table 4.6	Solvent systems used in TLC on silica gel plates	64

Acknowledgements

The author of this thesis wishes to thank the following:

Professor George Attard for his great support and dedicated supervising of my study. His deep knowledge and prudent learning attitude and timely encouragement have exerted a great influence on me. I also would like to thank him for his help during my writing of this paper.

Doctor Marcus Dymond for his advice and many useful discussions about the experiments which were very helpful for my early stage study.

Steve Hant, Mathew Cheetram, Maria-Nefeli Tsaloglou, and others for sharing the lab and computers.

My parents for spiritual support and encouragement.

My laptop that has to face an ugly face and a pair of deep and perplexed eyes day and night.

Chapter 1 Introduction to cell membranes &

membrane-enzyme interactions

1.1	General functions and properties of membranes	2
1.1.1	Composition and structure	2
1.1.2	Membrane proteins and functions	3
1.1.3	Organelle membranes and special local membrane structures	5
1.2	Membrane chemical composition and geometry	5
1.2.1	Molecular structure and common lipid families	5
1.2.2	Lipid solutions, polymorphism and phase preferences	8
1.2.3	Lipid molecular shape model and membrane curvature stress	10
1.2.4	Membrane curvature stress profile	11
1.3	Membrane-enzyme interactions	13
1.3.1	Functional classification of membrane associated enzymes	13
1.3.2	Protein construction	14
1.3.3	Membrane-protein association patterns	16
1.3.4	Examples of membrane protein interactions	17

The cell membrane, which forms the boundary of a cell or respective organelle, is one of the most important components of cells. Its composition and structural diversity and the many complex but fundamental functions it carries out, are all represent fruitful areas for research. It is generally accepted that most membrane functions are mediated by distinctive proteins which associate with membranes through different and specific mechanisms. Moreover, there is increasing evidence which suggests that organisms homeostatically regulate their lipid metabolism and the membrane compositions so as to maintain a series of properties constant or within an appropriate range [1,2]. Properties such as the spontaneous curvature stress, membrane hydrocarbon thickness, surface charge density and head group hydration are essential factors that modulate membrane—protein interactions, and which are involved in many cellular events. As a consequence, lipid membranes can no longer be regarded only as inert walls for functional proteins to embed in or lay on.

1.1 General functions and properties of membranes

1.1.1 Composition and structure

The most well known membrane is the outer cell membrane, also termed as plasma membrane or cytoplasmic membrane. It has a sheet structure formed by two monolayers consisting of a broad spectrum of lipids. A wide range of proteins associate with this bilayer complex. Figure 1.1 is a schematic diagram of the fluid mosaic model of a cellular membrane [3]. It shows that two layers of lipid molecules pack tightly with one layer's head groups facing the extracellular matrix and the other one's facing the cytosol. The hydrocarbon tails of lipids form the hydrophobic core, which is about 5 nm thick. Proteins are known to insert in the membrane to different extents or only interact with the polar head group region of a lipid cluster. Typically, the mass ratio of protein to lipids ranges from 1/4 to 4/1, and thus proteins may take up more than 50% of total membrane surface area [4]. Membranes are held together mainly by hydrophobic interactions among the long fatty acyl chains, while van de Waals force, hydrogen bonds and electrostatic interactions also exist in the hydrophobic core or head group area and effect the packing and dynamics of

membranes. Membranes are fluid structures in which lateral motion is observed for both lipid molecules and membrane proteins. The average diffusion rate for a lipid is about 1-2 μm per second [5,6]. The transverse diffusion of lipid across the membrane (flip-flop) is rare, which partially accounts for the asymmetry between the distinct layers of membrane in term of its lipid composition.

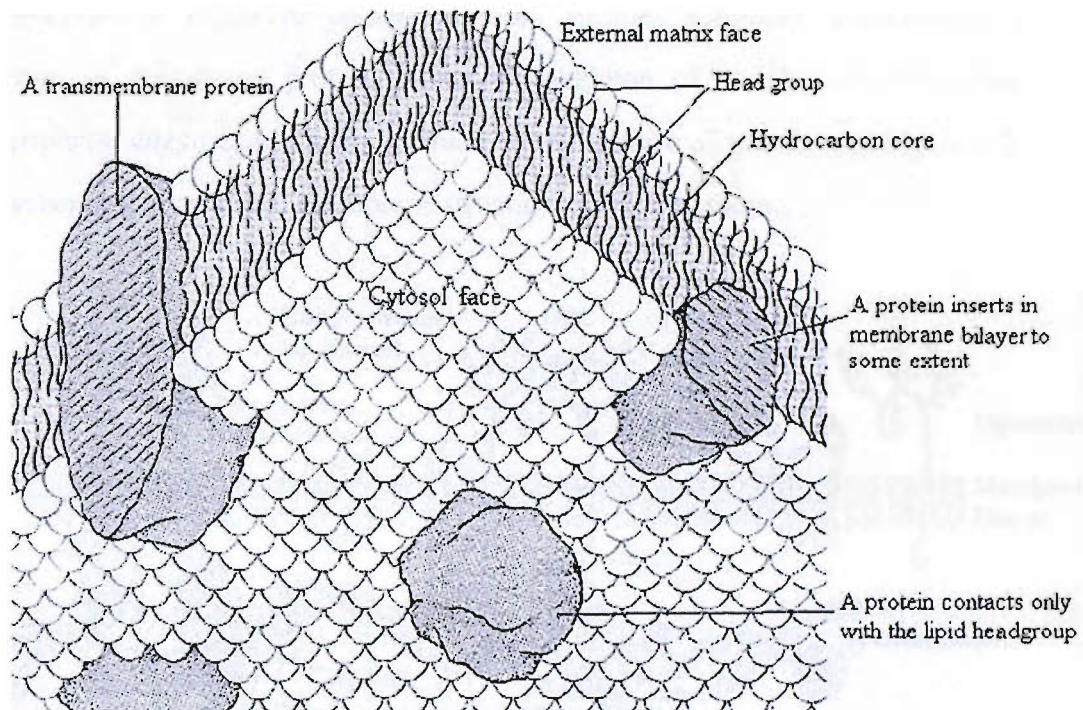


Figure 1.1 A schematic diagram of a membrane bilayer

1.1.2 Membrane proteins and functions

As one important component of biological membrane, proteins not only form the skeleton of the membrane but carry out most of the membrane functions, including substance transport; energy transduction; biological signal reception and transmission; and enzymatic reactions. These functions are conducted or mediated by distinct elements like pumps, channels, and enzymes within an environment formed by the surrounding membrane lipids as well as the intra- or inter- cellular matrix. The most significant property of a membrane is its selective permeability, which defines the boundary of a live cell. On one hand, the hydrophobic nature of the membrane hydrocarbon core impedes free flow of hydrophilic materials and thus serves as an osmotic barrier. Water and some small polar molecules can pass this barrier, while non-polar compounds can enter it and in fact dissolve into it. On the other hand,

transport (exchange) of most polar molecules, such as salts, amino acids, and other essential metabolites for life functions are carried out by special transport systems, i.e. above mentioned pumps, channels. In many cases, these processes take place against a concentration gradient and thus are energy consuming events. These are so called active transport, which are closely coupled to energy producing pathways, such as glycolysis or oxidative phosphorylation. Besides substance transporters, another group of membrane protein forms the skeleton of a cell, and also bind many peripheral enzymes and carbohydrates to the surface of membrane. Figure 1.2 shows a schematic drawing of membrane structure of an erythrocyte.

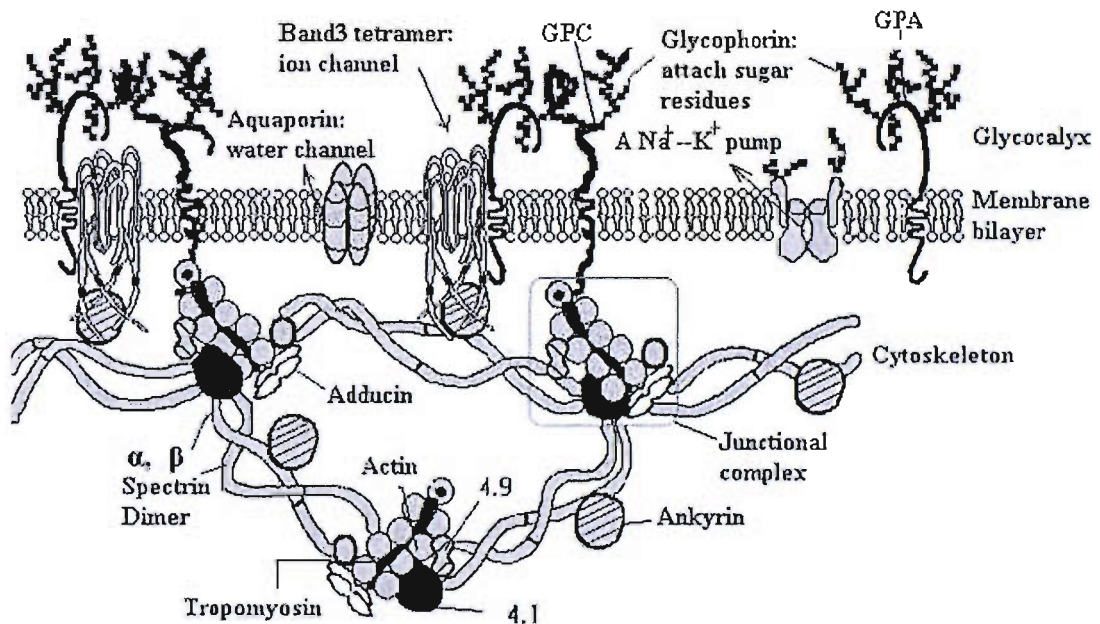


Figure 1.2 Schematic diagram of the erythrocyte membrane structure

Notes: Examples of shown membrane proteins are: Band 3, aquaporin, Na⁺/K⁺-ATPase, Glycophorin A (GPA) and Glycophorin C (GPC). Commonly, membrane protein have three domains: extracellular domain, attached by many carbohydrate units; transmembrane domain, where they aggregate as oligomeric complex or interact with each others; cytoplasmic domain, interact with other cellular components, such as Band 3 and GPC anchor the cytoskeleton to membrane bilayer.

This figure is from: <http://dwknowles.lbl.gov/membrane/membrane.html>.

1.1.3 Organelle membranes and special local membrane structures

In addition to a plasma membrane, eukaryotes also contain other intracellular membranes. These structures surround a variety of organelles contained within the cytoplasm. These subcellular membranes function similarly as plasma membranes and control communication between their inside environments and the cytosol. For example, the membrane of a lysosome, the major intracellular digestive system, prevents a series of hydrolytic enzymes like phosphatase, proteases and glycosidases from leaking out and digesting cell components. The nuclear membrane encloses the genetic information of life with a double membrane, which is notable for its pore system, termed as nuclear pores. These well defined pores appear to regulate the passive movement of molecules up to 9 nm diameter [7]. Some membranes, like those of the endoplasmic reticulum and Golgi apparatus, are even more bulky structures and seem to join or associate with each other closely—especially in the vicinity of nuclear membranes—and to form a continuous complex. Other special membrane structures like caveolae (a subtype of functional raft residing in plasma membranes) and lipid vesicles which contain proteins or lipids to specific destinations are also local membrane configurations exerting functions as membrane recruitment, substances transport and signal reception [7-9]. This diversity in membrane structures derives from specific lipid and protein composition.

1.2 Membrane chemical composition and geometry

1.2.1 Molecular structure and common lipid families

Lipids are one of the four classes of molecules essential for life. Unlike polypeptide, polysaccharide and nucleic acid, lipids are distinct in that, most lipids in biomembranes^{N1} are amphiphilic molecules with a hydrophobic fatty acid tail and a hydrophilic head group. Thousands of such amphiphiles, with different tails and head groups, are found in biological systems and this accounts for the diversity of membranes and membrane functions. This wide range of amphiphilic molecules can

N1: Besides of components of membrane, lipids also serve as fuel molecules, store energy, and transfer signals. These lipids may be present with different structures as found in membrane lipids.

be grouped into three main families depending on their molecular backbone structure. These are phosphoglycerides (also known as glycerophospholipids), sphingolipids (including sphingomyelin and glycolipids) and steroids. Table 1 briefly summarizes the molecular structure of these three families and a number of important lipid species in membrane composition.

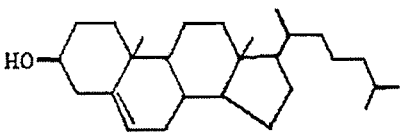
Name	Structural formulas	Name	Structural formulas
fatty acid	$\text{H}_3\text{C}-(\text{CH}_2)_n-\overset{\text{H}}{\underset{\text{H}}{\text{C}}}=\overset{\text{H}}{\underset{\text{H}}{\text{C}}}-\text{CH}_2-\overset{\text{O}}{\parallel}{\text{C}}-\text{OH}$	Cholesterol	
glycerol	$\begin{array}{c} \text{CH}_2\text{OH} \\ \\ \text{H}-\text{C}-\text{OH} \\ \\ \text{CH}_2\text{OH} \end{array}$	Sphingosine	$\text{H}_3\text{C}-(\text{CH}_2)_{17}-\overset{\text{H}}{\underset{\text{H}}{\text{C}}}=\overset{\text{H}}{\underset{\text{H}}{\text{C}}}-\overset{\text{H}}{\underset{\text{OH}}{\text{C}}}-\overset{\text{H}}{\underset{\text{NH}_2}{\text{C}}}-\text{CH}_2-\text{OH}$
Sphingomyelin	$\text{H}_3\text{C}-(\text{CH}_2)_{12}-\overset{\text{H}}{\underset{\text{H}}{\text{C}}}=\overset{\text{H}}{\underset{\text{H}}{\text{C}}}-\overset{\text{H}}{\underset{\text{OH}}{\text{C}}}-\overset{\text{H}}{\underset{\text{N}-\text{H}}{\text{C}}}-\text{CH}_2-\text{O}-\overset{\text{O}}{\parallel}{\text{P}}-\text{O}-\text{CH}_2-\text{CH}_2-\text{N}(\text{CH}_3)_3$ $\text{R}-\text{C}=\text{O}$		
Phosphatidate		Phosphoglyceride	
$\begin{array}{c} \text{O}-\text{CH}_2-\text{CH}-\text{CH}_2 \\ \quad \quad \\ \text{O}=\text{C} \quad \text{O} \quad \text{O} \\ \quad \quad \\ \text{R}_2 \quad \text{O}=\text{C} \quad \text{O}=\text{P}-\text{O}^- \\ \quad \quad \\ \text{R}_1 \quad \text{O} \quad \text{O}^- \end{array}$		$\begin{array}{c} \text{O}-\text{CH}_2-\text{CH}-\text{CH}_2 \text{O}^- \\ \quad \quad \\ \text{O}=\text{C} \quad \text{O} \quad \text{O} \\ \quad \quad \\ \text{R}_2 \quad \text{O}=\text{C} \quad \text{O} \\ \quad \quad \\ \text{R}_1 \quad \text{O} \quad \text{O}=\text{P}-\text{O}-\text{X} \\ \quad \quad \\ \text{O} \quad \text{O} \quad \text{O} \end{array}$ X: head group; R ₁ R ₂ : hydrocarbon tails.	
Phosphatidylcholine (PC)		Phosphatidylethanoamine (PE)	
$\begin{array}{c} \text{O}-\text{CH}_2-\text{CH}-\text{CH}_2 \text{O}^- \\ \quad \quad \\ \text{O}=\text{C} \quad \text{O} \quad \text{O} \\ \quad \quad \\ \text{R}_2 \quad \text{O}=\text{C} \quad \text{O} \\ \quad \quad \\ \text{R}_1 \quad \text{O} \quad \text{O}=\text{P}-\text{O}-\text{CH}_2-\text{CH}_2 \\ \quad \quad \quad \\ \text{H}_3\text{C} \quad \text{N} \quad \text{H}_3\text{C} \\ \\ \text{H}_3\text{C} \end{array}$		$\begin{array}{c} \text{O}-\text{CH}_2-\text{CH}-\text{CH}_2 \text{O}^- \\ \quad \quad \\ \text{O}=\text{C} \quad \text{O} \quad \text{O} \\ \quad \quad \\ \text{R}_2 \quad \text{O}=\text{C} \quad \text{O} \\ \quad \quad \\ \text{R}_1 \quad \text{O} \quad \text{O}=\text{P}-\text{O}-\text{CH}_2-\text{CH}_2 \\ \quad \quad \quad \\ \text{H} \quad \text{NH}_3^+ \end{array}$	
Phosphatidylinositol (PI)		Phosphatidylserine (PS)	
$\begin{array}{c} \text{O}-\text{CH}_2-\text{CH}-\text{CH}_2 \text{O}^- \\ \quad \quad \\ \text{O}=\text{C} \quad \text{O} \quad \text{O} \\ \quad \quad \\ \text{R}_2 \quad \text{O}=\text{C} \quad \text{O} \\ \quad \quad \\ \text{R}_1 \quad \text{O} \quad \text{O}=\text{P}-\text{O} \\ \quad \quad \quad \\ \text{HO} \quad \text{H} \quad \text{HO} \quad \text{H} \\ \quad \quad \quad \\ \text{H} \quad \text{H} \quad \text{H} \quad \text{H} \end{array}$		$\begin{array}{c} \text{O}-\text{CH}_2-\text{CH}-\text{CH}_2 \text{O}^- \\ \quad \quad \\ \text{O}=\text{C} \quad \text{O} \quad \text{O} \\ \quad \quad \\ \text{R}_2 \quad \text{O}=\text{C} \quad \text{O} \\ \quad \quad \\ \text{R}_1 \quad \text{O} \quad \text{O}=\text{P}-\text{O}-\text{CH}_2-\text{C}-\text{NH}_3^+ \\ \quad \quad \quad \\ \text{H} \quad \text{COO}^- \end{array}$	

Table 1.1 Formulas of lipid structure units and some common lipid species.

Among these family, phosphoglycerides are the most abundant lipid type in biomembranes, especially in prokaryotic membranes. As the name suggests, they are composed of a glycerol backbone, linking two fatty acid chains by an ester bond to the hydroxyls on C1 and C2 and one phosphate to the C3 hydroxyl (Figure 1.3). The latter group is in turn esterified to an alcohol, including choline, ethanolamine, serine, inositol etc. Some species only have one fatty acid tail, these are the lyso-phosphoglycerides. The two fatty acid chains may differ in length and the saturation (number of unsaturated bonds and their position within the carbon chain). The common number of carbon atom found in nature fatty acids is 14-20, and is predominantly even; a double bond usually has a *cis* configuration. A fatty acid is identified using a systematic name which contains this molecular information. For example, an 18-carbon-atom fatty acid with 1 single *cis* double bond at 9th carbon is represented as 18:1 *cis*Δ⁹, i.e. oleic acid, one common component in membrane lipid tail. The carbonyl oxygen of fatty acid together with glycerol, phosphate, and the polar head group form the polar region of a membrane lipid. Table 2 lists a schematic representation of common hydrocarbon chains.

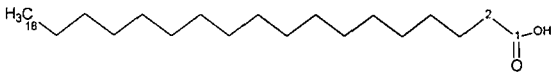
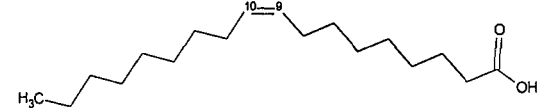
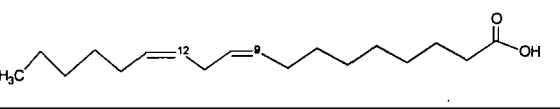
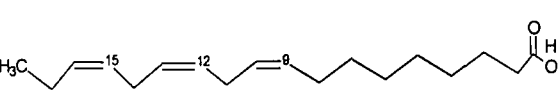
Fatty acids	Structure	Fatty acids	Structure
Myristic Acid 14:0	$\text{CH}_3(\text{CH}_2)_{12}\text{COOH}$	Stearic Acid 18:0	
Palmitic Acid 16:0	$\text{CH}_3(\text{CH}_2)_{14}\text{COOH}$	Oleic acid 18:1 <i>cis</i> Δ ⁹	
Palmitoleic Acid 16:1 <i>cis</i> Δ ⁹	$\text{CH}_3(\text{CH}_2)_5\text{CH}=\text{CH}-(\text{CH}_2)_7\text{CO}_2\text{H}$	Linoleic acid 18:2 <i>cis</i> Δ ^{9,12}	
Arachidic Acid 20:0	$\text{CH}_3(\text{CH}_2)_{18}\text{CO}_2\text{H}$	Linolenic acid 18:3 <i>cis</i> Δ ^{9,12,15}	

Table 1.2 Common fatty acids in membrane lipid tail domain.

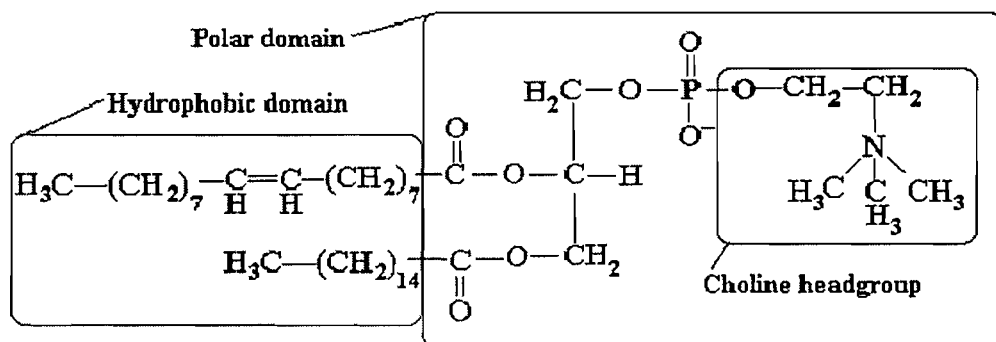


Figure 1.3 An example of phosphoglyceride structure:

1-Palmitoyl-2-oleoyl-phosphatidylcholine

1.2.2 Lipid solutions, polymorphism and phase preferences

Despite the high diversity of lipid species, a common property deriving from their hydrophobicity is that they form aggregate structures, such as micelles, when dispersed in water. There are two necessary conditions for aggregation: total concentration of amphiphiles must be higher than critical micelle concentration (CMC); and the temperature must be above the Kraft point. At concentrations lower than CMC, the dispersed amphiphiles exist as monomers while at temperature below Kraft point, the amount of dissolved molecules simply does not achieve CMC. By forming aggregates, the contacts between hydrophobic carbon chains and the polar environment are minimized and those between hydrophilic head groups and water molecules are maintained. This is a spontaneous process and mainly entropically driven by reducing the order arrangement of water molecules [5]. Though, the origin of hydrophobic force is too complex to be fully explained here, it is of biological importance and also functions in macromolecule folding and interactions.

A wide range of complex aggregate structures are induced as the concentration of amphiphiles is increased or as the temperature is raised. The phase transitions of different binary systems may depend, to different extents, on above factors. For example, a simple binary system of single-chain ionic amphiphile/ water can adopt phases in the following sequence: micellar solution—hexagonal phase (H_I)—lamellar bilayer (L_α)—inverse hexagonal phase (H_{II})—inverse micellar solution when reducing the water content [10]. Some uncharged lyso-phospholipids also fall into

this case, whose phase behaviour is mainly dependent on water content. For these amphiphiles, when water content is insufficient to “surround” the continuous oil phase, inverse micellar solution is formed. Alternatively, for many double-chain systems such as diacyl zwitterionic phospholipids, temperature appears to be more important for inducing phase transitions. A typical phase sequence displayed by diarachinoylphosphatidyl-ethanolamine/water system at water content over 20% to the excess water region is: L_{β} — L_{α} — H_{II} . Except temperature and water content, the transitions between these phases are also dependent on factors such as divalent cations and hydration status. Table 1.3 lists the main factors affecting phase behaviour. In general, factors which can reduce the repulsion between headgroup regions or increase the steric interactions in chain region facilitate non-lamellar phase [10]. Non-lamellar phases like cubic phase and oblique phase can also be formed under distinct conditions dependent on the amphiphiles types. This multiple choice in fact is one respect regarding lipid polymorphism: a simple binary amphiphile/water system alone can assume various structures under different conditions.

However, not all these phases are of biological significance. On the contrary, the dominant geometric structure of cellular membranes is a bilayer structure— L_{α} phase, even though a large amount of the lipids forming this lamellar phase, in isolation, preferably adopt non-lamellar phases under quasi-physiological conditions. Some structures like the inverted hexagonal H_{II} phase occur only transiently and locally in normal cells, but appear more and more relevant to membrane functions discussed in section 1.1.3.

Factor		Effects on phase behaviour (phase transition)
Head group domain	hydrophilicity	In general, hydrogen bonding and less degree of hydration tend to lead to stronger attractive interactions among headgroups domain, thus result in relative smaller cross section area for single lipid molecules, and favour non-lamellar phase.
	sterical structure	
	hydrogen bonding	
Hydro-carbon chain domain	chainlength	Longer chains imply more pressure within membrane hydrocarbon core; ether linkage is less hydrophilic than ester-linked one; and more unsaturated bonds in proper position increase fluidity within tail domain. These factor though less profound to those from headgroup domain, facilitate lose pack of chains, and decrease the $L\alpha$ - H_{II} transition hindrance.
	chain linkage	
	unsaturation	
	single chain	
Solvent property	temperature & pH	These exterior factors mainly function upon interfacial region, as to affect headgroup hydration and protonation status. Increasing temperature will results in more freedom for hydrocarbon chains to adopt conformations, and then bring about more fluidity in this domain.
	hydration	
	ions & other solute	

Table 1.3 Factors affecting membrane phase behaviour and their function tendency.

1.2.3 Lipid molecular shape model and membrane curvature stress

In order to rationalize the phase behaviour of amphiphilic materials, a molecular shape concept was proposed [11]. This model explains aggregate polymorphism and classifies amphiphiles mainly on base of molecular shape with respect to the head group and carbon chain regions. Type 0 lipids represent those with comparable sizes for the two regions, and thus bare an overall cylindrical shape; they form lamellar structures. Type I lipids have a relatively smaller cross-sectional area of the hydrocarbon chains compared to the larger head group region, so these “inverted cone” shaped amphiphiles pack optimally in H_I or micellar phases. For the opposite case, type II amphiphiles have a larger or more splayed chain area and favour configurations of H_{II} phase or inverted micelle. In fact, the majority of membrane amphiphiles belong to the last type which also appears to be the most important one concerning about membrane morphology and functions. See Table 1.4 for a schematic representation and examples.

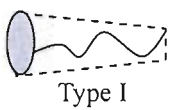
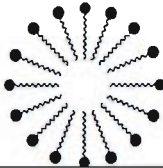
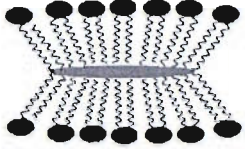
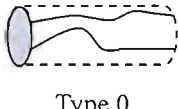
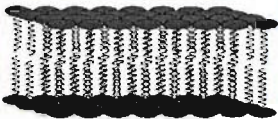
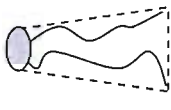
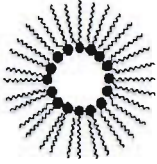
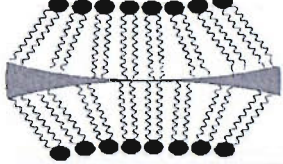
Amphiphile example	Molecular Shape	Phase preference	Tendency to curve in membrane bilayer
Lysophospholipids	 Type I		Positive curvature. 
PC & Sphingomyelin	 Type 0		Free volume shown as grey shading area.
PE & Cholesterol	 Type II		Negative curvature. 

Table 1.4 Lipid molecule shape model & curvature in a frustrated bilayer

Note: The molecular shapes of amphiphiles shown as geometric objects with dashed line are schematic representations, and act only as a guide to understand the gross feature of how they pack. They do not reflect the real situation of the molecular shapes which are fluid complex.

Using this description, it can be seen that each monolayer in a membrane bilayer may have a spontaneous tendency to curve either towards the polar region (due to type I amphiphiles) or towards nonpolar cone (due to type II amphiphiles). The corresponding structures and curvatures are termed as positive and negative. However, for a symmetrical bilayer to remain flat, the tendency to curve positively or negatively is offset by that from the apposing leaflet since they are hydrophobically coupled together. Consequently, the tendency to curve is frustrated and the unexpressed curvature is thus stored as potential energy with a latent ability to deform the bilayer structure.

1.2.4 Membrane curvature stress profile

Considering the interaction between amphiphiles molecules within a bilayer formed by type 0 amphiphiles, since there is no tendency for each leaflet to curve, the interfacial tension within each monolayer is internally balanced by forces from headgroup and chain regions. While for a bilayer built by type I and type II amphiphiles, due to the tendency to curve to a non-lamellar structure, the interaction within the headgroup and chain regions are different. Thus, the force from one region

may surpass that from the other region. However, the composition of force encountered by a lipid molecule must equal zero, for a stable bilayer. Particularly, a profile across one leaflet of a frustrated bilayer is shown in Figure 1.4, the internal tension mainly comes from three regions:

- 1.) from the head group region— F_h , induced by hydration and electrostatic effects (usually repulsive) and hydrogen-bonding effect (usually attractive);
- 2.) from the carbon chain region— F_r , usually repulsive due to steric repulsion;
- 3.) from transition parts of above two regions— F_c , a hydrophobic driving effect to minimize the polar-nonpolar interfacial area.

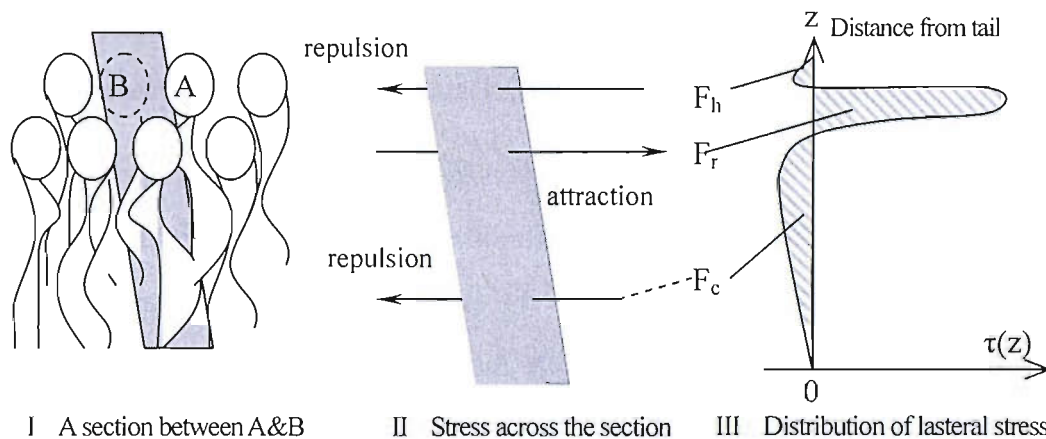


Figure 1.4 Schematic diagrams of lateral stress distribution within a bilayer.

The lateral tension distributed across this profile is nonuniform but must be balanced overall. That is, the net tension represented by the shading area shown in Figure 1.4, must equal zero.

If a protein which has a closed approximately cylindrical, is embedded in a lipid monolayer, the local interaction between amphiphiles is substituted to an amphiphiles-protein interaction. The original lateral tension stored in the vicinity of insertion is partially released which leads to a more stable state. Thus, a local redistribution of lateral tension will be introduced. Such an example of membrane-protein interaction is given in section 1.3.4.

1.3 Membrane-enzyme interactions

1.3.1 Functional classification of membrane associated enzymes

According to the broad range of catalytic reactions, enzymes bound to membrane can be principally grouped into five types [12]; they are:

Type 1.) involve in the biosynthesis of membrane components;

Type 2.) associate with information transfer;

Type 3.) participate in translocation phenomena;

Type 4.) act on locally concentrated substances;

Type 5.) being a number of organized multi-enzymes group, especial those enzymes in a metabolism pathway which catalyzing several continuous reactions.

Above classification involve a wide range of cellular events and various association manners among which lipid compositions of the membrane bilayer, particular type II amphiphiles, have direct influences on enzyme activity in many cases [13-15]. However, such a classification is not strict because one enzyme grouped in one category could be included in other(s) as well. Such enzymes as phosphokinase,^{N2} is a good example to illustrate this problem. There is ample evidence showing that the majority enzymes of glycolysis bind to cellular membranes at different sites and by different means [16-18]. These enzyme-membrane interactions bring sequential coupled enzymes to a closed vicinity—type 5, which pass metabolites one to another in a local concentrated situation—type 4; moreover, glycolysis is one of the pathways involving in energy metabolism, and several transfer processes are found to be pumped by this pathway—type 3. Thus, membrane-enzyme association appears to render profound regulation roles on post-translation and metabolic events. However, there have not been direct observations of PFK association with membrane lipids.

N2: Phosphokinase is the enzyme chosen in present study which catalytic the third reaction in a sequential of ten glycolytic reactions. And glycolysis is an important pathway in organism energy metabolism. More detailed properties of PFK and glycolysis pathway will be introduced in chapter 2.

1.3.2 Protein construction

Protein structures are commonly described hierarchically [5,19]:

- 1.) amino acid sequence—primary structure;
- 2.) short range interactions of these building blocks, which form special structures like α helix, β strand and β turn—secondary structure;
- 3.) spatial arrangement of such structural units into global configurations—tertiary structure;
- 4.) and last, crosslink and association of above global subunits to a more bulky oligomeric complex—quaternary structure.

Among these four level structures, the first one is the most basic and important structure in protein construction. All proteins in all species, from bacteria to humans are built from a repertoire of twenty amino acids. These building blocks have different side chains varying in stereo structure, hydrogen-bonding capacity and hydrophobicity. These properties (especially hydrophobicity) are not only essential for further constructions of proteins (secondary, tertiary and quaternary structures), but also important in membrane-protein and protein-protein interactions. A classification of the twenty amino acids according to their hydrophilicity is included in Table 3.2. Schematic representations of primary and secondary structures are briefly shown in Figure 1.5; also see PFK structures in chapter 3 as views for higher-level structures. In general, processes to form above structures are overlapped events when a new protein is synthesized. That is to say before proteins or enzymes are distributed to their final destination across membranes or transported within vesicular liposome and finally settled down (in lipid membranes or nearby) to perform their assumed functions, local secondary construction units are folded and three dimensional structures are partly formed during the polypeptide is continuously growing. So, membrane-protein interaction may occur in every level in the course of a protein achieving the final structure, i.e. the most stable state for a given polypeptide.

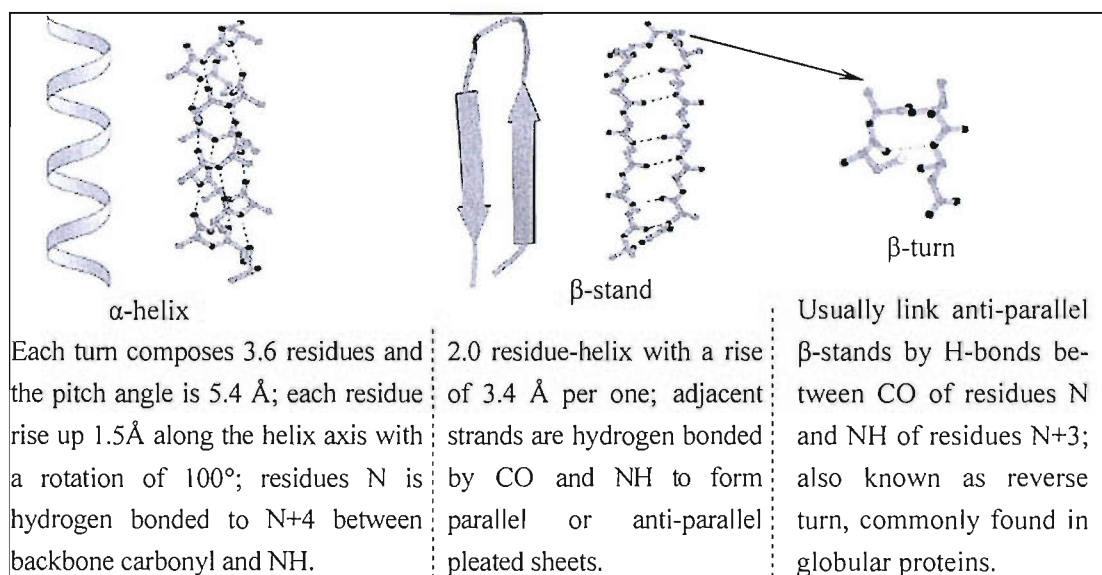


Figure 1.5 Main properties of primary and secondary protein structures

For membrane proteins, especially those spanning membranes, a model was proposed to mimic the process of membrane-protein association [20], which includes four steps. This is known as the four-step thermodynamic model:

- 1) By electrostatic interactions, a peptide with a size of around 18-20 residues is absorbed close to the membrane surface;
- 2) Through a series of interactions involving hydrogen bonding, electrostatic force, hydrophobic interaction, the attracted peptide is future partitioned into amphiphilic core and folded to a more ordered structure—usually an α -helix;
- 3) Driven by hydrophobic interaction, the formed structure inserts to the hydrocarbon core of the lipid bilayer to an extent decided by the thickness of membrane and overall protein outline;
- 4) To give a more stable system, two or more such subunit may associate with each other, to reduce the exposed polar face of the helix to the surrounded apolar environment or to meet with the balance decided by the interactions between the protein with both the extra-membrane domain and the inner-membrane domain.

Random coil \longleftrightarrow Folded structure \longleftrightarrow Insertion \longleftrightarrow Associated complex

The original model also considers free energies changes during partitioning, folding, insertion, and association; so it is more complex than addressed here, which only

involves a description about the processes. However, for some membrane associated proteins, especial non-transmembrane one, above processes may not be fully adopted. For example, they may only contact with the polar head groups of the amphiphiles or insert into the surface section of the membrane (cf. Figure 1.6).

1.3.3 Membrane-protein association patterns

To illustrate the patterns which are adopted during membrane-protein interaction, several different schematic models are proposed in literatures [21,22] and they are listed in Figure 1.6. The first case represents situations that the length of inserted motif and the thickness of membrane hydrocarbon core are different; and local thickening and thinning effects of bilayer occur to reduce these hydrophobic mismatches. Enzymes such as gramicidin A and a number of synthetic peptides can be sorted in this type [23,24]. The second model depicts that, after residing in membranes, protein will adopt particular structures as hourglass-like and barrel-like to perform their functions, this type is common for transmembrane enzymes such as porin [25] and alamethicin [26,27] involving in translocation events (case 3 in section 1.3.1). The last model stands best for peripheral membrane enzymes like CCT and protein kinase C [28,29], and thus is more related to the question of studying. This type of enzymes usually contains specific amphiphilic domain(s) which sense the surface charge of membranes and also possible anchor themselves by insert to the hydrocarbon core to some extent.

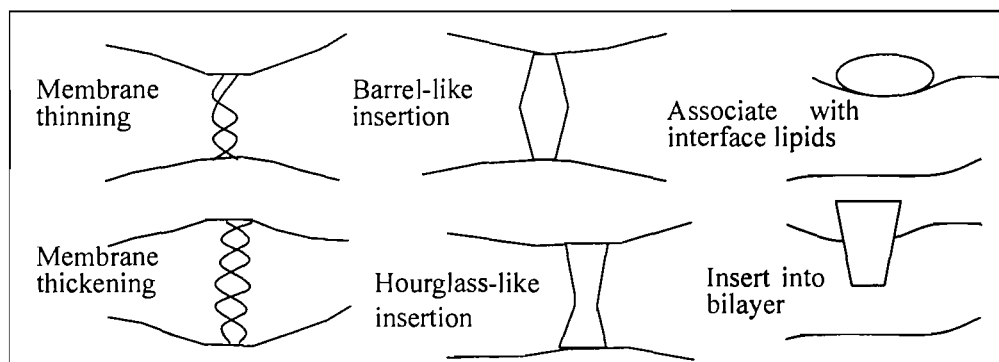


Figure 1.6 Membrane-protein association patterns

1.3.4 Examples of membrane protein interactions

From above, it appears that interaction between proteins and lipids has a double effect. On one hand, the immediate vicinity of lipids in contact with the proteins with particular shapes will change the ways to pack the bilayer and release part of the potential lateral curvature tension stored inside the monolayer, consequently result in a more stable system. On the other hand, by partitioning into the membrane bilayer, proteins will fold into its most thermal stable structure or a more (less) activated form to carry out biological functions. The following is an example of such interactions between enzyme phosphocholine cytidylytransferase (CCT) and membrane lipids.

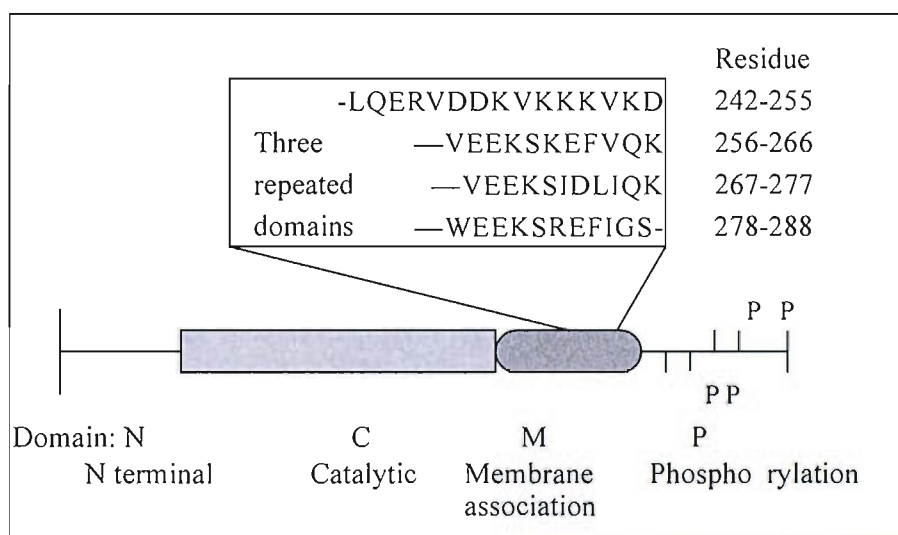


Figure 1.7 Functional domain of CCT & amino acids sequence of domain C [22]

In higher plants and animals, CCT (phosphocholine cytidylytransferase EC 2.7.7.15), catalyzes the rate controlling step in biosynthesis of phosphatidylcholine (PC), which is the most abundant lipid species of mammalian cell and a precursor important for other lipids synthesis. Figure 1.7 shows functional regions of CCT [22]. In cells, CCT were found either soluble in cytosol or associated with membrane bilayer. The former is favoured by phosphorylation of domain P, the C-terminal domain of CCT. In fact, this form, having low substrate-bonding affinity, is an inactive form due to the interaction between catalytic domain C and domain M [30]. Domain M contains a 3-time repeated peptide chain, each being 11-residue long, and have been proposed to be the principal domain associating with membrane lipids [31]. It was found that,

upon binding to membranes, the conformation of domain M is changed from a random coil to a well ordered amphiphilic α -helix. Consequently, the “autoinhibitory role of domain M” is removed and the enzyme-CTP bonding affinity is enhanced for more than 20 times [32,33]. Studies using tryptophan fluorescence quenching suggested that the reconstructed peptide (containing the above maintained three-repeated domain) insert halfway to the one layer of the artificial membrane—lipid vesicles [33]. Two factors are important to this interaction: negative charge density (of the lipids) on the membrane surface and the stored curvature elastic energy within the membrane. Specifically, lipids with negative charged headgroups like fatty acid and phosphatidylserine facility the association between membranes and CCT and give a more activated enzyme [34]. However, nature lipids [35] like diacylglycerol and zwitterionic lipids phosphatidylethanolamine can also activate CCT. And interestingly, these lipids are all type II lipids, which induce large amount of negative curvature tension in the constructed membrane structure. Some investigations [36,37] (using lipid vesicles as model membrane) were developed to relate enzyme activity to the composition of type II lipids of the reconstructed membranes. The results consist well with the theory that the stored curvature tension is a main factor in membrane-CCT association. It is also proved in these studies that comparing with type II lipids, type I lipids which induce positive curvature tension in membranes activate CCT to a less effective degree.

In addition to CCT, a number of other membrane associated enzymes are also regulated by non-lamellar phase favouring lipids. Protein kinase C, for example, is an extrinsic enzyme binding reversibly to membranes. Increased partitioning to membranes and a more activated enzyme is resulted by non-lamellar lipids [28,29,]. Rhodopsin is similarly activated by lipids with negative spontaneous curvature though it is a transmembrane enzyme which senses the lateral stress distributed in the whole bilayer [38]. Other extrinsic enzymes like phosphatidate phosphohydrolase: PLAs and diacylglycerol kinase [39] are found sensitive to membrane physic properties too. Thus CCT and other enzymes involving in synthesis of membrane lipids are regulated by the membrane-enzyme interaction, hence obtain a homeostatic

control of membrane properties and functions.

The purpose of this study is: to use lipid vesicles as model membrane and phosphofructokinase as the target enzyme, to explore links between variation in the phosphofructokinase activity and the vesicles lipid compositions.

Chapter 2 Introduction of Phosphofructokinase

2.1	Common properties	21
2.1.1	PFK families	21
2.1.2	Substrates specificity and ion requirement of PFK	22
2.1.3	PFK oligomeric conformation	22
2.1.4	Glycolysis pathway and the key role of PFK	23
2.2	Modulation of PFK activity by intermediate metabolites	26
2.2.1	By energy charge: ATP, ADP, and AMP etc.	26
2.2.2	Feedback regulation: citrate and PEP amplify the inhibitive effect of ATP	29
2.2.3	F2, 6BP and other effectors	30
2.2.4	Reaction and allostery mechanisms: the concerted model	31
2.3	Modulation of PFK activity by Phosphorylation.....	34
2.4	Regulation by binding to membrane related cellular components	35
2.4.1	Binding to band 3 proteins.....	35
2.4.2	Interaction with caveolin-3	37
2.4.3	Other interactions with membrane related elements	37

2.1 Common properties

Phosphofructokinase (PFK) catalyses the phosphorylation of fructose 6-phosphate (F6P) to fructose-1,6-bisphosphate (F1,6-BP), using ATP, PPi or ADP as phosphoryl donors. It is a well known enzyme in terms of its rate-limiting role in glycolysis and typical allosteric regulation properties. The first report of PFK catalyzed reaction was published some 70 years ago [40], but to date there is no explicit mechanism to fully explain its catalytic behaviour. PFK reaction particularly with respect to allosteric mechanism, phosphorylation, modulation by metabolic intermediates and interaction with cellular components, is of considerable interest. These will be briefly introduced in this chapter.

2.1.1 PFK families

Since glycolysis is well conserved throughout evolution, PFK is widely distributed in all domains of organisms including bacteria, archaea, and eukaryotes [41]. PFK can be classed into 3 families, according to the phosphoryl donors it use. The first family refers to ATP-dependent PFK (EC 2.7.1.11), found in Bacteria, Eukaryotes and yeast; it is the most widely distributed type. The second family use pyrophosphate (PPi) as substrate (EC 2.7.1.90). The enzymatic reaction is more reversible and subject to a less complex allosteric regulation in comparison with that of first family. This group includes PFK from plants, as well as bacteria, and protists [42]. Lastly, ADP-dependent PFK (EC 2.7.1.146) was uncovered in 1994 by Serve W. M. Kengen et al., and to date only found in domain of Euryarchaea [43]. These 3 groups can be further divided and other classifications are also possible according to different criterions. For instance, PPi-dependent PFK can be sub-divided on the base of different responses to F2,6-P regulation—sensitive or no effects; and ATP-PFK can be classified to those specifically using F6P as reactant and those taking a broader source of phosphor acceptors like fructose, ribose, adenosine, tagatose-6-phosphate, and fructose-1-phosphate [44]. The latter type is termed as PFK B family and found in *Aeropyrum pernix* and also co-exist with a F6P specific PFK, family A PFK in *E. coli* [45]; however, PFK of family B is not allosteric controlled by substances like

nucleotides, citrate and Phosphoenolpyruvate (PEP) which are either activator or inhibitor for common family A bacterial PFK [41,45]. Among these different types, ATP-dependent PFK is the most extensively investigated group due to its wide distribution and its importance from the view of evolutionism. Unless specially stated, PFK discussed hereafter belongs to this group. The enzyme tested in activity assays of the present study is an ATP-dependent, family A PFK from *Bacillus stearothermophilus*. More detailed analysis of this enzyme is given in next chapter.

2.1.2 S substrate specificity and ion requirement of PFK

As one important kinase, PFK needs divalent cations for activity. In fact, metal ion-ATP complex is the real reactant in catalytic reaction. Mg^{2+} is the most effective ion, which can be substituted by other cations like Mn^{2+} and Co^{2+} , with lower efficiency; Ca^{2+} is an inhibitor. NH_4^+ and K^+ are positive effectors with the former being more efficient [46]. For the other substrate F6P, PFK shows some substrate specificity with β -D-fructofuranose-6-phosphate ^{N1} being the only active isomer of F6P for the reaction [47]. However, despite this anomeric restriction, a number of nucleoside triphosphates and sugar phosphates are alternative reactants, but usually they bind to PFK with less affinity. For the majority of PFK, pyrimidine nucleotides are poorer substrates comparable with purine nucleotides [48]. Many of these intermediates serve as competitive analogs for the original reactants.

2.1.3 PFK oligomeric conformation

Most ATP-dependent PFK are homotetrameric enzymes which consist of four identical subunits packed as two layers of two. Exceptions are found in yeast [49] and certain bacteria [50] which contain an $\alpha_4\beta_4$ octamer and a dimer respectively. Crystal structures of PFK from some bacteria are solved at high resolution [51,52], which belong to space group I222 with a cell dimension 122.5, 84.5 and 61.5 Å. That is to say, the overall structure is asymmetric. The structure of PFK gives important information that all the active and allosteric effect sites lie in clefts among subunits.

N1: Except this β -furanose, the other two anomers of D-F6P are one cyclic α -furanose and one acyclic keto; these forms exist in a ratio of 76:19:5; PFKs bind two furanoses but only take the β -anomer in phosphorylation [54].

So, the entire tetrameric complex is the smallest active form with four identical sites for each substrate and effector. PFK from bacteria are about half smaller than those from various mammalian tissues. The molecular mass of each subunit for a bacterial PFK, range from 32000 to 38000 daltons, while those of mammalian PFK subunit are 75000- 95000. Moreover, mammalian PFK can aggregate into even larger complexes at high concentration [53,54]; and this aggregate-disaggregate equilibrium is a pH-dependent process which confers these enzyme fairly complicated modulation roles. A schematic representation of the homotertrameric structure is shown in Figure 2.1 and a more detailed analysis of BsPFK will be given in chapter 3.

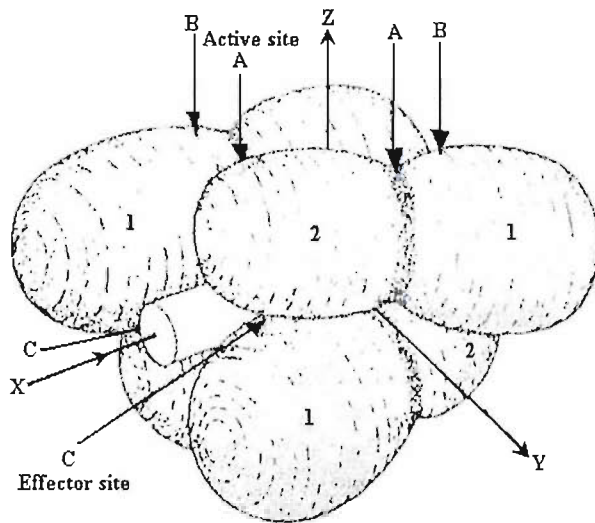


Figure 2.1 A schematic drawing of PFK tetrameric structure [55]

One subunit consists of two domains shown as 1 and 2; active sites A, B and effector sites C are buried between two domains of one subunit or the clefts between two subunits; one subunit contacts with other two and leaves the central of the complex a water channel along X axis.

2.1.4 Glycolysis pathway and the key role of PFK [56 and hereafter]

Glycolysis is one of the universal pathways for glucose metabolism which is highly conserved throughout evolution. A set of ten enzymatic reactions in glycolysis are nearly identical from bacteria to animals. However, glycolysis is different in these domains of organisms with respects to glucose uptake mechanisms (the entry of sugar in pathway) and to the ways of consuming the end product, pyruvate, under anaerobic conditions. Figure 2.2 shows the glycolytic flux, from one molecule of glucose to two molecules of pyruvate, which subsequently, are converted into either lactate (under anaerobic conditions) or into acetyl coenzyme A, (under aerobic conditions). The later metabolite represents the entry point for citric acid cycle and electron transport

chain, i.e. the aerobic way to liberate most energy from fuel molecules in animals.

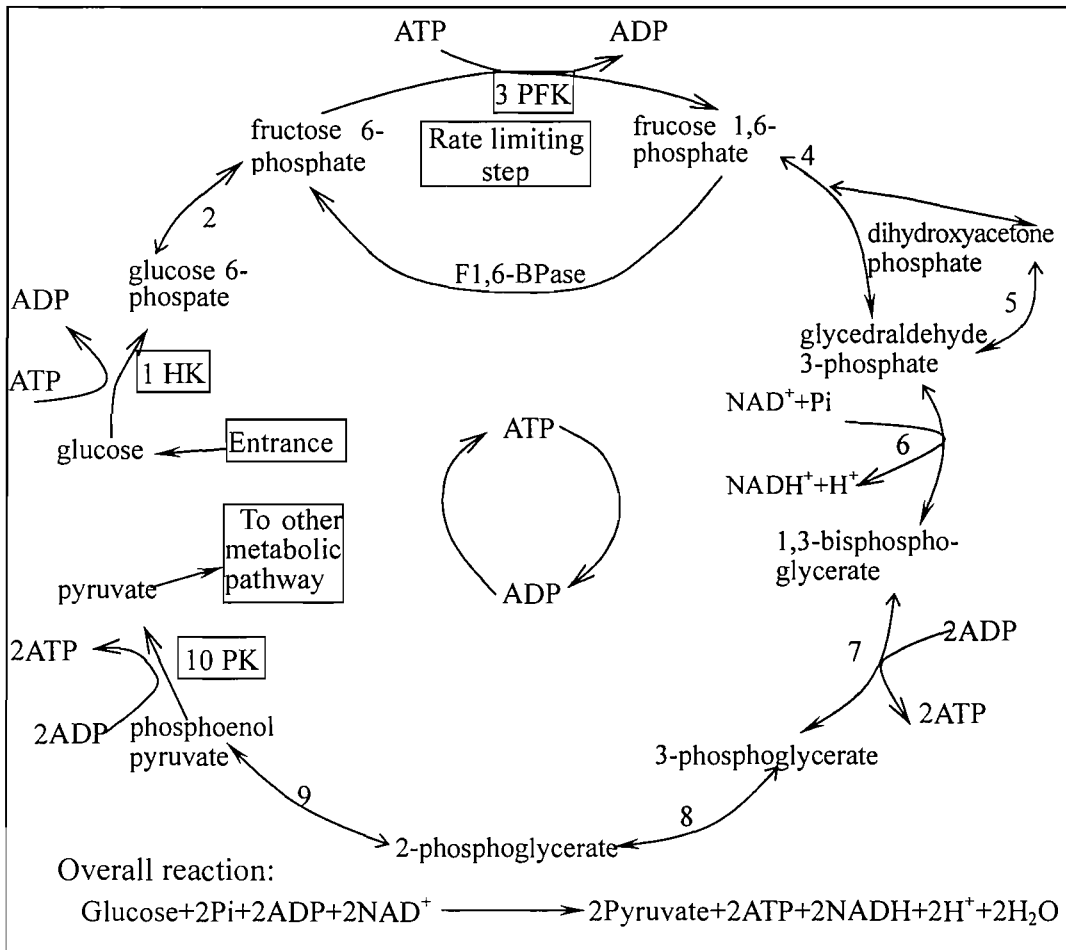


Figure 2.2 The flow of glycolytic pathway

Notes: Ten reactions are catalyzed by enzymes listed in Table 2.1, in which reaction 1, 3 and 10 are important steps for the whole pathway. For reaction 3, the opposite reaction in glucogenesis is catalyzed by fructose 1,6-bisphosphatase.

In the pathway showing in Figure 2.2, there are three irreversible reactions (1, 3, 10), each having a large negative free energy; thus are considered to be important for the regulation of the whole pathway. Generally speaking, irreversible reactions are usually highly regulated in metabolic pathways [46]. On one hand, the activity of enzymes catalysing these reactions is dramatically changed by means of allosteric activation and/or inhibition and phosphorylation. On the other hand, in irreversible reactions the rate of the forward direction is much higher than the reverse one. When the reaction is activated/inhibited, more effects will be induced on the forward direction than the reverse one; thus the net flow through the reaction is changed. In

contrast, reversible reactions are not capable of inducing significant control in the whole reaction flue. Reaction rates of the forward and reverse directions are not so different that the ratio of substrates/products is not subject to obvious variation even if the enzyme is activated/inhibited. So, reactions having large negative free energy are predisposed to be rate-limiting steps for the pathway. Specifically for glycolysis, these reactions are catalyzed by HK (hexokinase), PFK, and PK (pyruvate kinase) respectively, and all three are allosteric enzymes. Among these enzymes, PFK catalyzes the committed step of glycolysis, and sets the pace of glycolytic flux, while HK controls the trap of glucose and PK limits the outflow of the pathway.

Enzyme	Free energy (kJ/mol)		Enzyme	Free energy (kJ/mol)	
	$\Delta G^{\circ'}$	ΔG		$\Delta G^{\circ'}$	ΔG
Hexokinase	-16.74	-33.47	Glyseraldehyde 3-phosphate dehydrogenase	6.28	-1.67
Phosphoglucose isomerase	1.67	-2.51	Phosphoglycerate kinase	-18.83	1.26
Phosphofructo-kinase	-14.23	-22.18	Phosphoglycerate mutase	4.6	0.84
Aldolase	23.85	-1.25	Enolase	1.67	-3.35
Triose phosphate isomerase	7.53	2.51	Pyruvate kinase	-31.38	-16.74

Table 2.1 Glycolytic enzymes and free energy of each enzymic reaction

Notes: $\Delta G^{\circ'}$ is standard free energy change; ΔG is the free energy change under actual physiologic conditions, calculated using known concentration of reactants under typical physiologic conditions [56].

Hexokinase is allosterically inhibited by both its products: ADP and glucose 6-phosphate. The latter substance exists in equilibrium with fructose 6-phosphate, one of the substrate of PFK. Thus, inhibition of PFK leads to a higher concentration of G6P, thus an indirect inhibition of HK. Moreover, the main source of G6P is derived from the breakdown of glycogen; in this sense, the HK reaction is not necessary for glycolysis. The last exergonic reaction in glycolysis is catalyzed by PK. The products of this reaction is pyruvate, a multiple functional intermediate that can enter into other metabolic pathway or serves as building block e.g. in the synthesis of long

chain fatty acids. F1,6-BP, one of the products of PFK reaction activates PK to maintain the constant output of glycolysis. When ATP concentration is high or other signals like accumulations of acetyl CoA or long chain fatty acids occur, PK is inhibited and gluconeogenesis pathway (in which glucose is formed) is activated. The second phosphorylation of glucose, the first unique step to glycolysis pathway is catalyzed by PFK, which is actually an irreversible reaction *in vivo*. As described above, this enzyme sends signals to HK and PK; and appears to play feedback regulation and feed forward stimulation roles to them, respectively. Moreover, due to its complex allosteric mechanism and fully regulated by a number of important intermediates, PFK play an indispensable role in glycolytic flow and overall carbohydrate metabolism.

2.2 Modulation of PFK activity by intermediate metabolites

Organisms rigorously organise metabolism by controlling the activities of their enzymes which catalyze thousands of different reactions at the same time. The most important control strategies are: transcriptional control of the enzyme amount; and modulation of enzymatic activities; and the accessibility of reaction substrates. PFK, as an important enzyme in energy metabolism, is regulated by all above strategies. Particularly, some respects of PFK activity regulation such as energy charge, allosteric regulation, are briefly introduced in this section.

2.2.1 By energy charge^{N2}: ATP, ADP, and AMP etc.

As one of the ATP-generating metabolic pathways—catabolic, glycolysis is strictly subject to modulation by cell energy status. This can be partly drawn from the fact that the activities of several enzymes in this pathway including PFK are well regulated by normal cytosol ATP concentration which essentially limits the output of glycolysis to the required level. Moreover, ADP and AMP, reflecting low energy state of cells, enhance PFK activity by allosteric regulation or diminish ATP

N2: Energy charge, one index of the cell energy status, is calculated by: (amount of ATP and half amount of ADP)/(total amount of ATP, ADP, and AMP). For most living cells, the energy charge is in the range of 0.8 to 0.95 [5].

inhibition. Thus, PFK activity is well regulated by the energy status and functions as a control point in glycolysis and the whole energy metabolism.

Lardy et al. [54], found that in addition as one of substrates ATP, was also an important inhibitor of PFK. Since then, extensive kinetic studies have been carried out to explain this regulatory property of PFK from a variety of organisms and tissues. The adopted inhibitive mechanisms and the extent of inhibition, vary widely dependent mainly on the enzyme source. However, one common property of ATP inhibition is that upon binding ATP to PFK at either the allosteric site or the active site of F6P, the enzyme binding affinity with respect to F6P is decreased. For most eukaryote PFK, ATP (above the inhibitive concentration) binds to the effector site and induces a structure change in PFK. The resulted PFK-ATP complex consequently shows lower cooperative binding affinity to F6P. The original hyperbolic saturation curve of F6P, shown in Figure 2.3, is substituted by a sigmoidal one and the shape of the curve can be further shifted to right by adding more ATP.

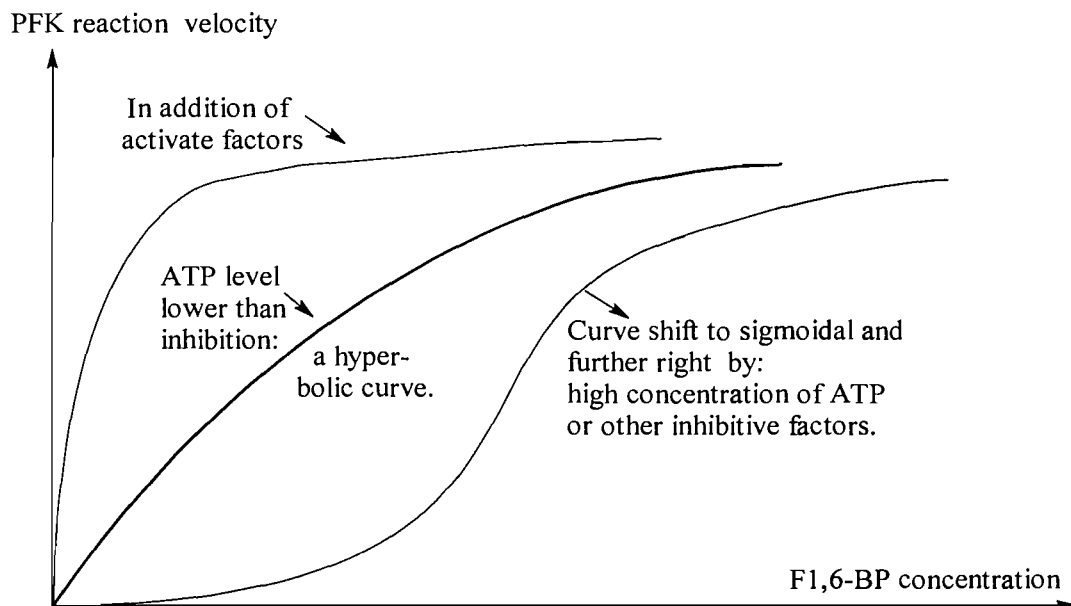


Figure 2.3 A schematic plot of PFK allosteric inhibition by ATP

Notes: The original curve of reaction velocity versus F1,6-BP concentration plot is a hyperbolic one, shown in thick line; it can be shifted to sigmoidal by increasing ATP concentration or other inhibitive effectors.

As to most Bacterial PFK, especially the best investigated one from *Escherichia.coli*, the F6P saturation curve shows sigmoidal properties regardless of ATP concentration. Due to the lack of a specific ATP allosteric site in bacterial PFK, inhibition of ATP is presumed to result from the binding of ATP to the F6P active sites abortively or binding to the T-state of the enzyme which disfavours the reaction flux. By either of these two means, it is equally to decrease the PFK binding affinity with respect to F6P. See section 2.2.4 and 3.1.2 for detailed explanation of the ATP inhibition mechanism. From above, it is not surprising that this inhibition caused by disfavoured binding can be relieved by F6P or by ADP [57].

For most PFK, a high concentration of magnesium ions can relieve ATP inhibition effectively [58], and it is proposed that free ATP^{4-} rather than MgATP^{2-} plays a more potent inhibitive role, just opposite with respect to substrate specificity of PFK. In the latter case, MgATP complex is the real substrate. Moreover, it has been reported that this modulation by ATP shows significant pH and temperature dependence in that the inhibitive extent and tendencies are different for PFK from different sources and organs [59,60]. The most extensively studied example is PFK from rabbit muscle. This enzyme is allosterically inhibited at low pH but completely loses this property under alkaline condition; at pH values up to 9, this PFK shows Michaelis-Menten kinetics with respect to both substrates. [61,] However, pH and temperature also affect the association-dissociation equilibrium for PFK from mammals. This equilibrium is also a potent factor to regulate PFK activity, so the ATP-inhibitive mechanism is difficult to correlate or ascribe to one special factor.

As to other elements in energy charge, ADP and AMP are common activators of PFK. Generally, these intermediates effectively counteract the inhibitive effect of ATP and synergistically enhance the effects of other activators such as F1,6P [62]. As analogs of ATP, these nucleotides compete with ATP through binding to ATP allosteric sites. Alternatively for most prokaryotes PFK, upon binding to effector sites, the active form of PFK is stabilized which facilitates the effective binding of substrate F6P. Other nucleotides such as ITP, CTP, UTP, and GDP (which can be regarded as part of the

energy status of a cell), also play inhibitive or activating roles on PFK. GDP is a potent activator of PFK, functioning in a manner similar to ADP [63]. Consequently, GDP is more commonly chosen instead of ADP in some kinetic studies to activate PFK and avoid the competitive interaction of ADP with respect to ATP. In [57], it is even proposed that all three here mentioned NTPs and ATP inhibit BsPFK to essentially the same extent if they are in present at a concentration above 10mM.

2.2.2 Feedback regulation: citrate and PEP amplify the inhibitive effect of ATP

3-phosphoglycerate, 2-phosphoglycerate and phosphoenolpyruvate (hereafter stated as 3-PG, 2-PG and PEP, respectively) are all phosphorylated intermediate metabolites of the glycolysis pathway (See Figure 2.2). For mammals, it was proposed that these metabolites in addition with citrate exhibit a synergistic inhibitive function with respect to ATP, but only if ATP is in present at or above a critical inhibitive concentration [64]. The effects are more pronounced at low pH and low temperature conditions. Particularly for citrate, its synergistic effect is supported by experiments, using citrate and ITP. The latter is a patent substrate of PFK but with a very weak inhibition. The results show no detectable inhibition of enzyme activity [65,66]; and more interestingly, citrate serves as an activator at sub-saturating concentration of ATP/ITP [67]. The opposite view was proposed that citrate (3-PG and PEP as well, respectively) can cause PFK inhibition alone when ATP concentration is not capable to achieve inhibition [68]. What is more, citrate is one of the effectors resulting in depolymerization of the active tetramer enzyme to inactive dimers [69]. From these views, it is reasonable to say citrate, alone can affect PFK activity. PEP is essential to regulate PFK activity in prokaryotes, since PFK in such organisms have only one allosteric binding site for PEP/ADP. Crystallographic studies show that a glutamate residue is responsible for binding both the activator and inhibitor [70,71]. Therefore, PEP and ADP exhibit antagonistic effects on enzyme activity, by means of increasing or decreasing the binding affinity of F6P to PFK (rather than altering the maximal rate of the enzyme turnover). This regulatory way is called the K-type regulation manner. See section 2.2.4 for definition of K- and V-type regulation of enzymatic

reactions. Steady-state fluorescence and kinetic experiments show that the PFK inhibition/activation by PEP/F6P are pH and temperature dependent and also affected by MgATP concentration [72,73].

2.2.3 F2,6BP and other effectors

Hers and Schaftingen discovered a strong activator of PFK [74], which proved to be F2,6-P, the most potent activator for mammalian and plant PFK. This factor allosterically regulates the enzyme activity by markedly decreasing the half saturation concentration of F6P and effectively diminishing the inhibitive effect of ATP. Under the physiological condition [53,75], ATP concentrations and F6P concentrations is about 3mM and 0.1mM, respectively. That is, ATP is well above the critical inhibitive concentration (or F6P concentration is far below saturating). While, F2,6-BP virtually relieves the inhibition by ATP and stimulates PFK (and eventually the whole glycolysis pathway) to proceed *in vivo*.

F2,6-BP is present in liver, brain, heart, skeletal muscle and other tissues. It is also formed by the phosphorylation of F6P, a reaction catalysed by PFK2 (EC2.7.1.105, see Figure 2.4), an enzyme resembling PFK. F2,6-BP also has an inhibitive action to fructose 1,6-bisphosphatase (EC3.1.3.11), which is an important enzyme in gluconeogenesis and plays the opposite role with respect to PFK. PFK2 itself is an interesting subject for investigation due to its coexistence with another enzyme (fructose 2,6-phosphatase, EC3.1.3.46) in a multi-domain protein. The phosphorylated and de-phosphorylated forms of this bifunctional protein correspond to FBP2ase and PFK2 respectively. From Figure 2.4, it can be concluded that F2,6-BP collects the signals from glucagon (corresponding to low level of glucose) or glycogen (high level of glucose), and express its information at the point of PFK activity, the committed step of glycolysis. Secondly, cyclic AMP, one crucial second messenger for many hormones, is also involved in this indirect regulation of PFK activity through phosphorylation of a bifunctional enzyme and lower the F2,6-BP level. Finally, cAMP alone is a weak activator of PFK and cAMP dependent protein kinase can directly phosphorylate PFK. [53,76]

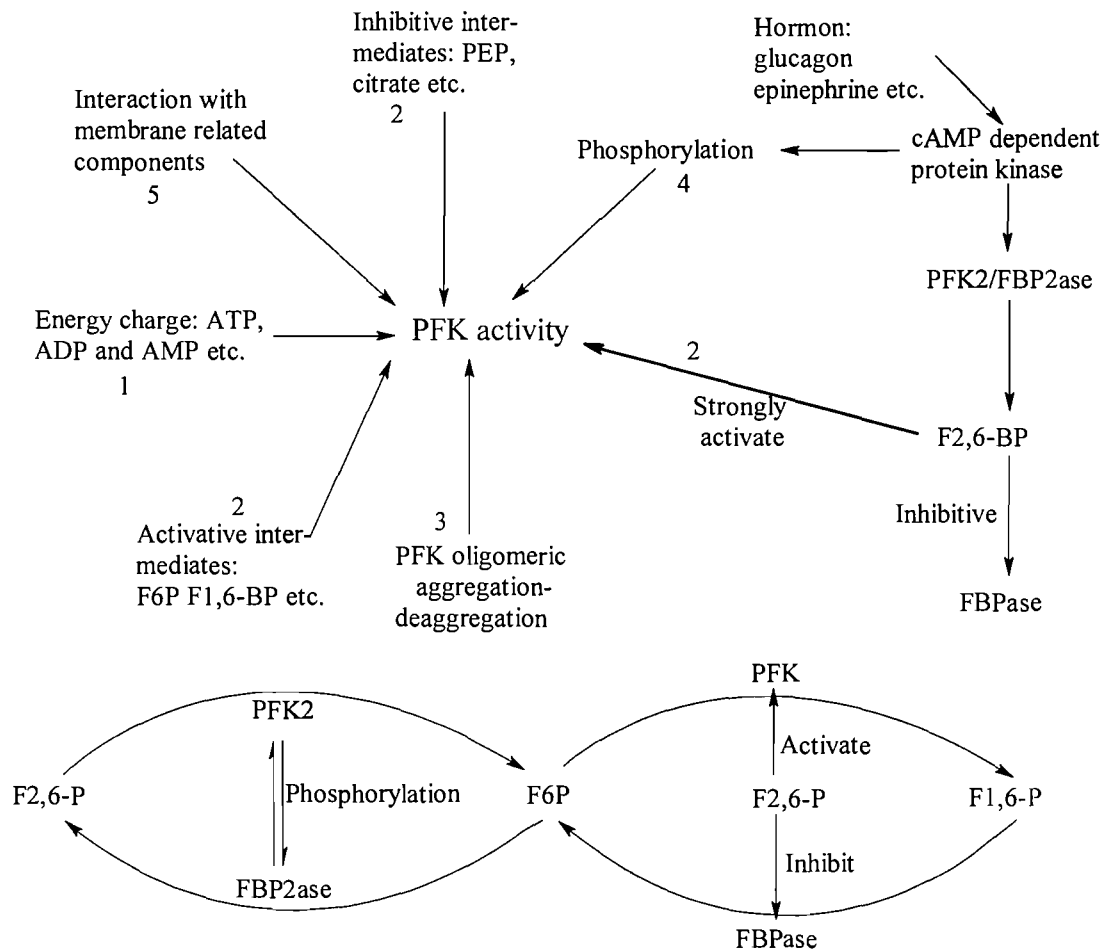


Figure 2.4 A schematic drawing of PFK regulation mechanisms

Notes: PFK activity can be directly regulated by 5 manners; manner 4 and 5 will be introduced later. Manner 2 involves many intermediates and other factors such as hormones regulations are also important for PFK activities. Except PFK, enzymes shown in Figure 2.4 are: FBPase, 1,6-bisphosphatase; PFK2, fructose-6-phosphate-2kinase; FBP2ase, 2,6-bisphosphatase. The latter two enzymes coexist in a multi-domain bifunctional protein and can transform to each other by a phosphorylation-dephosphorylation reaction.

2.2.4 Reaction and allosteric mechanisms: the concerted model

From above, PFK is classic example of allosteric enzyme whose activity is controlled by a series of physiological factors. Allosteric enzymes usually are oligomeric proteins symmetrically built by identical subunits and their kinetic properties do not simply fulfil the Michaelis-Menten model. Based on kinetic studies of enzyme activities, Monod, Wyman and Changeux introduced a model to explain the mechanism for allosteric enzymes [46,56]; and it was used to explain the complex catalytic behaviours of PFK. This is so called concerted model (also known as

Monod-Wyman-Changeux model or MWC model). The following are main points of the concerted model, which are explained using PFK as an example.

1.) The allosteric enzyme can exist in two different conformations, termed as the relaxed or R-state, and the tense or T-state. The symmetry of the structure is conserved in allosteric transitions; that is all the subunits within the oligomer must be all in either T-state or all in R-state; it does not contain a mixture of the two. For PFK, a tetrameric complex, exist in equilibrium in solution between R_4 and T_4 forms. In other words, though the two forms are able to convert from one to another but no asymmetry hybrids, such as R_3T_1 , R_2T_2 , and R_1T_3 exist.

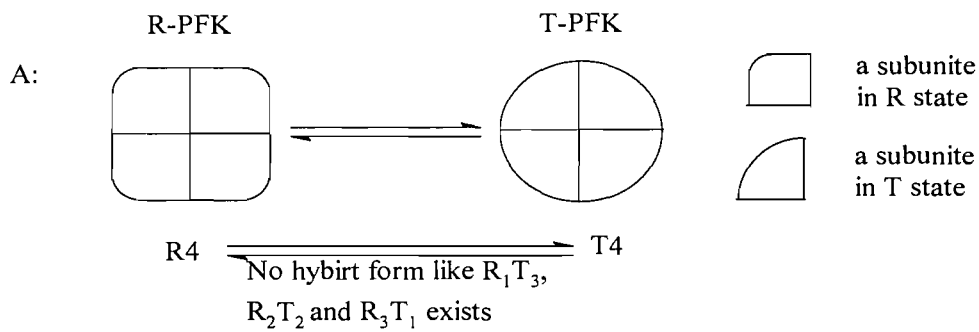


Figure 2.5A A schematic drawing of concerted model of PFK tetramer

2.) Substrates and effects bind R- form or T-form of enzymes with different affinities. In particular, T-state PFK show high binding affinity allosteric inhibitors such as PEP; and R-state PFK have high affinity to F6P and activators as ADP and cAMP; and ATP can bind to two forms of PFK with same affinity. However, in the absence of any ligands (substrate or allosteric effectors), nearly all of the enzyme molecules are in the T-state.

3.) The substrate-enzyme binding shows cooperative feature. In the case of PFK, F6P is more likely to bind the R-state PFK as it is the higher affinity form. On one hand, by forming R-PFK--F6P complex, the amount of free R-state PFK is reduced; consequently, the equilibrium is shifted to the right. So more enzyme molecules will exist as R-form and the overall enzyme/substrate affinity is increased. On the other hand, up to four molecules of F6P can bind to the same PFK because each of the four subunits of the tetramer contains one substrate binding site for F6P. Due to the R-state

PFK is the high affinity form, the more F6P molecules bind to PFK, the more difficult it will convert to the T-state PFK in the equilibrium. See Figure 2.5 for the concerted model of PFK. In result, one binding of F6P is in favour of next and further binding, a property known as positive substrate cooperativity. Substrate cooperative is usually measured by Hill coefficient n . An n value greater than 1 suggests positive substrate cooperativity, and vice versa; the maximum possible value of n is equal to the number of binding site.

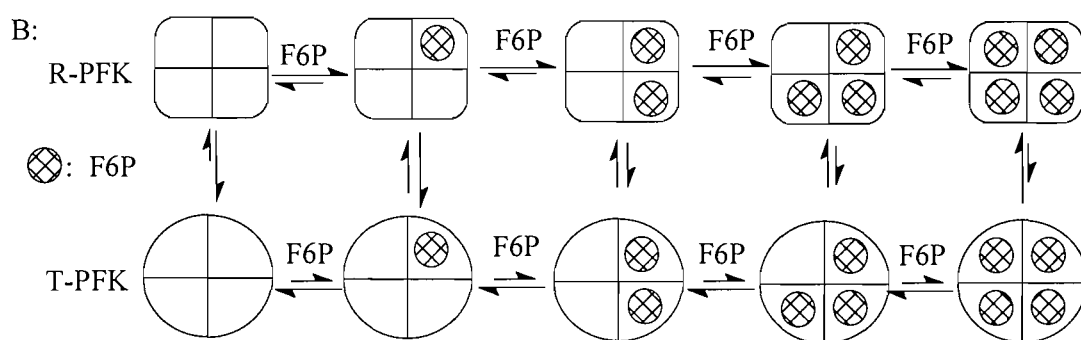


Figure 2.5B A schematic drawing of concerted model of PFK tetramer

Notes: F6P binds to R-PFK with higher affinity; F6P binding to PFK is positively cooperated because the more F6P bind to one PFK molecule, the more difficult the R-PFK will convert to the T-PFK (denoted by the arrows in each transition equilibrium). For PFK, a tetramer enzyme having one binding site on each subunit, the maximum Hill number is 4.

It is shown in Figure 2.3 that when adding activators like ADP to the reaction mixture, the $V/[F6P]$ plot is shifted to left, implying less F6P is required to achieve the V_{max} (or to saturate the enzyme). Moreover, when a very large amount of activator are added, nearly all of the enzyme will be converted to the R-state, consequently, the substrate can have no further cooperative influence and the curve becomes hyperbolic. From Figure 2.3, it also can be seen that all the lines are heading towards the same V_{max} value despite the different shapes. That is, all effectors regulate the PFK reaction by changing substrate binding property rather than altering the V_{max} of the reaction. In enzyme kinetics, these two situations are named as K-system and V-system, respectively.

The above mechanism of PFK allostery is mainly based on the kinetic properties of enzyme from bacterium. PFK from yeast and eukaryotes display more complicated

behaviours such as association—dissociation equilibrium of rabbit muscle PFK. The concerted model has been adapted to explain their reaction and regulation mechanisms [46]. It is difficult to ascribe the PFK activity variation to one single reason, because many factors may exert influence on the enzyme activity at same time and one factor can affect the enzyme by different means. However, one common rule is that, the positive effectors are in favour of the R-state PFK and increase the apparent F6P binding affinity, while the negative effectors do the opposite.

2.3 Modulation of PFK activity by Phosphorylation

Cyclic AMP (cAMP) dependent protein kinase phosphorylates a number of enzymes and thus is important for many cellular processes. PFK, the rate limiting enzyme of glycolysis, is also subjected to this regulation, but to a variable extent mainly dependent on the enzyme sources. The enzyme itself is purified with high or low phosphate form from muscle [77,78], liver, and heart [79,80], and can be further phosphorylated by the catalytic subunit of cAMP-dependent protein kinase, or dephosphorylated by alkaline phosphatase treatment [81]. The phosphorylation site is proved to be a serine residue located near the carbon terminus [82]. From literature reports it appears that the amount of phosphate incorporation varies widely and hence the resulting changes in enzyme kinetic properties are different even at similar incorporation levels. However some common observations can be noted:

- (1) The phosphorylation action is a complex process affected by factors such as buffer composition, pH, the original effectors of native PFK, and the aggregation state of the enzyme [83,84].
- (2) The active conformation of the enzyme, R-state PFK is more readily to be phosphorylated. Activators like AMP and F1,6-BP increase the phosphorylation rate, while inhibitors like citrate decrease the incorporation level; for a particular PFK, the final incorporation levels are similar for both the T-state and R-state PFK [82].
- (3) The higher the phosphorylation level, the more sensitive the PFK is to allosteric inhibition by ATP and citrate, and the less sensitive it becomes to be activated by AMP, glucose 1,6-bisphosphate (G 1,6-BP), and fructose 2,6-bisphosphate (F2,6-BP).

Moreover, the difference becomes more obvious at lower pH values [83,84].

(4) Despite the diversity (or even conflicting observations) in kinetic properties and variation in the resulting enzyme activity, this cAMP dependent reaction is responsible for the regulation of PFK activity *in vivo* [80,81] and possibly, for the reconstruction of PFK subunits which leads to different enzyme conformations [85,86].

In addition, PFK activity can also be regulated by this phosphorylation reaction indirectly. As shown in Figure 2.4, cAMP transduces the signal initiated by glucagon (in muscle, initiated by epinephrine) in two ways: phosphorylate PFK2/FBP2ase and remove the most potent activator (F2,6-BP) of PFK; simultaneous, phosphorylate PFK directly, and change the enzyme sensitivity to its effectors in the tendency of activity inhibition. Though the extent of this modification and adopted mechanism are far from clear, there is no doubt that they are metabolically essential.

2.4 Regulation by binding to membrane related cellular components

In general, glycolytic enzymes are highly soluble proteins and easily separated from the insoluble lipid membrane fractions [87]. This fact leads to the conclusion of its cytosolic location. However, *in vitro* immunoprecipitation/immunofluorescence has revealed a variety of potential binding interactions between PFK and special components in/on cellular membrane surface domains [87,88]. These components include anion transporter—band 3 in erythrocyte membrane [89]; lipids and signal transmitters—caveolin-3 in muscle membrane [90]; proton pump—H⁺-ATPase [91]; and filamentous actin in muscle membrane [90]. Other enzymes in the glycolytic pathway also show preferential association with some of these cellular elements (especially with band 3) [92]. These interactions, from a general view, lead to a localization of the glycolytic enzymes and thus link the glycolysis pathway with other essential cell events.

2.4.1 Binding to band 3 proteins

Band 3 is a predominant integral membrane protein which functions as an anion

transporter. The N-terminal segment of band 3 (located on the cytoplasmic side of the membrane, cf. section 1.1.2) functions as an attachment site for the spectrin-actin submembrane cytoskeleton of erythrocytes [6]. This segment of band 3 is also capable of binding to glycolytic enzymes like PFK, G3PDH, and aldolase [93,94]. The binding sites are thought to be located at the end part of this segment where more than half residues are acidic. Phosphorylation of band 3 residues (tyrosine 8 or 21) was reported to block the interaction between band 3 and with glycolytic enzymes [95] which in turn enhances the glycolysis pathway. Inhibition of glycolysis was observed by suppressing the same phosphorylation [92]. G3PDH, and aldolase appear to compete with PFK by binding at the same or overlapping sites on band 3 protein [96].

Similarly to phosphorylation of PFK, as discussed in the last section, this regulation is sensitive to high ionic strength, pH, and shows preference for different aggregated forms of the target enzymes. Moreover, this interaction shows opposite effects to PFK activity. On the one hand, the bound enzyme is no longer subject to the original allosteric inhibition by ATP and 2,3-bisphosphoglycerate; and the reaction velocity/[F6P] curve is converted to non-sigmoidal (see section 2.2). Consequently, it is assumed that binding occurs at the ATP/ADP activation site. On the other hand, this interaction appears to inhibit PFK by preferential binding to inactivated dimeric form of PFK, thus changing the association—dissociation equilibrium of the free PFK. In fact, these two aspects are related because the allosteric inhibition site is located in the cleft between subunits of the oligomeric enzymes, which is more opened in dimer form (see Figure 2.1). Considering the *in vivo* situation, this interaction is important to regulate PFK activity and the overall glycolysis pathway. Particularly for mammalian red cells, this regulation could be more significant. Red cells lack F2,6-BP, the most potent activator of PFK. Thus association of PFK with band 3 might be the main way to release the inhibition effect induced by millimolar concentration of ATP and 2,3-BPG [89]. According to overall glucose metabolism in the glycolysis pathway and the total amount of PFK available in cells, PFK activity is only expressed about 1% of maximum [88]. However, the theoretic PFK activity,

calculated under the physiological levels of inhibitory metabolites (ATP, F6P, 2,3-BPG ect.), should only be less than 0.1% of maximum. Thus, the band 3 associated PFK seems to account for the actual activity of this enzyme *in vivo* [88,89]. In addition, taking into consideration of the other two subsequent glycolytic enzymes (G3PDH and aldolase, see Figure 2.2 and Table 2.1) which also bind to the same or adjacent sites on the band 3 N-terminal segments, this interaction most likely and at least, enrich or redistribute these enzymes to such status that favour the further regulation of the entire pathway.

2.4.2 Interaction with caveolin-3 ^{N3}

Caveolin, an integral membrane protein, is one of the structural elements of plasmalemmal caveolae; and caveolin-3 is the specific isoform expressed in muscle cells. Immunohistochemical studies show that Cav-3 associates with several proteins and confers functions—such as cellular signal differentiation and structural stabilization and membrane recruitment—to this special membrane domain (also known as a lipid raft). Recently it has been reported that PFK and Cav-3 (possibly Cav-1 as well) form a tight complex which is facilitated by extra-cellular glucose and regulated by original activators of PFK [90]. Although this interaction is somewhat unusual and its mechanism and biological significance are far from clear, this local concentrating role couples PFK activity to other cellular processes [97,98].

2.4.3 Other interactions with membrane related elements

The above mentioned associations are special in terms of the involvement of several successive glycolytic enzymes for the case of band 3; and for the case of caveolin-3, a strong action which could link the glycolysis pathway to a number of other cellular events. Muscle PFK is also found to be activated by F-actin which shows a preference for the dephosphorylated form of the enzyme and consequently influences the equilibrium of PFK oligomerization [99]. This is thought to be important for the use

N3: Caveolae are 50–100-nm invaginated plasma membrane domains present in many cell types. They are enriched in glycosphingolipids and cholesterol and characterized by the presence of the integral membrane protein caveolin. Caveolin-1 and -2 are ubiquitously expressed [100,101]. Caveolin and caveolae seem to play a role in many different cellular processes.

of energy source during muscle contraction. Muscle PFK interacts with phospholipase-A2 thus builds a link between glycolysis and phospholipolysis [102].

To summarize, PFK the rate limiting enzyme in the glycolysis pathway, is subject to a series of modulation mechanism including:

- 1.) classic allosteric inhibition and activation by metabolites;
- 2.) association-dissociation equilibrium;
- 3.) phosphorylation—dephosphorylation;
- 4.) interactions with membrane-related compartments.

All these manners, by means of modifying the protein's functions and its cellular location to express these functions, give a comprehensive control of PFK activity and the whole of glycolysis. The latter manner—to locate the enzyme—may be considered as part of post-translational modification of PFK (also all other glycolytic enzymes); and it is a membrane involved process which involves the interaction of PFK and several membrane components. However, the purpose of this thesis is to study the interactions of PFK and membrane lipids. The particular PFK studied, is from *Bacillus stearothermophilus*.

Chapter 3 PFK from *Bacillus stearothermophilus*

3.1	General properties.....	40
3.1.1	Enzyme source.....	40
3.1.2	BsPFK reaction and regulation mechanisms.....	40
3.1.3	Experimental conditions: temperature- and pH-dependence.....	42
3.2	The primary and secondary structure of BsPFK	44
3.3	Three dimensional structure of BsPFK	46
3.3.1	Construction of BsPFK subunits	46
3.3.2	Subunits association	46
3.3.3	An analysis of BsPFK subunit amino acid using helix wheel.....	49

3.1 General properties

PFK from *Bacillus stearothermophilus*, noted as BsPFK hereafter, is one of the most extensively studied enzymes. Its structure at a high resolution was reported by Evans etc. [51,52]. As indicated in Chapter 2.1, this specific PFK is a relative simple enzyme and is less complex regulated than those from high organism.

3.1.1 Enzyme source

Bacillus stearothermophilus is a species of gram-positive and endospore-forming bacterium in the genus *Bacillus*. The distinguishing feature of this bacterium is that its spores are highly resistant to heat while its vegetative cells are sensitive to unfavourable conditions [103]. As the name indicates, *B. stearothermophilus* is a fat- and heat-loving species: it grows at temperatures between 30—75°C, with an optimum of 65°C [104]. It is also the source of several restriction enzymes, and is a popular research subject in terms of its inherent thermostability. Early investigations showed that some enzymes were stabilized when they were associated with the cell membrane. This led to the suggestion that membrane-enzyme association could contribute to the organism's stability under extreme conditions.

3.1.2 BsPFK reaction and regulation mechanisms

BsPFK is an ATP-dependent enzyme which transfers the terminal phosphoryl group from ATP to fructose-6-phosphate (F6P). This is a ternary reaction, in which PFK can bind either of the two reactants first, i.e. kinetically that is a sequential random reaction. The enzyme-F6P-MgATP ternary complex can be formed through two ways and binding of ATP to enzyme or to enzyme-F6P complex is the rate-limiting step of the whole catalytic reaction (non-rapid equilibrium). This conclusion was drawn from kinetic studies using low level ATP (ATP concentration is less than K_m , half of the saturating concentration, so that the inhibition effect of ATP is removed). Some investigations [57,105,106] showed that the maximum reaction speed remained constant by increasing the F6P concentration when the ATP was fixed; whereas the reaction velocity increased linearly when increasing ATP concentration stepwise and keeping the F6P concentration fixed. After this non-rapid equilibrium, the transfer of the γ -phosphate group from ATP to F6P is catalyzed and the final products, ADP and F1,6BP are released from the enzyme-products ternary complex enzyme-MgADP-F1,6BP, through a sequential random order. See Figure 3.1 for the reaction pathway.

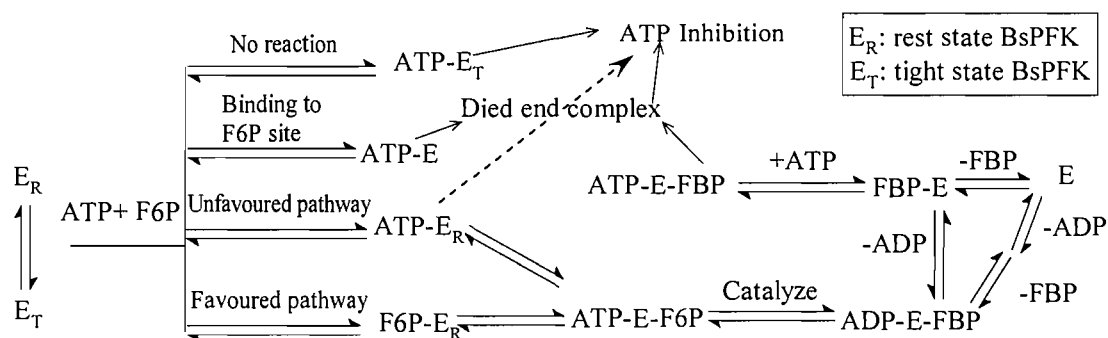


Figure 3.1 Schematic diagram of reaction flux and ATP-inhibition

Unlike ATP, Phosphoenolpyruvate (PEP) is an allosteric inhibitor of BsPFK. When binding to the allosteric sites, PEP diminish the substrate affinity to F6P, thus inhibit BsPFK heterotropically. This inhibition is reversed by F6P and ADP [108]. In this respect the BsPFK resembles that from *Escherichia.coli* (EcPFK). These two enzymes have about 55% homology and the same secondary structures [57,71]. Whereas EcPFK displays apparent homotropic cooperativity in the presence of saturating ATP, the saturation of BsPFK by F6P is cooperative only in the presence of the inhibitor PEP. BsPFK shows regulation mechanism which is similar to that exhibited by eukaryotes PFK (refer section 2.2.1). The original hyperbolic saturation profile with respect to F6P is switched to a sigmoidal one in the presence of respective inhibitors. For BsPFK, this inhibitor is PEP and for the other group of PFK, it refers to ATP. Though ATP is not an allosteric inhibitor of BsPFK, it inhibits the enzyme by different ways. To be more specific, the allosteric sites of BsPFK are located in the clefts between two subunits of the tetrameric complex and made up of a glycine residue at position 212. It was proved by site directed mutagenesis that the ability of ATP to inhibit the enzyme is unaffected by mutant GV212 [109,110]. So, this observation rules out the possibility that ATP inhibits PFK by binding to the effector site and regulates the enzyme allosterically. (The allosteric site binds effectors ADP, F6P, and PEP). Instead, several other possible mechanisms were proposed by different investigators to explain how ATP inhibits PFK, these include:

(1) By abortive binding of ATP at the active sites of F6P via its γ -P group:

Kinetic studies on the initial rates using a fixed and low ATP concentration showed that the double-reciprocal plots—($1/v$ versus $1/[F6P]$) converge at the left of the $1/v$ axis. This is usually seen in the case of noncompetitive inhibition [111]. This can be simply and hypothetically explained by the substrate-inhibition introduced by ATP.

Moreover, inhibitory studies using AMPPCP, an analogue of ATP, only display competitive inhibition with respect to ATP [57]. This further confirms the substrate-inhibition hypothesis because AMPPCP, having a differently orientated terminal phosphate group is unlikely to bind to F6P active site in the same way as ATP. Because this is a noncompetitive inhibition, it is relieved by adding more F6P.

(2) By binding to the enzyme-product binary to form a dead-end complex, PFK-ATP-F1,6-BP: this ternary shows a much lower dissociation constant when compared with the normal product-product-enzyme ternary complex, PFK-ADP-F1,6-BP. However, product inhibition studies of the reverse reaction (in which ATP is a product and F1,6BP is a reactant), show that the complex PFK-ATP-F1,6-BP does not form readily, and thus do not support this hypothesis.

(3) By performing the catalytic reaction under one disfavoured way: this is based on the fact that PFK could bind either reactant first and then the rest later. That is, the reaction could undergo through two alternative pathways but with one kinetically favouring another. As can be inferred from Figure 3.1, ATP binding to PFK first, is the disfavoured way. More importantly, BsPFK is an allosteric enzyme, which exists in an equilibrium between two forms, R- and T- state (see section 2.2.4). Experimental conditions such as effectors' concentration and pH play functional roles to control this equilibrium and thus adjust the level of the enzyme activity. Though ATP does not bind to PFK through allosteric site, by competing with F6P and binding to the active site, the T-state of PFK is favoured.

Altogether, ATP particularly at a concentration above saturation could inhibit BsPFK by means of: forming dead-end ternary complexes; binding to BsPFK prior to F6P binding (and changing the reaction flux through a disfavoured manner; or by favouring the T-state of the enzyme which displays a much lower BsPFK/F6P binding affinity. As a consequence, higher concentrations of F6P; and higher pH values or adding allosteric activators, which favour the R-state of the enzymes will diminish the effect of ATP inhibition.

3.1.3 Experimental conditions: temperature- and pH-dependence

It can be expected that BsPFK is more stable to extreme conditions such as temperature and pH, since the enzyme source is a thermostable bacterium. There are many studies of PFK activity over wild temperature ranges. Gebhard et al. studied

BsPFK activity at 60°C and pH 8.2, assuming this was the optimal condition for enzymatic function [112]. Braxton et al. compared the activity and allosteric property of BsPFK at pH 6 and at various temperatures as low as 6°C [113]. Besides the high catalytic activity at low temperature, another interesting phenomenon they discovered was that MgADP, a physiological activator of BsPFK at temperatures above 16°C, eventually changed into a weak inhibitor at 6°C. Thus, an entropy (as well as enthalpy) driving hypothesis was used to interpret this modulation mechanism. PFK allosteric inhibition by PEP showed similar temperature dependence [114,115], and further supported the thermodynamic character of enzyme allostery. Later, with the aid of site-directed mutagenesis, the PEP inhibition of BsPFK was re-examined, and the accepted allosteric mechanism was reevaluated [116].

Though BsPFK is highly active at low temperature, the activity is lost quickly, especially upon freeze-drying and freeze-thawing treatment. It was reported [117] that PFK from rabbit muscle lost nearly all the activity after freeze-drying and dissolution; addition of certain sugars and divalent cations could protect enzyme from denaturation and help maintain most of the catalytic ability. Trehalose and zinc are the most effective sugar and ion species respectively to maintain the enzyme activity during storage, while other sugars like glucose and galactose showed less efficiency. In the case of BsPFK, preliminary experiments showed that about 90% activity was lost after 24 hours if preserved with ice; and only a slight decrease of activity (3% per day) at -20°C. Each freeze-thawing cycle resulted in loss of about 24% activity. Preserving BsPFK with substrate F6P, does enhance the stability of enzyme (see section 5.5 for the optimization of experiment conditions). For the experiments discussed in this thesis, the enzyme was stored in a freezer in separate vials as a concentrated solution, and in the PFK assay, it was diluted to the desired concentration (see section 5.6).

As to pH dependence, there has been no direct investigation using BsPFK in activity study. However, EcPFK was studied over a pH range of 6-9 [118]. The enzyme-substrate binding affinity and substrate binding cooperativity and the catalytic rate constant showed apparent pH-dependence. BsPFK resembles EcPFK structurally and qualitatively. In literatures, pH values 7-8.2 are common assay conditions for BsPFK [57,105,113].

3.2 The primary and secondary structure of BsPFK

Amino sequence study of PFK is not only the basis to map the enzyme stereo-structure. It is also helpful to establish the mechanism of the enzymic reaction. Moreover, by comparing the gene and amino acids sequence of PFK from different sources, valuable information is collected which can elucidate the homology relationship between different organisms, and thus the origin and evolution of the glycolysis pathway. For example, a comparison of amino acid sequences [119] showed a marked homology between the N- terminal halves (C-terminal as well) of rabbit muscle PFK and BsPFK. This indicated that RM-PFK, which is about twice as big as bacterial PFK, evolved from a common ancestor of BsPFK via a process of gene duplication and divergence [109,120]. BsPFK is a homotremic enzyme composed of 34-kDa subunits, and each subunit is composed of 319 amino acids. The following figures show the complete amino acid sequence of one BsPFK subunit, and an analysis of its amino acids hydrophilicity. The amino acid sequence of BsPFK, RM-PFK and EcPFK are compared in Appendix.

Amino acid	Code	Hydrophobicity	Content	Amino acid	Code	Hydrophobicity	Content
Arginine	R Arg	-4.5	19	Glycine	G Gly	-0.4	46
Lysine	K Lys	-3.9	18	Alanine	A Ala	1.8	26
Asparagine, Aspartate	B Asx	-3.5	8,20	Methionine	M Met	1.9	5
Glutamine, Glutamate	Z Glx	-3.5	9,20	Cysteine	C Cys	2.5	3
Histidine	H His	-3.2	12	Phenylalanine	F Phe	2.8	7
Proline	P Pro	-1.6	7	Leucine	L Leu	3.8	22
Tyrosine	Y Tyr	-1.3	9	Valine	V Val	4.2	26
Tryptophan	W Trp	-0.9	1	Isoleucine	I Ile	4.5	30
Serine	S Ser	-0.8	12	Hydrophobic/Total residues		165/319	
Threonine	T Thr	-0.7	19	Percent of hydrophobic residues%		51.7	

Table 3.1 Hydrophobicity analyses of BsPFK amino acids

Note: Hydrophobic value is referred to Kyte-Doolittle scale. See Section 1.4 for explanation of protein hydrophobicity and hydrophobic scale. Data in above table are taken from: <http://www.cyber-dyne.com/~tom/Doolittle.html>.

Sequence No.	10	20	30	40
Amino acids	<u>MKRIGVLTSG</u>	<u>GDSPGMNAAI</u>	<u>RSVVRKAIYH</u>	<u>GVEVYGVYHG</u>
Note	Strand A: 3-9	Helix 1: 16-29	Strand B: 33-37	
50	60	70	80	90
<u>YAGLIAGNIK</u>	<u>KLEVGDVVDI</u>	<u>IHRGGTILYT</u>	<u>ARCPEFKTEE</u>	<u>GOKKGIQOLK</u>
Helix 2: 40-45	Strand C: 49-52 Helix 3: 54-57	Helix 4: 79-92		
100	110	120	130	140
<u>KHGIEGLVVI</u>	<u>GGDGSYQOAK</u>	<u>KLTEHGFPCV</u>	<u>GVPGTIDNDI</u>	<u>PGTDFITIGFD</u>
Strand D: 96-101	Helix 5: 103-114	Strand E: 119-124		
150	160	170	180	190
<u>TALNTVIDAI</u>	<u>DKIRDATATSH</u>	<u>ERTYVIEVMG</u>	<u>RHAGDIALWS</u>	<u>GLAGGAETIL</u>
Helix 6: 139-159	Strand F: 163-168	Helix 7: 175-184; Strand G: 188-190		
200	210	220	230	240
<u>IPEADYDMND</u>	<u>VIARLKRGE</u>	<u>RGKKHSIIIV</u>	<u>AEGVGSVDF</u>	<u>GROIQEATGF</u>
Helix 8: 198-210	Strand H: 216-221	Helix 9: 227-238		
250	260	270	280	290
<u>ETRVTVLGHV</u>	<u>ORGGSPATAFD</u>	<u>RVLASRLGAR</u>	<u>AVELLEKKG</u>	<u>GRCVGIQNNQ</u>
Strand I: 242-246; Helix 10: 248-252	Helix 11: 258-276	Strand J: 282-287; Strand K: 290-295		
300	310	319		
<u>LVDHDIAEAL</u>	<u>ANKHTIDQRM</u>	<u>YALSKELSI</u>		
Helix 12: 296-300	Helix 13: 308-316			

Table 3.2 Amino acids of BsPFK

Note: Hydrophobic residues are shown with colour; residues shown in black are those on the subunit surface (using structure files from PDB and analyzed by Cn3D program); totally, 13 α -helices and 11 β -strands are underlined [51,52]; the secondary structural units also consist of 17 β -turns and 3 β - α - β units located at residues 3-37, 96-123 and 188-221.

From the above tables, it can be seen that: On one hand, BsPFK subunit consists of a high percentage of hydrophobic residues, and some of these residues are located on the subunit surface where the oligomeric association may occur. On the other hand, there are a large amount of charged residues on the subunit surface, especial 19 Arg and 18 Lys. According to the three dimensional structure of BsPFK given below, it

can be seen that many of these charged residues lie at or in the vicinity of substrate/effector binding sites.

3.3 Three dimensional structure of BsPFK

Different structure maps were built up for R- and T-state of BsPFK [52,109]. Generally, R- and T-state crystals were formed in the presence of the enzyme activator and inhibitor respectively. Figure 3.2 shows a schematic map of R-state BsPFK [51].

3.3.1 Construction of BsPFK subunits

It is apparent that one BsPFK subunit consists of two domains. The protein chain, starting from N-terminal, first forms the main part of the first domain (Strands A to E and helices 1 to 5) then crosses to domain two through the long helix 6; by following strands F to I and helices 7 to 9, the chain returns to domain one for the strand J and K and helices 10 to 12; the final helix 13 expands to domain two again. Approximately, domain one is made up of residues 1-134 and 254-304; and domain two of residues 135- 254 and 305-319. Both domains have a central α - β - α sandwich unit.

3.3.2 Subunits association

One subunit contacts with two other subunits and forms two interfaces. Taking the upper subunit in map I as an example (the lower one in map II), it forms association by packing helices 1, 3, 11 upon helices 7, 6, 13 in another subunit. The β -band between stands J and K is also in contact with its equivalent across the X-Z plane. The interaction between the subunits shown in map II is relative loose. The main force is the contacts between helix 6 and helix 3 of these two subunits. Along this interface, there is a channel of ordered water molecules between the two β -stands from each subunit.

Besides the force from native subunits, substrates and effectors binding to BsPFK also strengthen the association within the tetramer. From map I, two ADP molecules seem to bridge two subunits shown by binding to the enzyme effector sites. This site is located near the vicinity of C-terminal of one subunit and N-terminal of the other. Three arginine residues Arg 154 from the upper subunit and Arg 21 and Arg 25 from the lower one, bind the diphosphate group of ADP. Residues His 215 and Thr 155 also contribute to bind the ribose ring of ADP. However, this site is specific for

phosphate group and has no specificity for base. So, ATP and AMP do not bind to this site while GDP is one potent activator of BsPFK. In the T-state BsPFK, this site binds to PEP as inhibitor. Moreover, the active site for the cooperative substrate F6P is also made up of residues from two subunits. In map II, the upper subunit in map I interacts with a different subunit and forms two F6P binding sites. That is, F6P links two BsPFK subunits by bridging His 249 from the lower subunit and Arg 162, Arg 243 from the upper one. The Asp 127 from the lower subunit forms a hydrogen bond with the 1-hydroxyl group and drags F6P close to the ATP terminal phosphate group where the base catalyst reaction happens. Thus, 4 linkages in total are formed involving two pairs of subunit association. In addition, in the lower subunit Arg 252, Met 169, Glu 222 and Asp 127 serve to bind the sugar ring of F6P; and Asp 103 involves in binding of Mg^{2+} . The ATP binding site lies in the cleft between two domains of one subunit and is not clearly resolved. It consists of residues of helix 5; and a loose ordered loop between helix 3 and 4; and Arg 171 from the other domain.

The above discussion also agrees well with the fact that:

- 1.) The entire tetramer enzyme is the minimum unit for fully enzymatic active and activity regulation;
- 2.) The ATP inhibits the enzyme activity though a non-allosteric mechanism due to its lack of ability to bind the effector sites;
- 3.) The binding of ATP to enzyme is a slow and rate limiting step in the entire reaction process due to its particular but rather complex contact with the enzyme.

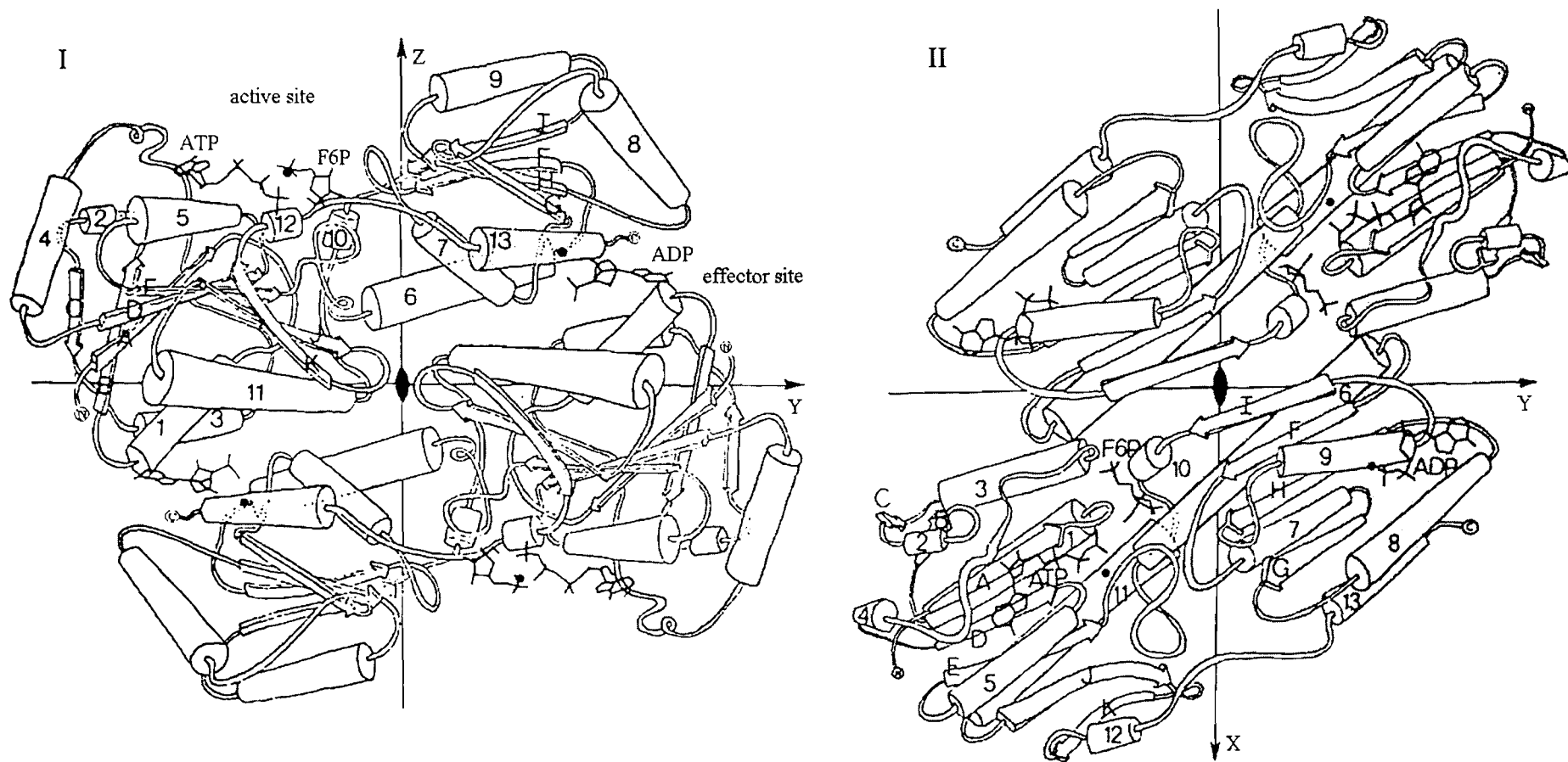


Figure 3.2 A schematic representation of BsPFK three dimensional structure.

Note: map I and map II both show two subunits of the R-state enzyme tetramer, viewed against X and Z axis respectively; the other two subunit lie behind the one shown: map I represents the situation of relative tight interaction while map II shows the other case; α -hilexes are represented by cylinders and β -strands by arrows; related binding sites and enzymetic reactants and effectors are labelled out [51].

3.3.3 An analysis of BsPFK subunit amino acid using helix wheel

On the BsPFK subunits surface, except those residues involved in subunits association and ligands binding, there still are some highly active expose regions where interaction between enzyme and free solvent ligands could possibly happen. As is apparent from the Figure 3.2, helices 4, 5, 8, 9 and 11 have exposed areas. Figure 3.3 is a further analysis of the amino acids within these regions. The applied tool is called helix wheel plot.

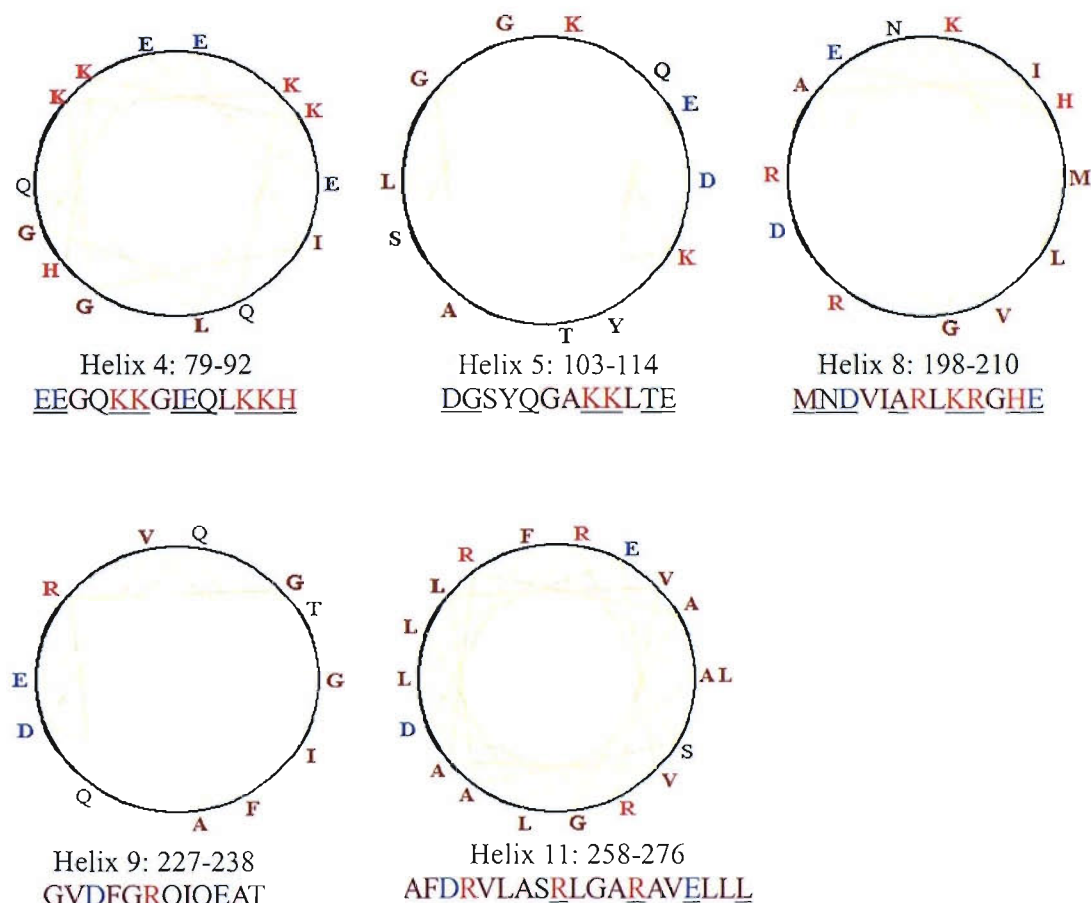


Figure 3.3 Helix wheel plots of exposed helices from BsPFK

Note: hydrophobic residues are shown in **brown**; basic residues in **red**; acidic in **blue**; on the enzyme surface (taken off those residues involved in subunit association), accessible residues are underlined.

From above analysis, after supplying the interaction face for subunit association and active/effector binding sites, the exposed surface area are mainly within several ordered regions. These include helices shown in Figure 3.3 and strands C and K. From the helix wheel plot, helix 4, 5 and 8 consist of many charged residues and helix 9 and 11 include concentrated nonpolar regions. Strand C and K are in close contact with helix 4 and 9 respectively and contain readily charged amino acids. Helix 4 and

strand C are near the N-terminal region where the enzyme chain starts with a few basic charged residues. From the structure map Figure 3.2, helix 4 is far from the active site and seems at one end of the subunit left side. On the other end, helix 8 is near the C-terminal part and on the side of the parallel strands complex. Despite the high percentage of hydrophobic amino acids in helix 9 and 11, the organization of these residues is not well ordered. Some of these hydrophobic residues are mixed with charged and polar residues and face outside; others are buried in the subunits interaction cleft. So, as a well soluble cytosol enzyme, BsPFK has a rather polar surface; there is no obvious and well ordered hydrophobic structural unit which can be commonly found in membrane protein, for example, CCT.

As introduced in chapter one, CCT is a peripheral membrane enzyme which consists of a special membrane binding domain—domain M. Interaction between the hydrophobic residues of domain M and the membrane lipids is one major driven force for membrane—CCT association. Upon binding to membranes, CCT activity is strongly enhanced [31-33]. However, BsPFK lacks a hydrophobic domain. Close interactions between BsPFK and membrane is unlikely unless the overall protein confirmation is adapted. Even if BsPFK could associate with membrane (lipids) to some extent, the interaction is expected to be a loose contact and only occur on the enzyme and membrane surface areas. The enzyme activity might be partly lost because the associated membrane could block the substrate—enzyme binding or result in low accessibility of the enzyme active sites.

CHAPTER 4 Experimental Methods

4.1	Experimental process.....	53
4.1.1	Buffer solution.....	53
4.1.2	Preparation of LUVs.....	54
4.1.3	PFK assay procedure	55
4.1.4	Separation and autoradiography	56
4.2	Optimization of the separation experiment	56
4.2.1	Nature of the problem.....	56
4.2.2	Separation methods.....	57
4.3	Charcoal methods	58
4.3.1	Experimental procedure.....	58
4.3.2	A combined method of active charcoal and TLC	59
4.4	Separation using thin layer chromatography—TLC	59
4.4.1	Selection of TLC plates	59
4.4.2	Visualization of the chemical contained spots on TLC plates.....	60
4.4.3	TLC using DEAE cellulose plates.....	62
4.4.4	TLC using normal cellulose plates	62
4.4.5	TLC using PEI cellulose plates	63
4.4.6	TLC using silica gel plates	63
4.5	Termination of enzymatic reaction	64
4.5.1	EDTA chelator	65
4.5.2	The effect of Copper (II).....	65
4.5.3	Denature PFK by low pH	66

The most widely employed PFK assay protocols are continuous and indirect methods, applying spectrophotometer or fluorometry [111,121]. That is either coupling the formation of F1,6-BP to the oxidation of NADH, using auxiliary enzymes aldolase, triose phosphate isomerase, and α -glycerophosphate dehydrogenase or coupling the production of ADP to pyruvate kinase and lactate dehydrogenase reactions, which regenerate ATP [122,123]. Relative reactions are depicted in Figure 4.1.

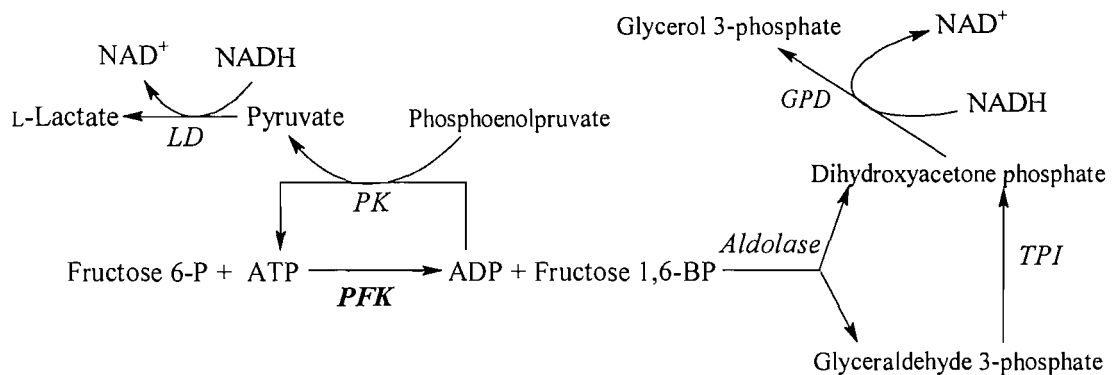


Figure 4.1 Coupled assays of PFK by linking FBP or ADP to the oxidation of NADH
 Auxiliary enzymes: Aldolase (E.C 4.1.2.13); TPI, triose phosphate isomerase (E.C 5.3.1.1); GPD, Glycerol 3-phosphate dehydrogenase (E.C 1.1.1.8); PK, pyruvate kinase (E.C 2.7.1.40); and LD, lactate dehydrogenase (E.C 1.1.1.27).

Due to its simplicity, rapidity and commercial availability of the auxiliary enzymes and other chemicals involved, perhaps this is also by far the most commonly used spectrophotometric assay technique. However, as several other enzymes and substances are introduced in the assay system, more complex interactions between enzymes and substrates or, in our case, between enzymes and lipid membranes are to be brought in as well. Some of these interactions may interfere with the catalysis or even distract the reaction from the desirable way. For instance, phosphoenolpyruvate, one reactant for pyruvate kinase, is a potent allosteric inhibitor of PFK [121]. Another problem is that, to find out the possible sources of bursts and lags in the progressing curves and to collaborate these factors to a proper condition, are not an easy job. Thus, intensively and systematically study is usually required to achieve the optimum assay conditions, under which PFK is expected to perform at maximum speed. Unfortunately, compromises are inevitable since an optimum condition for one enzyme is not always the one for the other(s) [124]. Another continuous assay protocol is to measure the H^+

production, utilising high sensitive pH metre [111]. This method does not require auxiliary enzymes, and the matrix of reagents is relatively less complex, but it is limited by the sensitivity of the pH metre.

In our study, the main aim is to study the interaction between PFK and lipid vesicles. So, the PFK reaction is studied under constant pH and temperature but with different vesicle environments: without lipid vesicles, with vesicles, and with vesicles having different lipid compositions. A proper assay incubation time is also important to give valid measurements but not too long to pass the initial reaction term. (See footnote N1 for more details.) The appropriate ratio of vesicles versus PFK is also required to adjust to provide enough interactions between PFK and vesicles but still leave certain potential for further modulation (by changing the lipid composition and then creating more activity binding sites). Extensive preliminary experiments were undertaken to look for optimized assay conditions which include: a suitable reagent to stop the enzymatic reaction; separation of the radio-labelled substances; proper PFK and vesicle concentrations and reaction incubation time. The results of these experiments will be discussed in next chapter. The experimental process will be introduced in this chapter first. It is helpful to understand the discussion of following sections.

4.1 Experimental process

4.1.1 Buffer solution

50mM Tris-HCl (pH 7.4 under 37°C), is used as buffer solvent, 5mM MgCl₂, 5mM (NH₄)₂SO₄, are added to give proper ion strength and essential divalent cations, Mg²⁺. Basically, this solvent was prepared at laboratory condition and adjusted to a pH which will give desired condition—pH 7.4 under assay temperature. For this aim, buffer pH variation following temperature was examined and listed in Table 4.1. Unless stated otherwise, this buffer solution was used to prepare all other reagents.

Temperature/°C	18	20	25	30	33	37	dpK/dT
pH—first run	8.15	8.06	7.91	7.74	7.56	7.4	-0.032
pH—second run	8.13	8.05	7.84	7.6	7.53	7.4	K ⁻¹

Table 4.1 Buffer pH at different temperature

4.1.2 Preparation of LUVs

Materials: DOPC, DOPA, DOPE, OA, lyso-OPA, and DOG, were purchased from Avanti lipid, either in chloroform solutions or in solid form. In some case, suitable dilution was needed before the following procedures. For the full name of the lipids, see Glossary and Abbreviation in appendix.

Lipid mixtures in chloroform solutions were transferred through a 100 micro-litre syringe to 2ml amber glass vials and dried under nitrogen gas and evaporated under vacuum to remove trace residual chloroform. 200µl water was added and vortexed well with the dried lipids; then lyophilized again for at least 4h. Buffer was added and the mixtures vortexed for 10 min, plus 20 min resting. Then they were sonicated for 20 min and rest for 30 min. Four freeze-thaw cycles were followed using liquid nitrogen and a water bath. In each cycle, vesicles were thawed at 37°C for 10 min and resting at room temperature for 20min. After the last thawing, vesicles were stored in freezer and used within at most 4 weeks after preparation. A Coulter N4 Plus Particle Sizer was used to determine the mean vesicle diameters. When using these vesicles in enzyme assays, they were rested about one hour to thaw and further diluted to 2.5mM. The stated amount of the diluted vesicles solvents were then added in assay mixture. The final lipids concentration of the total lipids was 0.5mM.

Mainly 5 systems of lipid vesicles were studied; they were DOPC/DOPE, DOPC/OA, DOPC/lyso-OPA, DOPC/DOPA, and DOPC/DOG. For each vesicles system, the ratio of each above two lipids was changed and 7 compositions of one vesicle system were experimented at one time. But the total lipid concentration was kept at constant

(0.5mM in final assay medium). Table 4.2 list compositions of DOPC /DOPE vesicles and the amount needed in preparation. For composition of other vesicle systems, see Appendix 2 for details.

Compositions*	10:0	9:1	8:2	7:3	6:4	5:5	4:6
Amount of DOPC / μ l	100	90	80	70	60	50	40
Amount of DOPE / μ l	0	18.9	37.9	56.8	75.7	96.7	113.6
Total lipids	2.544 mmol in 167.6 μ l buffer						

Table 4.2 Lipid composition of DOPC/DOPE vesicles

Note: Compositions* refer to the molar ratios of DOPC to DOPE, which were preserved as chloroform solution at concentration of 20 mg/ml and 10 mg/ml respectively.

4.1.3 PFK assay procedure

Materials: ATP, F6P, and PFK from *Bacillus stearothermophilus* were purchased from Sigma™; all were in powder form. γ -³³P-ATP was from Amersham Biosciences Limited™. Half life of ³³P is 25.4 days. Different volume of normal ATP was used to dilute the concentrated radioactivity ATP and give 4×10^4 — 8×10^4 c.p.m activity in a single assay. The volume of normal ATP needed was calculated, according to the decay of radioactivity. That is to say, fresh radio-ATP solution was prepared each time just before using it in enzyme assays. PFK was dissolved in F6P solution and separated into 2ml vials. They were then kept in freezer till usage.

Assay conditions were: 50mM Tris-HCl buffer, pH 7.4, 37°C, MgCl₂ 5mM; (NH₄)₂SO₄ 5mM; F6P 1.0mM; ATP, 0.1mM γ -³³P-ATP (3.6-7.2Ci/mol); the final assay volume was 50 μ l. For different batches of BsPFK, the amounts of enzyme used in each assay were adjusted to give a desired activity (see section 5.5 for optimization of assay conditions). When vesicles were used, 3 parallel assays were tested for each lipid composition. In total, for each vesicle system, there were 3x7 assays with vesicles (7 different lipid compositions) and 3 assays without vesicles as controls. The concentration of the total lipids and PFK; the reaction incubation period; and the reagent used to stop the reaction

flux were examined and fixed for PFK assays. The final conditions will be given in chapter 5.

4.1.4 Separation and autoradiography

After the PFK reaction was stopped, the assay mixture was loaded on TLC plates or treated with charcoal; the separation was then developed. The spots which contain radioactive chemicals (ATP and F1,6-BP) were visualized by using reagents to be discussed in section 4.4.2 or by autoradiography. In the latter case, autoradiography films were enclosed with TLC plates in a cassette and exposed overnight with dry ice; they were then treated with CEATANK developer solution and CEAFIX fixer. The black spots shown on those films were corresponding to radioactive spots on TLC plates. The indicated spots were then cut down from the plates and inserted into scintillation vials. A scintillation fluid was added and radioactivity was determined.

4.2 Optimization of the separation experiment

4.2.1 Nature of the problem

After the enzyme assays were terminated, separation of two radio-labelled substances (product FBP and unreacted ATP) was needed. Without a satisfactory separation, it is not possible to obtain an accurate measurement of enzyme activity, and the optimization of assay work-up procedures and other reaction conditions depend critically on a reliable separation. In addition, a clear separation is helpful to judge whether the termination is achieved or not; and to estimate the progress of the reaction before measuring the radioactivity.

As mentioned previously, assays of PFK activity that are more widely reported in the literature are based on continuous spectrophotometric or fluorometric measurements, which usually do not require a reaction termination step or the separation of products and reactants. Since such methods are not studied to our purposes, the following three main problems had to be considered before attempt the separation.

(1) In PFK reaction, the γ -phosphate of ATP is transferred to F6P to form F1,6-BP. The reaction mixture is very complex and the compounds that need to be separate (F1,6-BP

and ATP) are present at very low concentrations. In addition, the presence of high concentration of buffer ions (Mg^{2+} , NH_4^+ , Cl^- etc.) is undoubtedly the biggest problem for effective separation [125]. More particular, in one 50 μ l assay, the total added ATP (3.6-7.2Ci/mol) is 5.0 nmol and the F1,6-BP produces, is less than 1.0 nmol^{N1}. As to the measurable radiolabelled ATP and F1,6-BP, the amount is even lower. The medium also contains considerable amount of protein and lipids. In addition, F6P and ADP exist as the same level as F1, 6-BP and ATP, and they strongly interfere the separation.

(2) There are many samples to be separated. For each vesicle system, there are 24 identical samples to cover 8 lipid composition points. This means that effective but time-consuming separating techniques, which are suitable for single or small number of experiments, are not suitable here. However, one advantage of using thin layer chromatography is that many samples can be treated parallel. Techniques of thin-layer chromatography—TLC, are shortly introduced in section 4.4.

(3) Separation procedures should be as simple as possible. The half-life of phosphorus 33 is 25.4 days and the activity decay is about 3% per day. In order to obtain an accurate measurement and more importantly, to limit radiation contamination to a level as low as possible, a simplified assay protocol is helpful.

4.2.2 Separation methods

Based on above discussion, thin layer chromatography was chosen to attempt the separation. Firstly, a solvent system (isopropanol/acetone/ammonia/water: 3/2/1/4, solvent 1 in Table 4.3) was used, but this gave poor results. Then a more systematic study of TLC was undertaken. This involved testing 4 types of TLC plates (plates coated with different sorbent materials as stationary phase, see section 4.4), and a range of solvent systems as mobile phase. Since substances like nucleotides and their derivatives are strongly absorbed on active charcoal, two methods based on charcoal

N1: For an enzymatic reaction, if the substrate concentrations are well above the enzyme saturating concentrations, the reaction rate remains constant at the beginning stage. In present study, reaction conversion is controlled below about 20% to make sure that the reaction rate is unchanged.

were also studied [126,127]. Experiments were carried out first with non-radioactive compounds and then the best (promising) separation results were selected and checked in PFK assays with radiolabelled compounds. Samples used in these two circumstances were prepared differently. For the latter study, autoradiography was used to locate the spots (strands) of F1,6-BP and ATP. As to experiments using non-radioactive chemicals, after each experiment, distinct spots of ATP, ADP, F1,6-BP, and F6P were visualized by spray reagents (see section 4.4.2 for details). However, this method was far less sensitive than autoradiography. So, more concentrated samples were applied on TLC plates. As long as a reasonable observation (separation and visualization of spots) was achieved, other conditions like buffer ions and pH value were kept same as in enzyme assays.

4.3 Charcoal methods

Active charcoal, is a selective absorbent for nucleotides and derivatives, and widely used in research related to the synthesis and metabolism of nucleotides [128]. Theoretically, it could be used in our study if the charcoal absorbs ATP effectively and leaves the F1,6 BP in solution.

4.3.1 Experimental procedure

Active charcoal was obtained from Sigma, and was washed with 0.12M HCl twice and then suspended in 0.12M HCl solution (5% w/v). After a vigorous shaking, 100 μ l of the above suspension was added to the stopped reaction mixture. The whole mixture was then thoroughly vortexed and allowed to rest for 10 min. The mixture was then centrifuged at 14000 r.p.m until the charcoal was precipitated. 100 μ l of the supernatant was measured and added in scintillation vials, and radioactivity was counted. This method is referred as method A hereafter. In addition, 50 μ l above supernatant was visualized on silica TLC plate and chromatographed; radioactive chemicals were labelled by autoradiography and counted in scintillation. This provided an independent verification of method A. However, method A is not potent separation method.

4.3.2 A combined method of active charcoal and TLC

A fairly simple technique has been reported [126] for the separation of Pi, P₂IPi, from ATP. In principle, it can be a possible method to explore enzymic reactions. A suspension was made up of 10% acid-washed active charcoal and 90% ethanol, and shaken well before using. Charcoal spots of 20µl suspension were formed at the origin part of TLC plates through a pipette tip. The plates were then dried in a fume hood before loading on different volumes of assay mixture. The plates were finally developed and results checked using autoradiography. This method is called method B hereafter. It was found later that ATP and F_{1,6}-BP could not be separated effectively using this method because charcoal absorbs these two chemicals unselectively (see section 5.4.2).

4.4 Separation using thin layer chromatography—TLC

There are a number of the advantages of TLC, in terms of its simplicity, time saving, commercial availability, and ease with which it can be adapted to specific requirements. A discussion of these factors as well as the theoretical background like the partition between the stationary phase and mobile phase, and the physical parameters of solvent system, are beyond the scope of this thesis. However, a brief introduction of the properties of each type of plates is helpful for a better depiction.

4.4.1 Selection of TLC plates [129,130]

The most common sorbents in pre-coated TLC plates are Silica gel, Aluminium, Cellulose, and Polyamides. Separation on these plates behaves extremely differently, even though they are treated in the same way and applied to separate same chemicals. Generally speaking, silica gel coated plates are the most widely used because this type of plates is easy to be modified to meet with different requirements. As to the specificity of above mentioned sorbents, the situation is: inorganic stationary phase like Silica gel and aluminium are used mainly with lipophilic (hydrophobic) compounds; cellulose, on the other hand, is an organic medium and mainly used to separate hydrophilic reagents such as sugars, inorganic ions, and nucleotides. The

behaviour of the latter sorbent is determined by its water content, which interacts with the cellulose cover through hydrogen bonds. Thus, partition between this water and the developing solvents dominate the separation of target chemicals. For a special task, the native sorbents can be further treated by different methods, particularly by changing the water content and chemical modification reactions. Two examples of such derivatives of cellulose are DEAE (diethylaminoethyl) cellulose formed by reaction; and PEI (poly-ethylenimine) cellulose. Both are strong basic anion exchangers. In the literature, many clear separations of sugar or/and nucleic acid derivatives have been reported using DEAE and PEI cellulose plates [131-134]. The above three cellulose plates and Silica gel plate were tried to obtain the separation of the assay mixture in present study.

4.4.2 Visualization of the chemical contained spots on TLC plates

Several reagents were tried to visualize distinct spots of F6P, FBP, ATP and ADP. (See Table 4.3 for more details, the number of each reagent list in this table is also the reagent referring number.) Basic experimental procedure was to apply the reagent on developed TLC plates and treat the plates in an oven (cellulose plates) or with a hair drier (silica plates). Except for the DEAE cellulose plate, all other plates were pre-covered with fluorescent material, so the spots of ADP and ATP are visible directly under a UV lamp. As to DEAE plate, after running TLC, the plate was cut into halves, the half with ATP and ADP was dipped into fluorescein/ethanol 2% solvent and spots labelled using a UV lamp; the half with F6P, FBP on it was treated with spray reagent. For a detailed discussion of chosen of spray reagents for visualization in TLC, please refer [130,135].

Reagent 3 were chosen and used routinely as a spray reagent because it was applicable for all types of TLC plates and easy to prepare. Reagents 1 and 2 are specific sprays for phosphate and derivates; the advantage of these reagents is to show spots with different colours [135]. (Plates give a light blue background upon drying.) However,

cellulose plates cannot be subjected to high temperature, and some reagents (especially those prepared with acid), cannot be used with these plates. For example, when reagent 1 was used, cellulose plates are easily charred and giving a very deep colour; consequently spots corresponding for compounds were undetectable.

Spray reagents & preparation	Observation and procedure
1. Molybdenum blue: 1.3% MoO ₃ in 100ml 4M H ₂ SO ₄ .	Only on silica plate; four substances show blue color, without obvious difference after treat the plate in an oven (about 100°C) for 5 minutes.
2. Ammonium molybdate: 1g salt dissolved in 8ml H ₂ O+ 3ml 7% HClO ₄ , filled up to 100ml with acetone .	On silica plate: F6P dark blue; FBP grey blue; ATP yellow; ADP light yellow; at RT overnight or in an oven for 10 min; on cellulose plates: only F6P shows up on blue back ground.
3. Sulphuric acid: 2% in methanol.	Spots of FBP and F6P show brown color after charring the plate above 200°C; ADP, ATP weak brown.
4. Silver nitrate [135]	Only F6P shows black color on brown background.
5. Ninhydrin: 0.2g in 100ml methanol.	F6P brown (red if treated for a shorter time); FBP dark yellow; ADP, ATP not visible. The whole plate turned into pink due to the ammonia ion in buffer.
6. Nitric acid	No obvious effect.

Table 4.3 Tested spray reagents to visualize spots on TLC plates

Note: Except reagents 1, 2—for phosphate; and 4—for sugars; other spray reagents are commonly used in visualization procedure in TLC; there is no particular reason to choose them. Reagent 3 could give a better effect if more concentrated sulphuric acid are applied. However, as the destructive procedure (heating and charring) used this reagent is not suitable to use this reagent in the final enzyme assay experiment to locate the strands of ATP and F1,6-BP. That is, the charred products usually fluoresce, which will cause very strong quenching in scintillation measurement [130].

4.4.3 TLC using DEAE cellulose plates

Because the sample spots were easily spread on cellulose plates during loading, more concentrated solution were prepared (to reduce the amount of loading water) and give a suitable size of sample. Otherwise, after the plates are developed, the spots carrying the chemicals will spread even worse. A number of hydrochloric acid solutions were tried to attempt the separation. The acid concentrations were gradually increased. Typically, the solvent front moved up 8cm after developing for 20 minutes; then the spots of each compound were located using the processes described in section 4.3.2.

Concentration of HCl/(M)	Rf of F6P	FBP	ADP	ATP	Note
0.015	0.49 of 7.8cm		0.33	0.10	Spots spread as inverse triangle shape; spots of FBP were slightly darker than background and blurred.
0.030	0.62 of 8.0cm		0.58	0.13	
0.045	0.85 of 7.5cm		0.84	0.26	

Table 4.4 Solvent systems used in TLC on DEAE cellulose plates

Note: The third solvent (0.045M HCl) gave the best separation and was checked in a radio-assay, result see section 5.3.

4.4.4 TLC using normal cellulose plates

Quite a few solvent systems were tested using this type of plate; Table 4.5 lists those which gave relatively better results. Other solvent systems like: isopropanol/ammonia/water: 7/1/2; ethylacetate/acetone/water: 7/4/1; methanol/ammonia/water: 4/1/5; butanol/pyridine/water: 6/4/3 [130,136,137], were also tested according to different literatures, but gave poor results due to the similar mobility of substances (particular those of ADP, ATP, FBP). For all tests, TLC plates were developed for 30 minutes to get 6-7.5cm of solvent front. Spots of nucleotides were marked under a UV lamp; those of sugar phosphates were visualized using spray reagent 3 (Table 4.3). Although spots of FBP were unclear, very light yellow spots appeared near the position

close to F6P. Spots of ADP and ATP spread and streaked a lot (from the start line to top of spots); so R_f values in Table 4.5 were calculated using the distance between the top of the spot to base line.

Solvent system	Solvent front/cm	R_f of			Distance from F6P and ATP
		F6P	ADP	ATP	
Methanol/water/Formic acid 8 / 0.5 / 1.5	7.5	0.52	0.24	0.20	2.0 cm
Methanol (96%)	7.0	0.54	0.14	0.07	2.0 cm
Methanol / formic acid 8 / 2	6	0.38	0.08	0.08	1.7 cm
Methanol/ water 8 / 2	6	0.30	0.17	0.15	Poor separation
Methanol + HCl (conc.) 9ml + 0.3ml	7.5	0.67	0.24	0.29	3.0 cm

Table 4.5 Solvent systems used in TLC on normal cellulose plates

Note: The last solvent system: methanol/HCl (conc.) gave the best separation and was checked in a PFK radio-assay, result see section 5.4.

4.4.5 TLC using PEI cellulose plates

For this strong basic anion exchanger sorbent, solvents of alkali metal salts are common mobile phase. 0.75M, 1.5M and 2M LiCl were tested [131,132]. TLCs were run in the same direction as in pre-treated process.^{N2} Solvent front was developed about 8cm after 20 minutes' running. Due to the low mobility of all four substances, results were poor.

4.4.6 TLC using silica gel plates

Compared with plates coated with cellulose sorbents, silica gel plates are easy to handle. They withstand relatively high temperatures and the original spots do not spread a lot during sample loading. So, a wide range of solvent systems was tested using silica gel plates. Table 4.6 lists some of these systems, in which solvent 1 and 2

N2: Plates were pre-treated with water or 0.2M LiCl solvents as usually described in the literatures for this particular plate—run TLC without loading any samples.

gave promising separation, and were further tested in radio-labelled assays. After running the TLCs, spots of nucleotides were located with a UV lamp and spots of sugar phosphates were visualised with spray reagent 3; this was done by dipping the dried plate in reagent solution and heating the plates with a heating gun to a high temperature—brown spots showed up shortly. Spots of ADP and ATP also showed weak yellow on white background upon heating.

Solvent system volume ratio	Solvent front/cm	Rf of				Notes
		F6P	FBP	ATP	ADP	
P/A/H: 5/1/4	9.0	0.31	0.2	0.2	0.31	A: ammonia; P: pyridine; I: isopropanol and H: water. Pyridine quenches UV light, use spray reagent 3 to locate spots.
P/A: 9/1	Less polar, $R_f = 0$					
I/ P/A/H: 3/2/1/4	9.1	0.38	0.29	0.21	0.44	
Above solvent systems referred to reference [138].						
M/A: 5/5	6.7	0.45	0.22	0.15	0.22	M: methanol; T: acetone.
M/A/H: 5/2.5/2.5	7.1	0.63	0.55	0.32	0.39	
M/A/H: 5/1/4	8	0.80	0.73	0.40	0.55	
T/A/H: 5/1/3.5	7.9	0.41	0.19	0.09	0.18	
Above solvent systems referred to references [136,139].						
I/Pr/A/H: 3/1/1/5	8.6	0.58	0.52	0.30	0.50	Pr: propanol; D=distance between spot centres of ATP and FBP
A/I/H: 1/5/4	6.9	0.55	0.51	0.36	0.54	
A/Pr/H: 1/5/4	10.5	0.57	0.50	0.36	0.54	
I/T/A/H: 3/2/1/4 solvent 1	7.6	0.49	0.46	0.24	0.39	D = 1.7cm
T/A/H: 5/1/3.5	7.9	0.41	0.19	0.09	0.18	
A/T/H: 1/4/5 solvent 2	10.6	0.75	0.72	0.53	0.70	D = 2cm

Table 4.6 Solvent systems used in TLC on silica gel plates

4.5 Termination of enzymatic reaction

Before the PFK activity assay could be examined, the study of reaction termination (to stop the PFK assay at desired time points) was required. There are several ways to denature proteins such as heat; using detergents, urea and guanidine; and adding

hydrogen bonding organic solvents to assay mixture. Taking into account the difficulties faced in following steps, such methods as addition of reagents like high concentration of 8M urea or 6M guanidine; and large volume of organic solvents were not studied, because they would bring more interference to the separation task. Heat is obviously the simplest way to denature proteins. But PFK from different sources, have different capability to stand with extreme environment such as high temperature and high acidic conditions. PFK from some bacteria has a temperature optimum of 93°C and maintain 60% activity after treated at 100°C for two hours [140]. To BsPFK, as discussed in chapter 3, the optimal function temperature was 60°C [103]. What is more, ATP and sugar phosphate could be hydrolyzed under high temperature. So, to stop BsPFK reaction by heating is not practical for our study.

4.5.1 EDTA chelator

Divalent cations were required for PFK activity. Mg-ATP complex was in fact, the real active substrate in the reaction pathway. High concentration of EDTA (normally 50mM, depended on the ATP and buffer condition) was used as discontinuous PFK assay method [112,141], to stop the reaction output. In our experiment, 27 and 80mM EDTA (final concentration), were tried (results see section 5.1). From the spots of product corresponding to F1, 6-BP, it could be drawn that both above amount of EDTA were not to stop the reaction completely. This may be explained by the residue enzymic activity left in absence of divalent cations and/or the enzyme activation by buffer ammonium ions present in a fairly abundant amount.

4.5.2 The effect of Copper (II)

Heavy metal salt is another way to denature proteins. Cu^{2+} was capable of irreversibly inhibiting enzyme function by reacting with their sulfhydryl groups. The Cu^{2+} inhibition of PFK from various sources was studied in details [112], including BsPFK, which was shown to lose most of activity in presence of Cu^{2+} at a concentration above 0.5mM. In our experiment, final concentration of 1mM CuCl_2 was used to attempt terminating of the enzymatic reaction. Results see section 5.1.

4.5.3 Denature PFK by low pH

As introduced in chapter 2, PFK require the entire tetrameric structure for full active [55]. In addition, high hydrogen ion concentration will destroy hydrogen bonds on protein surface and result in protein denature. In present study, 10mM HCl (final concentration) was tried to denature PFK and consequently stop the reaction flux.

Chapter 5 Optimization of TLC Separation

& assay Conditions

5.1	Termination of the PFK reaction	68
5.2	Separation using charcoal	70
5.3	TLC on cellulose plates	73
5.4	TLC on silica gel plates	74
5.5	Assay condition optimization	77
5.6	Final experimental conditions	81

In this chapter, the proper way to stop the PFK reaction is discussed first. Then the optimized separation procedures are given. Finally, assay conditions such as reaction period and enzyme concentration are studied and adjusted to give a desired conversion. Since, preliminary study, BsPFK activity was shown to increase slightly in the presence of lipid vesicles. This fact was taken into consideration when adjusting assay conditions.

Unless specially stated, the term concentrations used in this chapter, were referring the final concentrations (of reagents or ligands) when the reaction had been stopped or inhibited. For example, “HCl 10mM” means, adding HCl to the assay mixture and the final concentration of HCl is 10mM. Assays stopped by EDTA are referring to start the reaction and then stopped it by EDTA; while assays inhibited by EDTA means to add EDTA before “start” the reaction. If EDTA could inhibit PFK effectively, there should be no product of radio-labelled F1,6-BP showing on autoradiographies of TLC plates. And thus, EDTA could terminate the reaction flux at the point needed.

5.1 Termination of the PFK reaction

Three reagents were investigated to terminate the enzymatic reaction. These were EDTA (27mM and 80mM), CuCl₂ (1mM) and HCl (10mM). The rationale behind the choice of these reagents is discussed in section 4.5. Because during the course of these experiments, the separation had not been achieved, a testing solvent (0.7M NH₄Cl) was used to “separate” the assay mixture. As shown in the following figures, the separation in these experiments was very poor, but it is possible to tell whether the respective reagent could terminate the reaction.

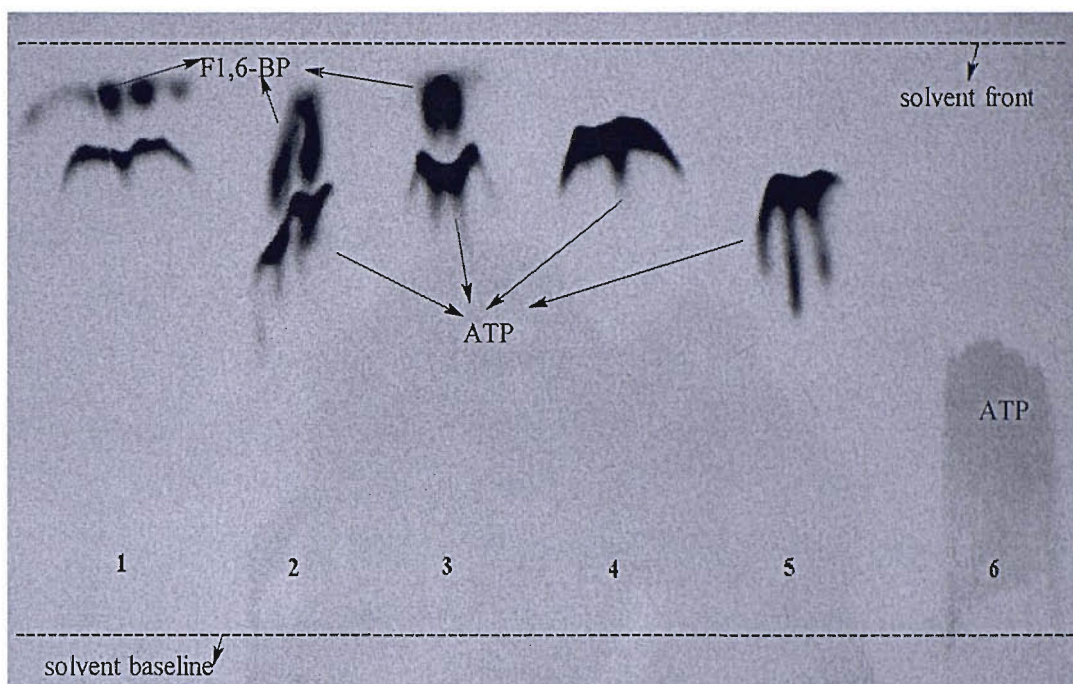


Figure 5.1 Study of PFK assay termination by EDTA solution

Notes: Panel 1, assay stopped by 27mM EDTA; panels 2 and 3 assays inhibited by 27 and 80mM EDTA respectively; panels 4 and 5, ATP added in 27 and 80 mM EDTA solution respectively; panel 6, only ATP buffer solution.

Figure 5.1 shows the results of experiments using EDTA to stop the PFK reaction. The concentrations of EDTA solution were much higher than the concentration of Mg^{2+} (5mM), which is essential for PFK activity. However, there still are very dark spots representing the radioactive product F1,6-BP showing up in panels 2 and 3. So, EDTA could not stop the reaction effectively. In literature [112,140], the reaction flow (PFK and auxiliary enzyme reactions) was stopped by 50mM EDTA, and the product of PFK reaction (F1,6-BP or ADP) was coupled to the oxidation of NADH (See section 4.5). The reason why EDTA did not work in our experiment could be the different enzymes and different assay protocols used in present study. In addition, by comparing the radiochemical spots of different panels in above figure, it can be seen that the spots in panels 1 to 5 (with EDTA) are more compact than that in panel 6 (only ATP in buffer without EDTA). This suggests that though EDTA solution cannot stop the enzymatic reaction effectively, it may help to separate ATP from F1,6-BP.

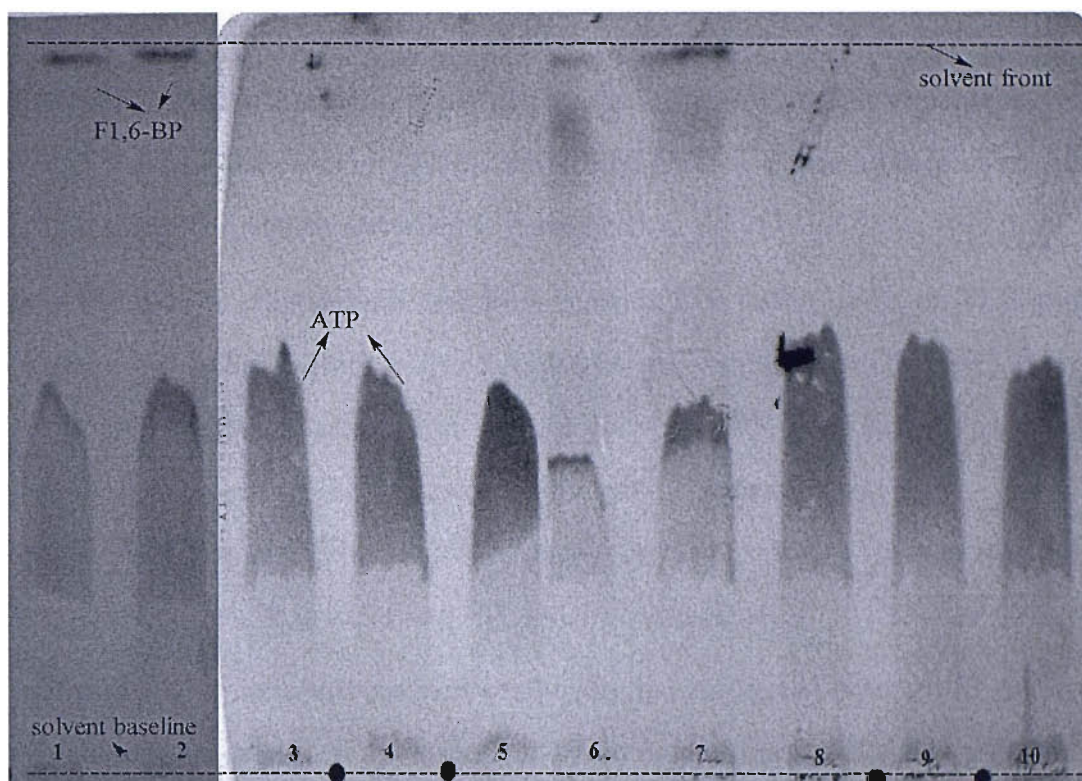


Figure 5.2 Study of PFK assay termination by CuCl_2 and HCl solution

Notes: Panels 1 and 2, assays stopped by 10mM HCl solution; panels 3 and 4, assay inhibited by 10mM HCl solution; panel 5, ATP in 10mM HCl solution; panels 6 and 7, assay stopped by 1.0mM CuCl_2 solution; panels 8 and 9, assay inhibited by 1.0mM CuCl_2 solution; panel 10, ATP in 1.0mM CuCl_2 solution.

The above figure shows the results of experiments using CuCl_2 or HCl solution to stop the PFK reaction. By comparing panels 1 and 2 with 3 and 4; and panels 6 and 7 with 8 and 9, the spots corresponding to product F1,6-BP are disappeared in panels 3, 4, 8, and 9, implying that both CuCl_2 and HCl solution can stop the PFK reaction properly.^{N1} However, these experiments were checked again after the separation of ATP from F1,6-BP were achieved later (see 5.4.4).

5.2 Separation using charcoal

Section 4.2 described the experimental processes using active charcoal to separate ATP and F1,6-BP. Figure 5.3 shows the result of method B and Figure 5.4 shows the

N1: Though there was no spot corresponding to F1,6-BP shown up, the plates (containing the region corresponding to F1,6-BP) were cut and the radioactivity measured in scintillation, the activity was comparable with background. This indicated that there is no radioactive chemical in these region, that is PFK is completely inhibited and no F1,6-BP produced.

double check result of method A. Studies on method A and B came to very similar conclusions, namely that active charcoal absorbs ATP (ADP) on the expense of F1,6-BP, and it cannot absorb ATP (ADP) completely. Method B was studied using silica gel TLC plates and will be discussed in detail here.

1.) In Figure 5.3, elliptical-labelled areas indicate UV visible spots on TLC plates visualized by UV light. (Both ATP and ADP spots are visible under UV light.) There is no radioactivity from these zones, so they are possibly ADT spots. Below these labels, there are diffuse zones that show low radioactivity in panel 1, 2, and 3. They are possibly ATP lost from the charcoal spots (very dark spots). These suggest that charcoal is not capable to absorbing ATP (ADP) completely.

2.) In assay 1, as the given reaction conditions, the amount of product (F1,6-BP) in theory should be enough to be visualized by autoradiography, but there is no radio-spots corresponding to F1,6-BP shown up in Figure 5.3. In assay 2, PFK concentration is increased (and thus the amount of radioactive product F1,6-BP), there was no observation of a significant increase of F1,6-BP radioactivity. This indicated that F1,6-BP was absorbed on charcoal as well.

3.) However, if the total radioactivity was increased in assay 3, the increase of radioactivity is apparent within all there regions (charcoal spot, ATP zone, and F1,6-BP spot). This implies that the total absorbance ability is limited.

4.) In addition, panel 4 and 5 show the cases when only ATP is applied on TLC plate. It seems that, without the disturbance from sugar phosphates, PFK, and HCl (60mM, reagent to stop the reaction), the ATP absorbance upon charcoal is better than that in assay 1, 2 and 3.

5.) In methods A (separation using charcoal suspension), 50 μ l clear suspension was taken from the total of 150 μ l assay/charcoal suspension mixture and the radioactivity was then counted. However, even assuming all the radioactivity came from F1,6-BP, i.e. ATP was completely isolated, it was too low to give a reasonable high radio-activity (the radioactivity of product F1,6-BP should give a much higher radioactivity

at the experimental condition). That is to say, charcoal absorb F1,6-BP. When method A was double tested (in TLC and autoradiography), this is more obvious. When 50 μ l above liquor was concentrated and loaded on cellulose TLC plates (See panel 2 and 5 in Figure 5.4), there are no radioactive spots. This suggests that most radioactivity remains on charcoal.

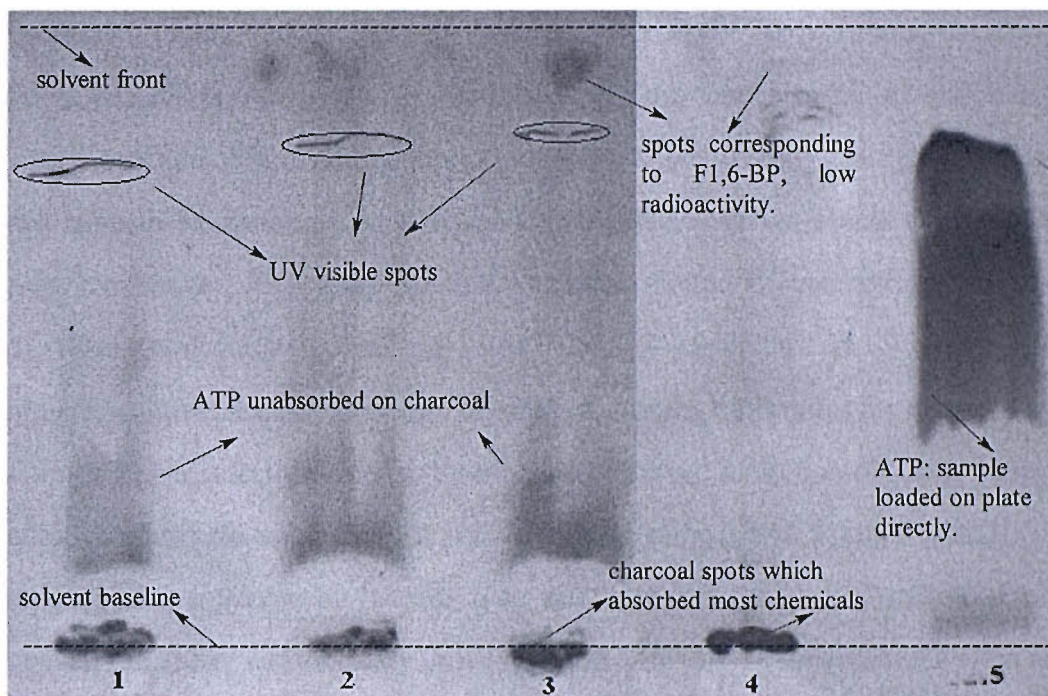


Figure 5.3 Autoradiography of separation result using charcoal-TLC method

Notes: assay 1, assay using low concentration of PFK; assay 2, assay using high concentration of PFK (all other conditions were same as assay 1, so more product of F1,6-BP yielded than assay 1); assay 3, PFK concentration kept same as assay 1 but higher radioactive ATP applied (total concentration were same in assay 1, 2 and 3, while assay 3 used 7.2Ci/mol radioactivity compare with 3.6Ci/mol in assay 1 and 2); panel 4, only ATP; samples were all loaded on charcoal spots except panel 5, in which ATP solution was loaded on TLC plate directly; chromatography was developed using testing solvent (0.7M NH_4Cl) and more than one plates were used for these experiments, two auto radiographies which showed clear results were edited in this figure.

From above, the use of active charcoal was not effective for completely removing the nucleotides without appreciable lost of F1,6-BP. Similar problems were discussed in [126] too; in which the low concentration of reagents was considered as one cause. In fact, in comparison with the assay condition in [126], the amount of radioactive reagents used in present study was even lower.

5.3 TLC on cellulose plates

Figure 5.4 is an autoradiography of three types of cellulose plates used in present study. As can be seen, the spots of each radiochemical stretch a lot, leaving ATP and F1,6-BP undetectable. Overall, separation on these plates is very poor; and the positions of spots is quite different from those achieved in previous experiments (Experiments using unradiolabelled chemicals. Compare with section 4.4.3). One possible answer for these differences is that the substances to be separated are in different medium. Since cellulose plates absorb solvent easily, samples loaded on plates have to be concentrated unless a much higher total radioactive are used. In present experiment, 55 μ l assay mixture was concentrated (frozen dry) to about 10 μ l and 1-3 μ l concentrated mixture was then loaded on TLC plate before chromatographed. So, concentration of other chemicals, buffer ions for example, are a few times higher than that used in experiments described in section 4.4.3. In literature, a radiotracer enzyme assay for PFK was developed using α,β,γ - ^{32}P labelled ATP [142]. Sharp separation was achieved on both cellulose plate and PEI cellulose plate. However, the buffer and auxiliary ion (Mg^{2+} and NH_4^+ etc.) concentrations were more than 10 time lower than that using in present study.

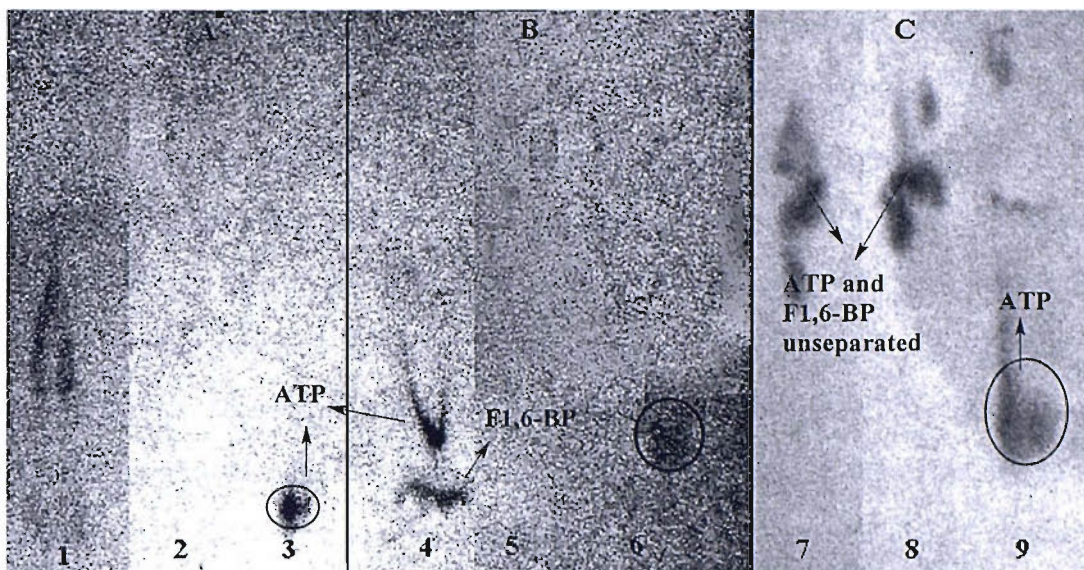


Figure 5.4 Autoradiography to check the TLC separation on cellulose plates

Notes: Plates A, B, and C are PEI plate, normal cellulose plate, and DEAE plate respectively; TLC solvents used with each type TLC plates are 1M NH_4Cl Methanol/HCl (concentrated) 9ml/0.3ml and 0.045M HCl respectively; in panels 3, 6 and 9, only ATP are loaded on plates; assay 1, 4, 7 and 8 are stopped by 10mM HCl solution; in assays 2 and 5, reaction medium were mixed with 100 μl charcoal (in 0.12 HCl) suspension and 50 μl clear sample was concentrated by frozen dry method and then loaded on plates; more samples was loaded on DEAE cellulose plate than on PEI and normal cellulose plates because the latter two types plates absorb solvent easily and are very difficult to dry; and so, on DEAE plate the spots show deep colour while on the other two plates, spots are unclear.

5.4 TLC on silica gel plates

In experiments studying separation of ATP and F1,6-BP, many solvent systems were tried using silica gel plate. Some of them were listed in Table 4.4 and only solvent 1 and 2 were checked under assay condition using radiolabelled chemicals (run PFK reaction and reaction mixture was then separated using TLC method and result was finally checked in autoradiography). As was mentioned previously, solvent 1 was used as final working solvent but gave a poor result. From Figure 5.5, there are two indicated radioactive regions shown up on plate 1, but the edge of F1,6-BP spots is unclear and ATP spots are incompact. Similar as the separation on cellulose plates, the TLC separation is different in under assay condition using radiolabelled chemicals and in experiments using normal chemicals. Particularly, F1,6-BP has a better mobility than ADP in radio-assays while in experiments using nonradioactive chemicals, ADP has a bigger reference value (see Table 4.4.6). Solvent 2 gave a better separation than

solvent 1 in experiments using non-radioactive chemicals because spots of ATP and F1,6-BP were separated with a long distance. However, when the separation result of solvent 2 was checked (under assay condition) in autoradiography, the result is even worse than that of solvent 1. As shown on the right of Figure 5.5, though there are two obvious regions corresponding to F1,6-BP and ATP, the edges of these regions are not clear and they overlap. The region corresponding to ATP is too big, so it is not practical to cut down the whole region for further experiments. This phenomenon is often seen when the TLC plate is overloaded. As discussed in the beginning of this chapter, the target substances to be separated are in low amount and in a complex medium. Simply to concentrate the assay mixture or reduce the loading amount are not suitable here because the former way will bring more serious disturbance while the latter will reduce the radioactivity and thus the accuracy in measuring procedure.

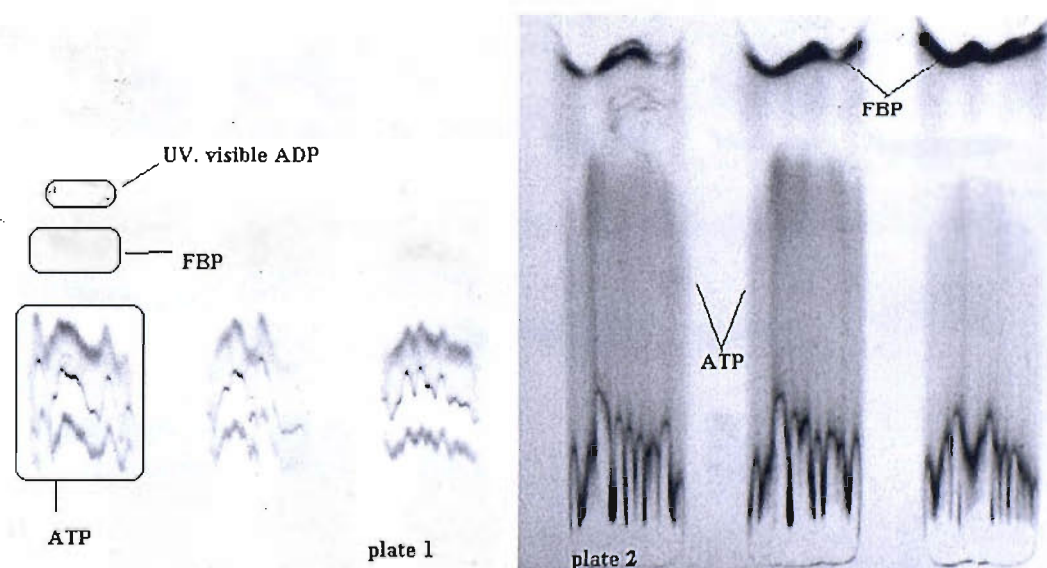


Figure 5.5 Autoradiography to check the TLC separation on silica gel plates

Notes: Plate 1 was developed using solvent 1 (isopropanol/acetone/ammonia/water: 3/2/1/4) while plate 2 was developed using solvent 2 (ammonia/acetone/water: 1/4/5); all samples loaded on TLC plates were PFK assay medium and all assays were stopped using EDTA solution.

One common problem for all the separations is that the spots spread too much on the plates and sometimes streak from the baseline to solvent front. Previously, it was concluded that adding EDTA solution is not able to stop the PFK reaction, but seems helpful to maintain the spots of chemicals compact in TLC (see ATP, F1,6-BP spots in Figure 5.1 and F1,6-BP spots in Figure 5.5). Enlightened by this observation, a series of EDTA solvents were tried on silica gel plates in an attempt to improve the separation. The concentrations of EDTA solvent tried were 40mM, 80mM, 120mM, 160mM and 320mM; the autoradiography check of these experiments is shown in Figure 5.5.

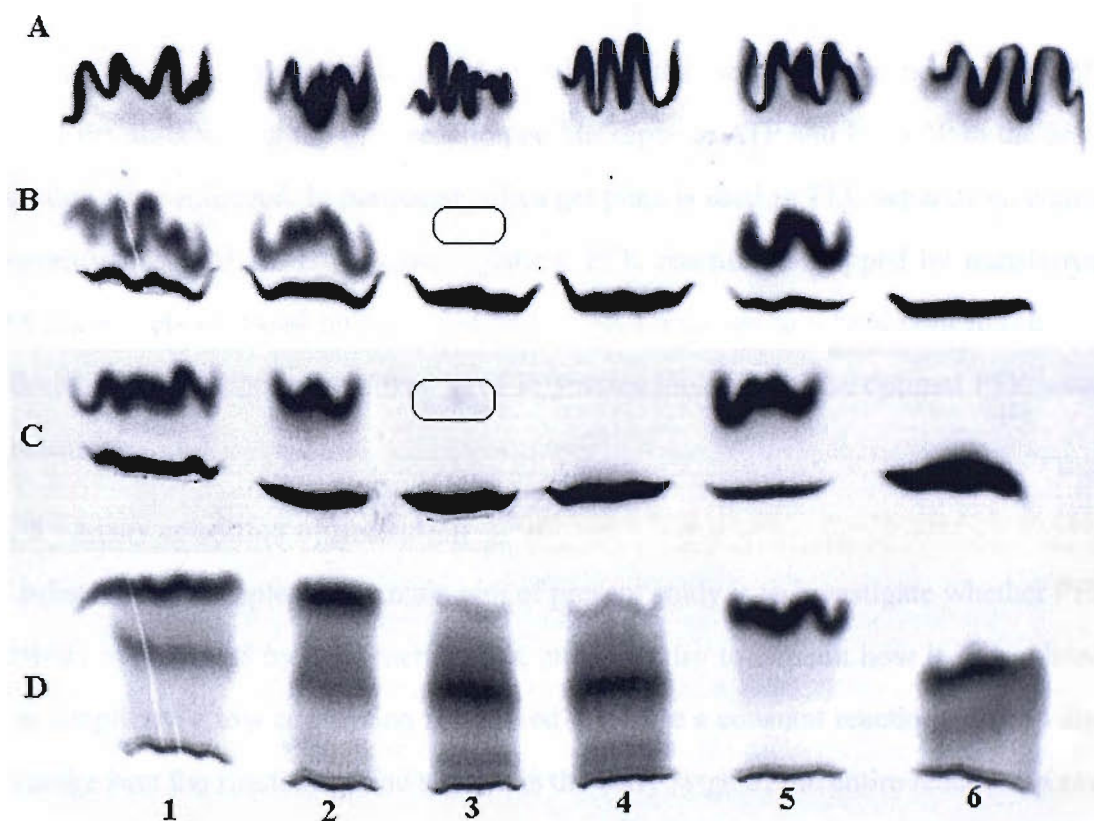


Figure 5.6 Autoradiography of TLC separation using a number of EDTA solvents

Notes: Plates A, B, C and D are all silica gel plates and developed using 320mM, 160mM, 120mM and 80mM EDTA solvents respectively; assay 1, PFK assay stopped by CuCl_2 solution; assay 2, stopped by HCl; assay 3 and 4, assays inhibited by CuCl_2 and HCl respectively; 5 assay not stopped (without adding CuCl_2 and HCl); panel 6, only ATP; labelled areas show low radioactivity on TLC plates which were indicated by the light colour on the autoradiography.

Among the series of concentration, 160mM and 120mM EDTA solvent give sufficient separation and the latter is the best one because the edge of two radioactive regions is clear. There is enough distance between these two regions which will facilitate following experiments. At the same time, the effect of reaction termination by both CuCl_2 and HCl were also checked with these experiments. As labelled out in Figure 5.6, for each assay inhibited by CuCl_2 , there is very weak radioactivity corresponding to the product (F1,6-BP), though theoretically, the concentration of Cu^{2+} used in these experiments is enough to fully inhibit PFK. However, when a 10mM HCl solution was tested in assay 3, no radioactive spots corresponding to F1,6-BP are detected.

Further experiments (using HCl solution to stop PFK reaction and 120mM EDTA solvent for separation) were repeated and the results were found to be reproducible. Thus, the aims to stop the PFK reaction and to separate ATP and F1,6-BP in the assay mixture were achieved. In particular, silica gel plate is used in TLC separation; elution solvent is 120mM EDTA aqueous solution. PFK reaction is stopped by transferring the assay vials to liquid nitrogen and adding HCl aqueous to a final concentration of 10mM. These methods were then used in studies looking for the optimal PFK assay conditions.

5.5 Assay condition optimization

As discussed in chapter 4, the main aim of present study is to investigate whether PFK activity is regulated by lipid membranes, and if so, try to explain how it is regulated. For simplicity, a low conversion is required to assure a constant reaction rate and also to make sure the reaction period studied is the early stage of the entire reaction *in situ*. At the same time, the PFK to vesicle ratio should be adjusted properly not only to obtain an apparent variation in PFK activity (if any) but also to leave enough room for further interaction through adjusting the lipid composition and lipid species of the vesicles.

Figure 5.7 shows the reaction conversion studied under different vesicles concentration and incubation time. From the graph, for all the incubation time studied (5, 8, 10, 15 minutes), the increase in PFK reaction conversion are all apparent when

adding 0.5 M DOPC vesicles, especially when long time were tested (10 min and 15 min). By adding more vesicles 1 M DOPC, there is more increase in conversion (in compare with the case that 0.5 M DOPC was used) when short time was tested than when long time was tested. When PFK activity was tested for 5 minutes and for 8 minutes with vesicles of different compositions (total lipid mass is 0.5 molar), the trends in the variation of conversion are similar except for the last date point. These experiments indicate that vesicles made up of total 0.5 M lipids will give a sufficient enhancement in PFK activity and this enhancement is more apparent when short reaction periods are studied.

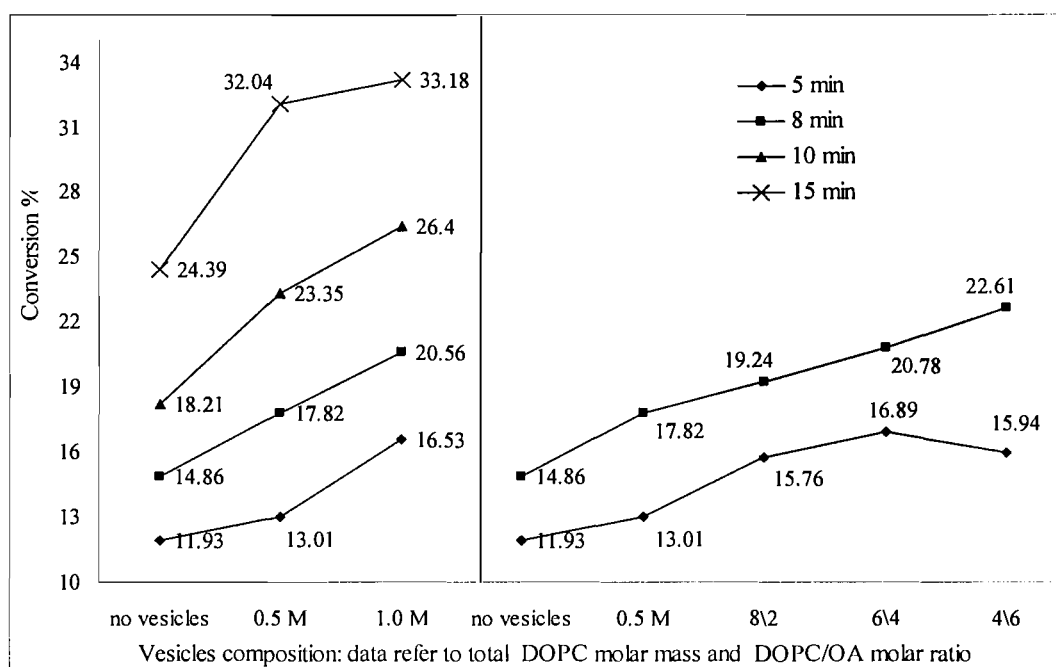


Figure 5.7 Optimization of PFK assay condition

Notes: Reaction conversion—Y-axis was studied as function of vesicles concentration and incubation time. The labels of X-axis refer to the total lipids concentration and composition of vesicles. The results shown in left and right half of this figure are for two experiments; they are included in for a better comparison.

Figure 5.7 shows the results of PFK activity tested for different incubation times. Due to more than one batch of PFK was used the enzyme activity may be different under same condition.^{N2} For the entire time range tested, 3 minutes to 8 minutes, the reaction

N2: The total enzyme activity for all PFK batches were same, 100 units. Every batch was in different purity, 0.8mg~2.3mg. Same dilution of each batch of PFK (same units but different mass) may give different activity. See conversion data of Figure 6.6 and 6.7.

conversion follows the incubation time linearly. So, the time range studied has not passed the initial reaction period under experimental condition. All these assays were tested in absence of vesicles and 3 minutes incubation time will give a high enough conversion, 15%, so PFK is high active enzyme under present experiment condition *in situ*. Considering the regulation rule of vesicles to PFK activity (apparent enhancement from above experiments), short incubation time or low amount of PFK is required to give a low reaction conversion. In addition, PFK from *Bacillus stearothermophilus* is high active at low temperature, about 6% conversion was gained if running the PFK reaction on ice for 2 min, which is required to preparing one set of PFK assay.^{N3} The shorter the reaction incubation time is, the more error will be expected to evaluate the PFK activity. For above reason, PFK reaction was studied at different enzyme concentrations and time periods to achieve a proper conversion. And for different batches of PFK, the conditions were rechecked and adjusted to maintain a constant enzyme activity.

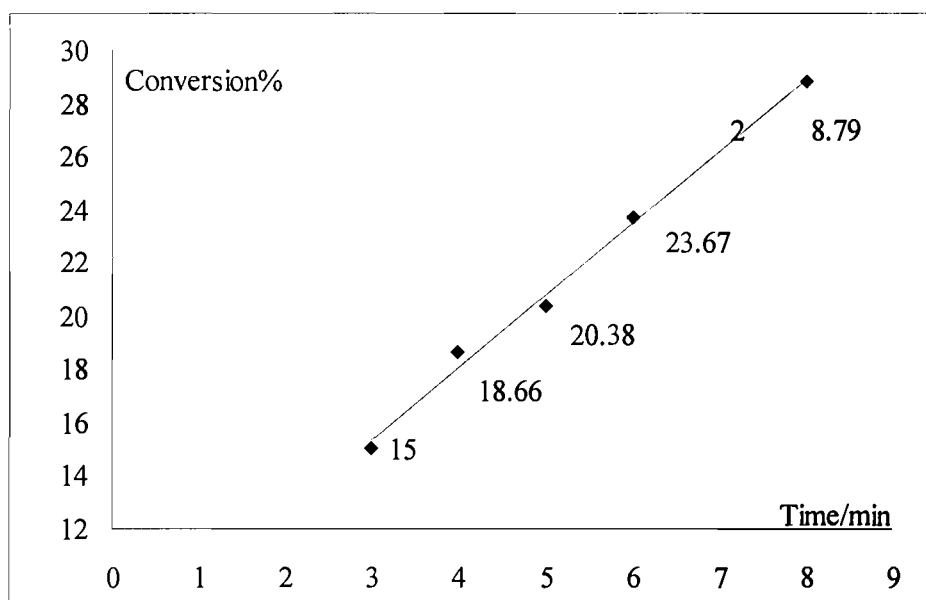
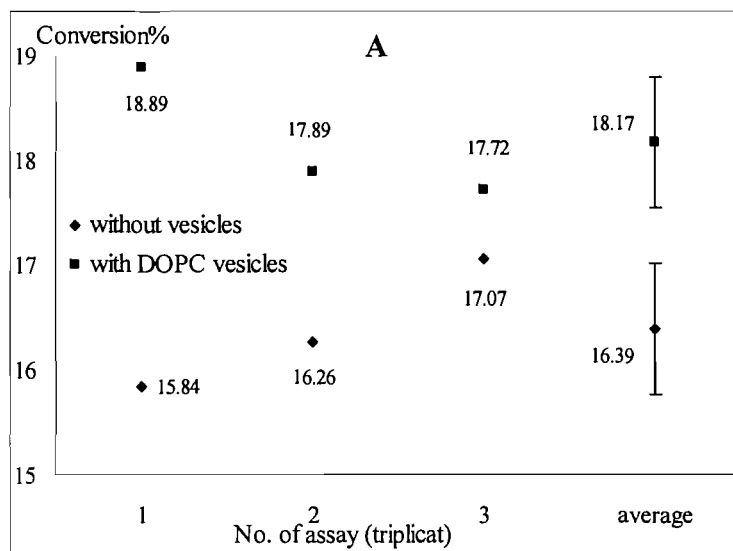


Figure 5.8 PFK activity tested for different assay incubation time

N3: PFK assays are set on ice before adding ATP to start the reaction. One set experiment usually contains 24 assays, which are triplicate assays for 7 compositions of one vesicles system and 3 control assays without vesicles. Adding ATP to all 24 assay vials takes about 2 minutes. All vials are then quickly transferred to hot water bath and timer starts. That is to say, the first few assays have already run for 2min at low rate during the whole preparation process. See section 5.3 details of experiment process.

Figure 5.9 shows possible errors in assay preparation and in TLC procedure. The error range (standard deviation/ average conversion) from TLC procedure is about 1%; while that from PFK reaction is about 4%.



A: Error in assay preparation.

Three parallel assays were tested for two PFK reactions, one without vesicles and the other with 100% DOPC vesicles. Errors, more specific the variation in conversion, resulted from reaction and TLC separation procedure.

B: Error in TLC procedure.

Two PFK assays were tested, one without vesicles and the other with 100% DOPC vesicles. Each assay medium was then equally separated into 3 samples, and each sample was separated in TLC. Variations in reaction conversion corresponded to errors from the TLC procedure.

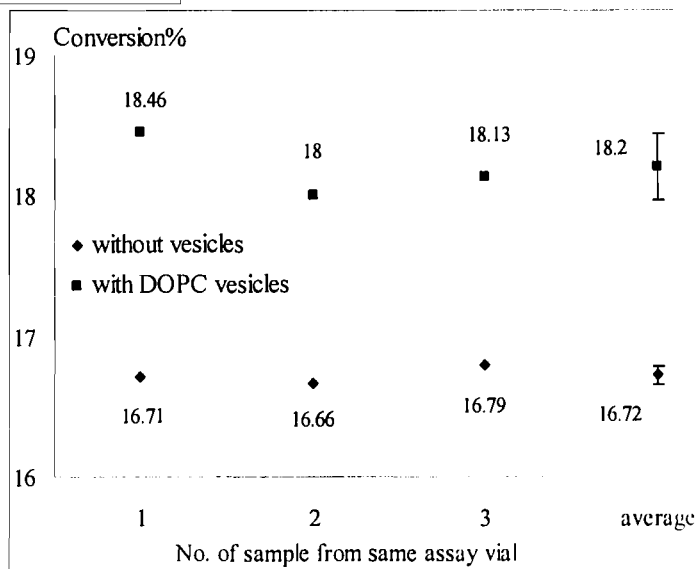


Figure 5.9 A&B PFK assay error range study

From above comparison, it appears that more error (variation in reaction conversion%) occurs during reaction stage. The possible reasons are:

1.) High activity of PFK, and extremely diluted PFK solution: PFK is highly active at experimental conditions. For the purpose of enzymatic active study, the original PFK sample (100 units, 0.8~2.3mg powder) is required to dilute thousands of times. For example, the last batch PFK (2.3mg, used in study with 5 different vesicles systems) was diluted 5.33×10^5 times in different steps. The final assay medium contained 4.31×10^{-6} mg, (1.875×10^{-4} units) PFK. For such a trace quantity, it is difficult to keep

the enzyme concentrations same in all assays;

2.) Parallel assays starting at different time points during preparation: as described in N5, during preparation of PFK assays (about 2 minutes is needed to prepare for one vesicle system), the reactions could start at different time. Though, these reactions happen at low temperature (on ice), low amount of product are yielded. This leads to the errors in final results.

3.) PFK activity unstabilized during storage: fresh reagents, particular enzyme solution and radioactive ATP solution, are prepared just before usage. However, PFK loses activity during storage and radioactivity of ^{33}P decays about 3% everyday. Different dilution methods are required for every new experiment which possibly results in errors.

To reduce above errors, two principles were followed in experiments; and these can also be taken as part of the PFK assays conditions.

1.) No more than 30 assays (one vesicle system) are tested at one time. This reduces the products yielded during preparation to a neglectable level.

2.) Avoid using different reagents (different batch of PFK and PFK solution made at different time) in same study. If time permitted, try to finish all the assays for one study in one go (all the reaction procedures, leave the separation work later). For example, the experiments discussed in next chapter are studies of PFK activity variation in vesicles systems. The same enzyme solution was used for all five vesicles systems; this saved the trouble to make new enzyme solution (but different dilutions) and radioactive ATP solution for every experiment using different vesicle systems.

5.6 Final experimental conditions

From above study, a reagent was found to stop the PFK reaction effectively; the assay mixture can be separated by TLC; and assay conditions were adjusted to give a proper PFK activity. Thus, the PFK activity assays can be studied. The final experimental conditions were:

PKF assay medium was 50 μl containing 5mM MgCl_2 , 5mM $(\text{NH}_4)_2\text{SO}_4$, 50mM Tris-HCl buffer (pH 7.4 under 37°C), 1mM F6P, 0.1mM ATP and 4.31×10^{-6} mg BsPFK.

The reaction was triggered by addition of radioactive ATP solution (7.2Ci/mol). The reaction was then stopped by immersing the assay vials in liquid nitrogen and addition of 5 μ l 0.011M HCl (the final concentration of HCl is 1mM).

About 30ul above assay mixture was then loaded on TLC plates and the plates were developed with 120mM EDTA as elution solvent. 100mL solvent was made up of 4.5g EDTA + 10mL ammonia (35%) + 88mL H₂O.

TLC plats (Silica gel 60) were developed for 2 hours to get a solvent front of about 16cm. Then the plates were dried and results checked with autoradiography. The indicated spots were then cut down from the plates and radioactivity was determined. The activity of blank areas from the same TLC plates was taken as background.

In data treatment, the production of FBP equals that of ADP, so conversion of ATP to ADP was calculated by:

$$\text{Conversion \%} = \frac{\text{radioactivity of FBP} - \text{background}}{\text{total radioactivity} - 2 \times \text{background}} \times 100\% ;$$

then the average and standard deviation of every three parallel assays were taken.

However, attention must be paid when performing experiments especially in TLC separation process. Sometimes the chromatography is not good enough to separate the two radioactive chemicals; and PFK activity is not stable especially during long period of storage.

Chapter 6 BsPFK Activity in Five Vesicle Systems

6.1	Results of two parallel experiments.....	84
6.2	Data analysis and discussion	90
6.2.1	PFK activity variation.....	90
6.2.2	Possible links between lipids vesicles properties and PFK activity	91
6.2.3	A comparison of PFK with CCT	92
6.3	Further work	93

Notes: all original data and converted data used to generate the plots in this chapter are given in Appendix 5.

Two sets of experiments were developed in this section (hereafter named as experiment one and experiment two), in each experiment, PFK activity was tested in the same five vesicle systems. That is, experiment two is a repeated study of experiment one. The results were given below. PFK activity in each vesicle system, specified by conversion%, was then compared with that in other systems and also transversely, compared with that in the same vesicle system but in repeated experiments.

6.1 Results of two parallel experiments

The following figures give the PFK activity tested in two experiments and for each vesicle system. Since different vesicle systems were studied at different time, and more importantly, a different batch of PFK was used in the second experiment, difference between the PFK activities was observed within assays tested under the same conditions. For a better comparison, in each vesicle system the relative activity—vesicle composition plot was inserted to conversion%—vesicle composition plot. The X-axes (vesicles compositions) of these two plots are same. More precise, PFK reaction without vesicles was tested as control assay and the resulting activity was taken as the unit activity 1. In DOPC/DOG system, PFK activity with 100% DOPC vesicles was set as unit activity.^{N1} The relative activity was calculated using activity at each vesicle composition point divided by unit activity. In following figures, the shown error bars correspond to the \pm standard deviation of the triplicate assays.

The five vesicle systems tested in experiments were made up of lipids DOPC and increasing amount of DOPE, OA, DOPA, lyso-OPA and DOG, respectively. For the lipids names, see appendix of Glossary and abbreviation; for the composition of each vesicle systems, see vesicle preparation procedures in section 4.1.2. The specific PFK activity—vesicle composition plots of these experiments are also list in Appendix 2 for reference; however, the shape of the curves are exactly the same as

N1: DOG is one of the lipid species giving strong negative curvature stress in membrane construction. High content of DOG in lipid vesicles will result in the cracking of the bilayer structure and formation of other lipid phases.

shown in conversion%—vesicle composition plots.

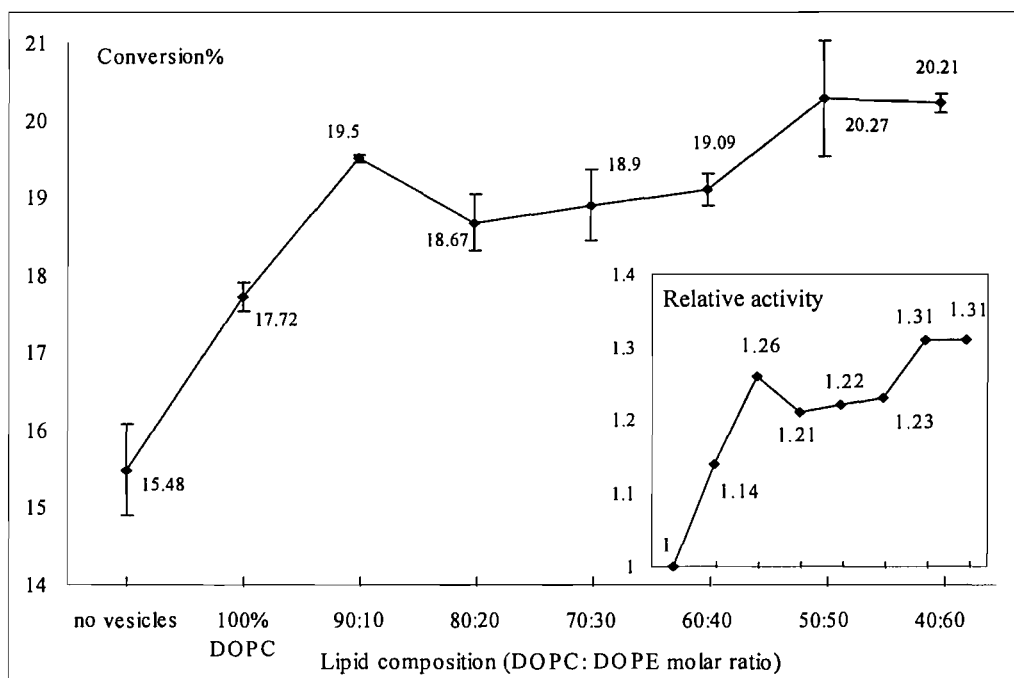


Figure 6.1 PFK activity in DOPC/DOPE vesicles

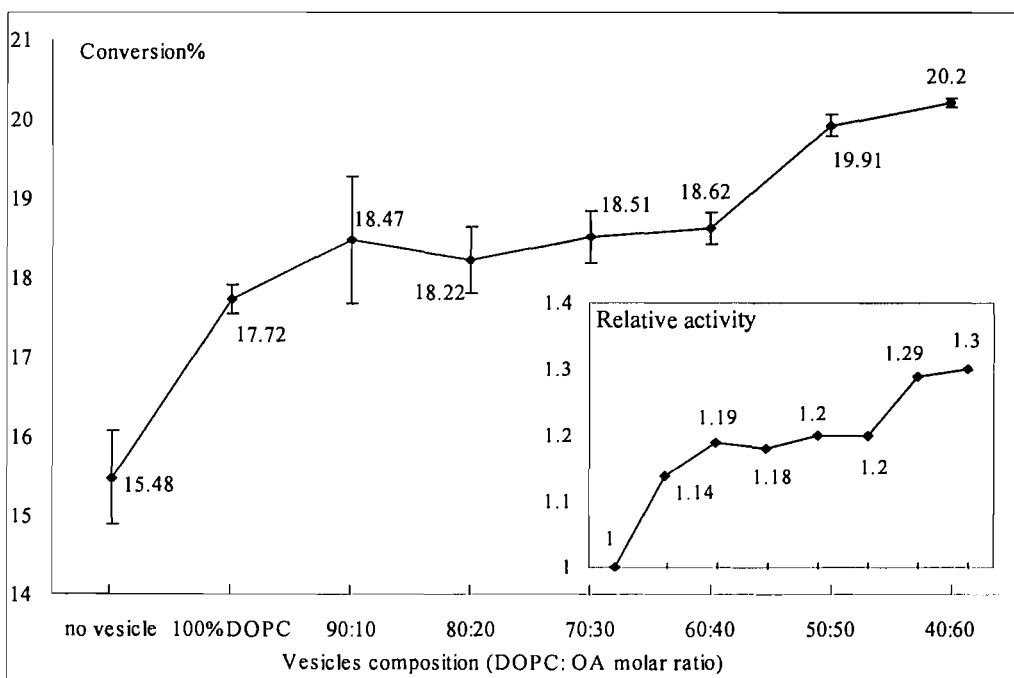


Figure 6.2 PFK activity in DOPC/OA vesicles

Note: Above two systems were examined at one go, and thus use same control assays, which are assays without vesicles and with 100% DOPC vesicles.

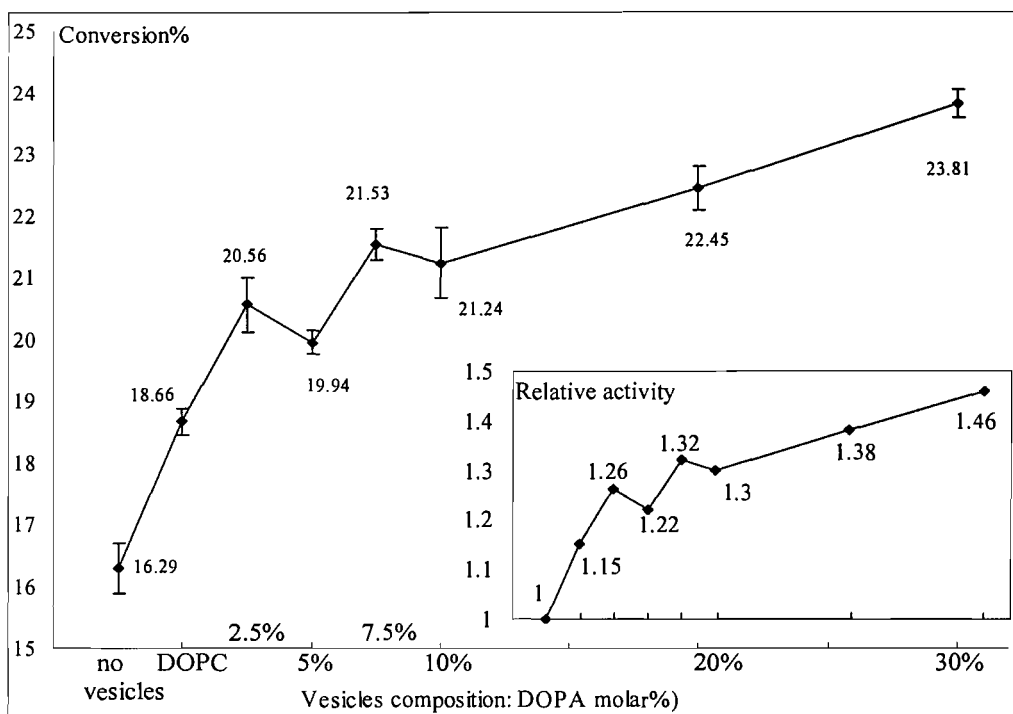


Figure 6.3 PFK activity in DOPC/DOPA vesicles

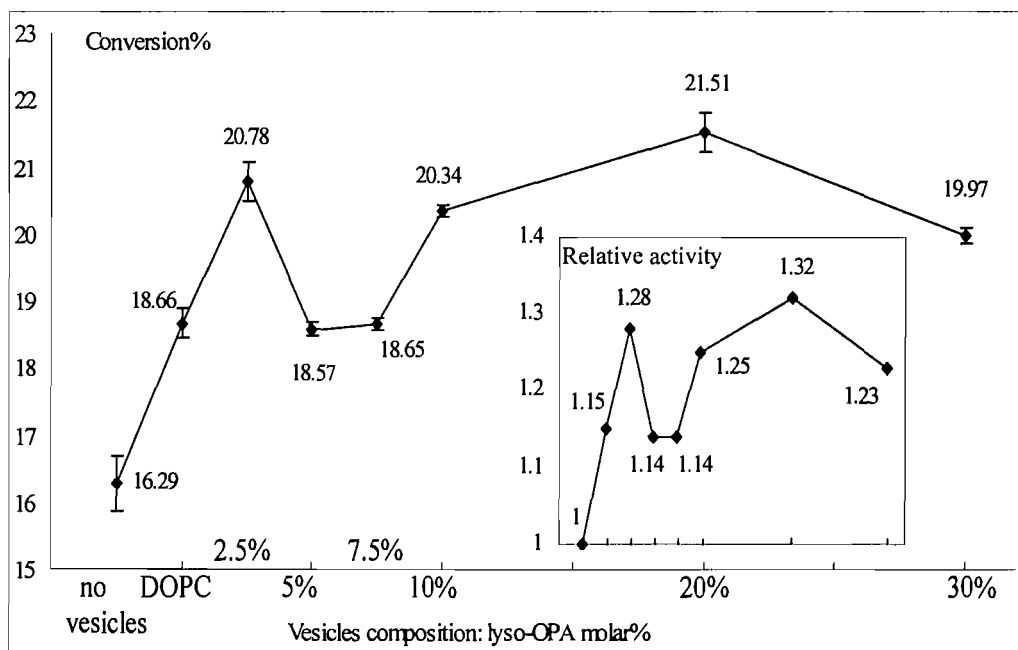


Figure 6.4 PFK activity in DOPC/lyso-OPA vesicles

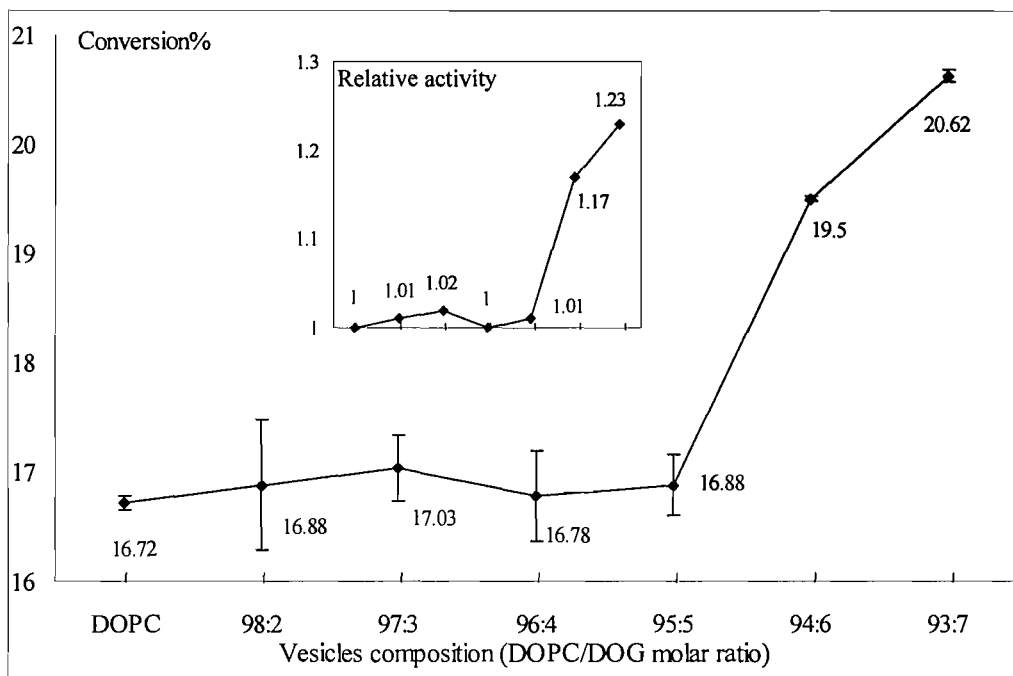


Figure 6.5 PFK activity in DOPC/DOG vesicles

Above figures show the results of experiment one while the following figure show the results of experiment two, which was experimented about two month later using a new batch of PFK.

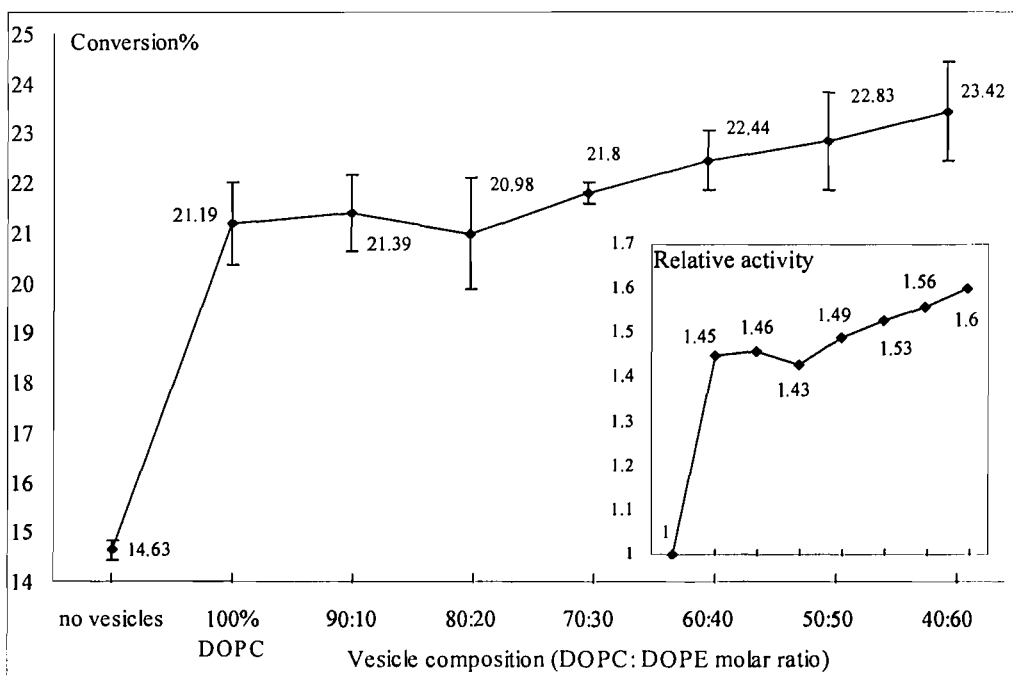


Figure 6.6 2nd PFK activity in DOPC/DOPE vesicles

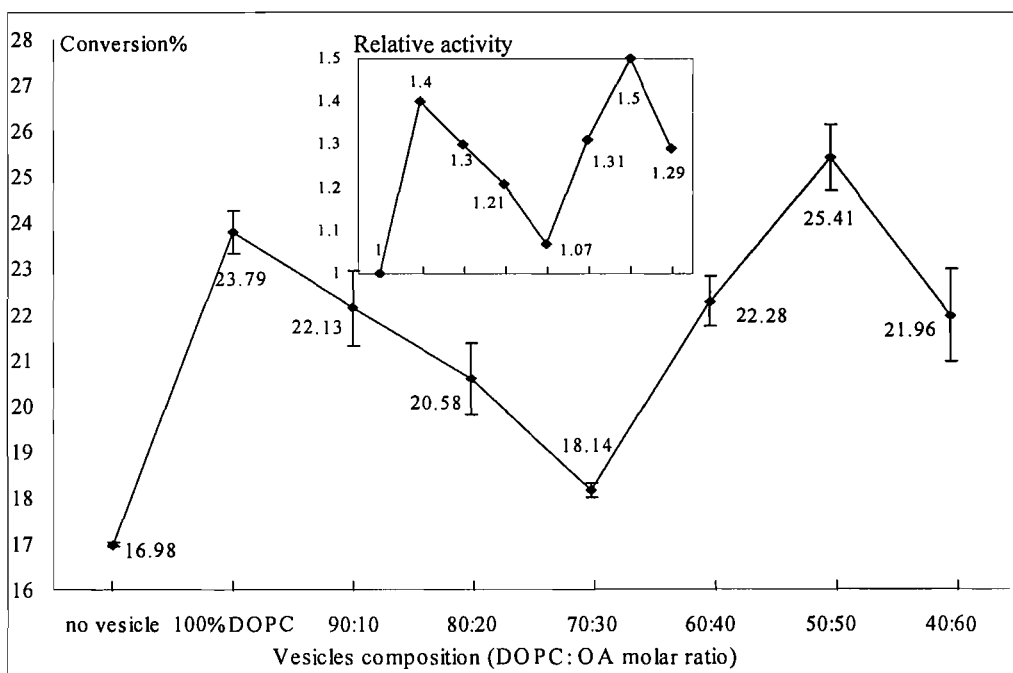


Figure 6.7 2nd PFK activity in DOPC/OA vesicles

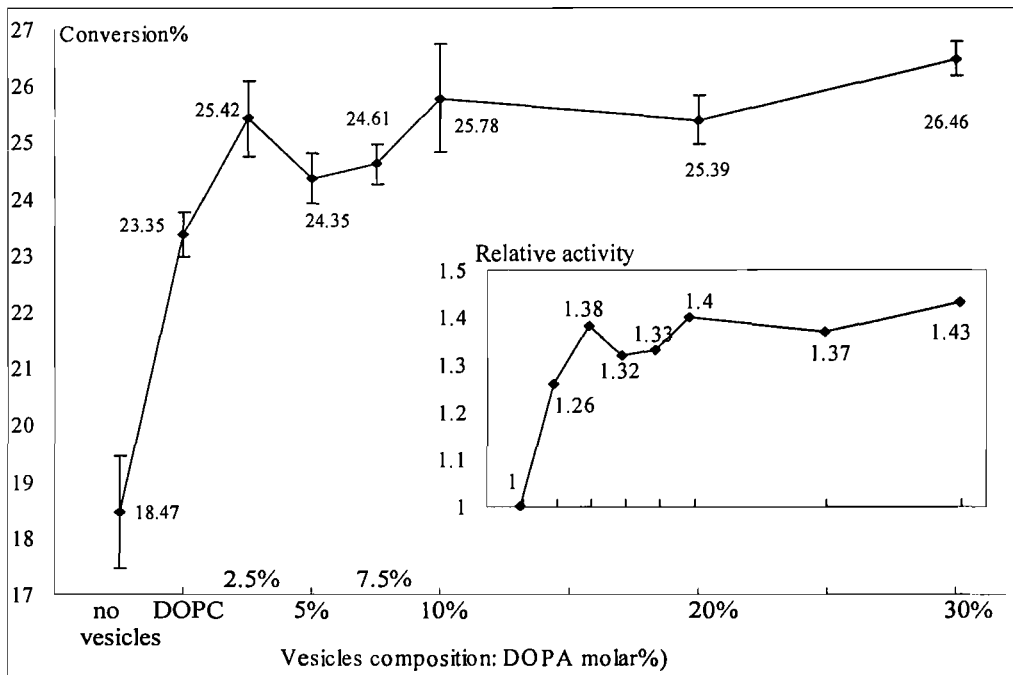


Figure 6.8 2nd PFK activity in DOPC/DOPA vesicles

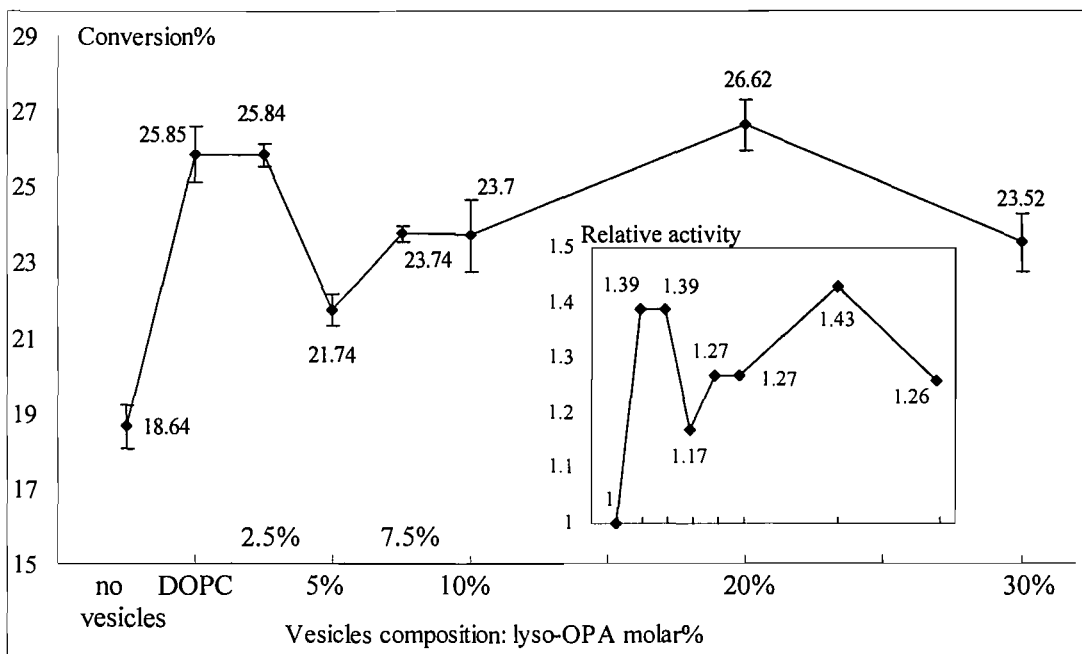


Figure 6.9 2nd PFK activity in DOPC/lyso-OPA vesicles

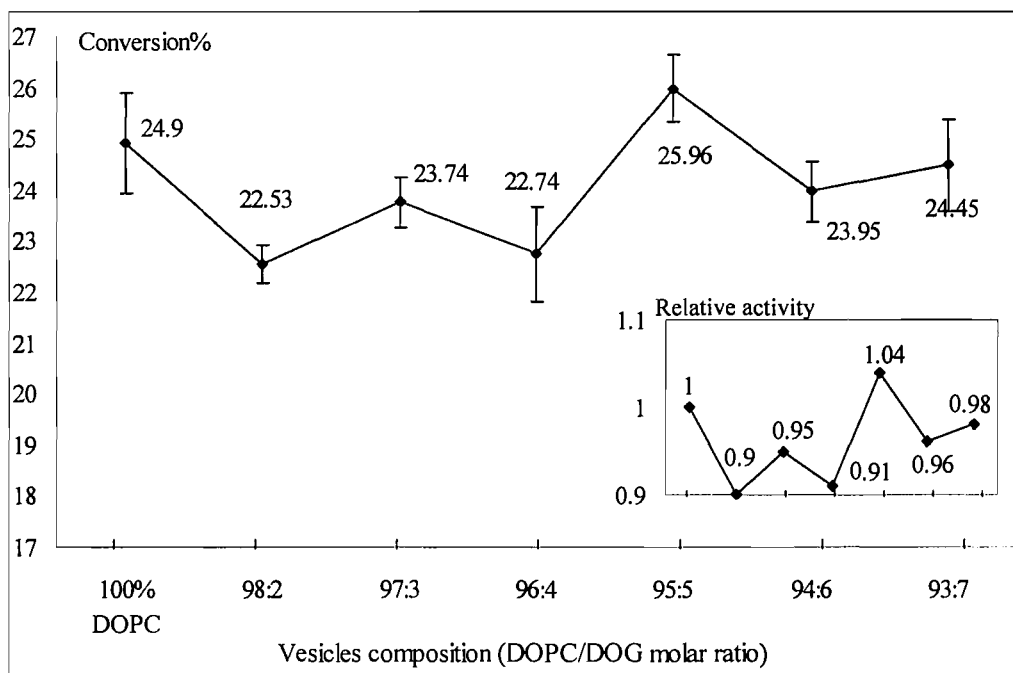


Figure 6.10 2nd PFK activity in DOPC/DOG vesicles

Note: All the assays in the second experiments were tested at one go, but different control assays (assays without vesicles and with 100% DOPC vesicles) were specially tested for each vesicle systems.

6.2 Data analysis and discussion

6.2.1 PFK activity variation

In total, five vesicle systems are studied, in all of which BsPFK activity shows obvious variation. More specific, BsPFK activity are all slightly but virtual increased at the presence of vesicles and seems to be further enhanced when the compositions of type II lipids are increased. Several common observations (for all system except DOPC/DOG system) can be noted from above figures. First, within the whole range of the lipid compositions studied, the increase of BsPFK activity is no more than twice of the native activity (without vesicles). This is more obvious from the insertion of each figure. Secondly, in comparison with control assays, BsPFK activity is most significantly enhanced when 100% DOPC vesicles is used. This increase accounted for more than 50% of the total activation. Thirdly, the enzyme activity seems increased step by step when type II lipids contents are gradually increase in vesicle. This observation is apparent in DOPC/DOPA, DOPC/lyso-OPA systems. Last, though the overall variation tendency is the an enhancement of enzyme activity, BsPFK activity are decreased at some lipid compositions. That is, enzyme activity is not always increased when the composition of type II lipid is increased.

Above discussion is only a simple analysis of the BsPFK activity according to the experiment data. Variation of enzyme activity is observed for five tested vesicle systems, but the tendency is not very clear. Moreover, there is distinct difference between the results of two parallel experiments. One the one hand, due to the difficulty in handling the enzyme assay and TLC separation experiments, a mild change in experiment condition could lead to obvious artificial errors. On the other hand, for each lipid composition the fluctuation of PFK activity is sometimes more than 5% of the average activity (see error bar in above figures), indicting the systemic error is possibly big.

6.2.2 Possible links between lipids vesicles properties and PFK activity

This study has tested a hypothesis of regulation role of model membranes on PFK activity. As stated in chapter 2 that PFK activity was expected to be inhibited upon interacting with lipid vesicles. The bases to presume this are:

1.) There has not been found any specific domain(s) in PFK protein to give a potent interaction with membranes and consequently to enhance its catalysis. On the contrary, BsPFK is a well soluble cytosol enzyme and has a rather polar surface; the interaction between BsPFK and membranes (if any), could be only possible on the surface areas and this interaction is expected to be a loose electrostatic contact. Due to the tetrameric structure of BsPFK, the association between the enzyme and membrane will cover one or more of the symmetrical BsPFK surfaces. Consequently, the active sites available for substrates are reduced.

2.) Even if the active sites of BsPFK are intact upon association with membranes, the free diffusion of enzyme and reactants molecules are expected blocked by the lipid vesicles. As discussed in chapter 3, one of the reactants, ATP could inhibit BsPFK by several manners. In this study, the concentration of F6P is ten times as that of ATP. Under this condition, the inhibition of BsPFK by ATP is minimized and the majority of enzyme exists in R-state which is more active than its T-state. However, this effect is reduced by the presence of vesicles which block the effective collision between BsPFK and F6P molecules.

3.) The binding of F6P to BsPFK is cooperative, in which one binding of F6P to BsPFK facilitates binding next F6P to other active sites. If BsPFK does associate with membrane and the face contain active sites is in contact, the total active sites are reduced.^{N2} And consequently, the positive substrate cooperativity is decreased too.

N2: According to the structure given in chapter 3, BsPFK consists of six faces, two of which contain four active site for binding F6P and ATP; they are referred to as face A and B hereafter. Other two faces of the enzyme embody binding sites for allosteric effectors; they are face C and D. The remained two faces are termed as face E and F.

However, the results of this study show the opposite outcome. That is instead of an explicit decrease, BsPFK active are slightly enhanced by the presence of lipids vesicles. Without the aid of the structural information showing how BsPFk associate with the vesicles systems, it is difficult to ascribe the observation to one particular membrane property. Two regulatory mechanisms are given as following to link the function of BsPFK and properties of lipid vesicles.

If any of the face A or B is in contact with vesicles, the total active sites of one BsPFK are reduced from 4 to 2. But the saturating states of other 2 active sites may not be changed. What's more, BsPFK may contact vesicles with other 4 faces which do not embody the active sites. That is, all the four active sites are possibly intact. Particularly, as shown in Figure 2.1, if face E and F (the face outside the paper and the one opposite) are in contact with lipid vesicles, all the active sites and allosteric sites are intact; and all the enzyme activity and allosteric property are possible remained. In addition, Schirmer et al. had found that the difference between T- and R- status of BsPFK was mainly a rotation of one pair of subunits relative to the other pair [114], thus the active sites are opened more widely to adopt an active, R-state enzyme. This conformational adjustment is theoretically possible when BsPFK interacts with lipid vesicles by its E or F face. Suppose this was the real case, BsPFK activity could be enhanced by fixing one side (face E or F) on vesicles and adopt the R-state conformation more easily.

The driven force for the association of the BsPFK and membrane could not be discussed with the limited data in this thesis. Is it only an electrostatic interaction between the polar headgroups of the lipids molecules and protein's ionisable residues? Or it is due to a more stable conformation formed when the membranes associate with the enzyme and partly release the stored curvature energy within the frustrated bilayer structure? More investigation is needed to answer these questions.

6.3 Further work

Though the BsPFK activity is shown varied by presence of lipid vesicles, the adopted mechanism and the biological significances of the regulative role of interaction between membranes and PFK activity could not be drawn from the limited data in this thesis. Further experiments will need to study more membrane systems and locate the specific link(s) between membrane properties and enzyme functions. More investigation will be required to study the properties of the model membrane used in terms as surface charge and stored curvature tension within the bilayer structure.

Further studies are also needed to optimize the enzyme assay conditions and separations process in TLC. A more deep understand of the enzyme properties such as its cold liability and storage condition are also help to explain of data and reduce artificial errors in experiments.

References in Chapter One:

01. Kent, C., (1997) *Biochim. Biophys. Acta* **1348**, 79-90.
02. Österberg, F., Rilfors, L., Wieslander, A., Lindblom, G., & Gruner, S. M., (1995) *Biochim. Biophys. Acta*, **1257**, 18-24.
03. Singer, S. J., & Nicholson, G. L., (1972) *Science*, **175**, 720-731.
04. Kim, K. S., Neu, J., & Oster, G., (1998) *Biophys. J*, **75**, 2274-2291.
05. Stryer, L., (1995) *Biochemistry 4th ed.* New York. **Chapter 11**, 263-290.
06. Thomas, E. Andreoli., (1986) *Membrane Physiology 2nd ed.*, Plenum Publishing Co., New York. **Chapter 2**, 33.
07. Evans, W. H. & Graham, J. M., (1989) *Membrane Structure and Function*, Oxford University Press. **Part 1**, 1-10.
08. Galbiati, F., Razani. B., Lisanti. MP., (2001) *Cell*, **106**, 403-411.
09. Anderson, R. G. *et al.*, (1992) *Science*, **255-5043**, 410-411.
10. Seddon, J. M., (1990) *Biochim. Biophys. Acta*, **1031**, 1-69.
11. Martonosi, A. N., (1985) *The Enzymes of Biological Membranes*, 2nd edition, Plenum Press, **Volume 1**, 131-195.
12. Finean, J. B. & Michell, R. H., (1981) *Membrane structure*, Elsevier/North-Holland Biomedical Press, **Chapter 5**, 161-210.
13. Vikström, Susanne., Li, Lu. & Wieslander, Åke., (2000) *J. Biol. Chem.* **Vol. 275**, No.13, 9296–9302.
14. Christopher D. Stubbs, Simon J. Slater., (1996) *Chemistry and Physics of Lipids*, **81**, 185-195.
15. Yang, F. Y. & Hwang, F., (1996) *Chemistry and Physics of Lipids*, **81**, 197-202.
16. Philip S. Lows, P. Rathinavelu, & Marietta L. Harrison., (1993) *J. Biol. Chem.*, **Vol. 268**, No. 20, 14627-14631.
17. Clarke, F. M. & Masters, C. J., (1975) *Biochim. Biophys. Acta.*, **381**, 37-46.
18. Jan, Gutowicz., Grzegorz, Terlechi., (2003) *Cell. Mol. Bio. Letts*, **Vol 8**, 667-680.
19. Chang, R., (2000) *Physical Chemistry for the chemical and biological sciences*, 3rd ed., Sausalito.

20. White, S. H. & Wimley, W. C., (1999) *Annu. Rev. Biophys. Biomol. Struct.*, **28**, 319-365.
21. May, S., (2000) *Curr. Opin. Coll. Interface Sci.*, **5**, 237-243.
22. Gil, T., Ipsen, H. J., & Mouritsen, Ole G., (1998) *Biochim. Biophys. Acta.*, **1376**, 245-266.
23. Harroun, TA., Heller, WT., Weiss, TM., Yang, L., & Huang, HW., (1999) *Biophys. J.*, **76**, 937-945.
24. Morein, S., Strandberg, E., & Killian, J.A., (1997) *Biophys. J* **73**, 3078-3088.
25. Cowan, S.W., & Schirmer, T. *et al.*, (1992) *Nature*, **358**, 727-733.
26. Doyle, D.A., & Wallace, B.A., (1997) *J. Mol. Biol.*, **266**, 963-977.
27. J.A. Killian, K.N.J. Burger, B. de Kruijff, (1987) *Biochim. Biophys. Acta.*, **897**, 269-284.
28. R.M. Epand, (1987) *Chem. Biol. Interact.*, **63**, 239-247.
29. M. Mosior, E.S. Golini, R.M. Epand, (1996) *Proc. Natl. Acad. Sci.*, USA **93**, 1907-1912.
30. Mouritsen, O.G., Kinnunen, P.K.J., (1997) *Biological Membranes. A Molecular Perspective from Computation and Experiment*, Berlin, pp. 463-502.
31. Hogan, M., Zimmermann, L., Wang, J., Kuliszewski, M., Liu, J., & Post, M., (1995) *Am. J. Physiol.*, **267**, L25-L32.
32. Yang, W., Boggs, K. P., & Jackowski, S., (1995) *Biochim. Biophys. Acta.*, **270**, 23951-23957.
33. Simon J. Dunne, Rosemary B. Cornell & Joanne E. Johnson. *et al.*, (1996) *Biochemistry*, **35**, 11975-11984.
34. Arnold, R.S. & Cornell, R. B., (1996) *Biochemistry*, **35**, 9917-9924.
35. Jamil, H., Hatch, G., & Vance, D.E., (1993) *Biochem. J.*, **291**, 419-427.
36. Attard, G. S., Templer, R. H., Smith, W. S., Hunt, A. N. & Jackowski, S., (2000) *Proc. Natl. Acad. Sci.*, **97**, 9032-906.
37. Davies, S. M. A., Epand, R. M., Kraayenhof, R., & Cornell, R. B., *Biochemistry*, **40**, 10522-10531.
38. Brown, M.F., Epand, R. M., *Lipid Polymorphism and Membrane Properties*,

Academic Press, San Diego, CA, 1997, pp 285-356.

39. Cornell, R. B., Arnold, R. S., (1996) *Chem. Phys. Lipids*, **81**, 215-227.

References in Chapter Two:

40. Dische, Z., (1935) *Biochem. Z.*, **280**, 248-264.

41. Ron S. Ronimus, Hugh W. Morgan., (2001) *Extremophiles*, **5**, 357-373.

42. Mertens E., Lador US, Lee JA., Miretsky A, Morris A, Rozario C, Kemp R.G., Müller M., (1998) *J. Mol. Evol.*, **47**, 739-750.

43. Ronimus, RS, de Heus E, Morgan HW., (2001) *Biochem. Biophys Acta.*, **1517**, 384-391.

44. Schumacher, MA, Scott DM, Mathews II, Ealick SE, Roos DS, & Brennan RG., (2000) *J. Mol. Biol.*, **296**, 549-567.

45. Daldal, F., (1984) *Gene*, **28**, 337-342.

46. Hofmann, E., (1976) *Rev. Physiol. Biochem. Pharmacol.*, **Vol. 75** 1-68.

47. Nicholas, C. Price., & Lewis, Stevens., (1989) *Fundamentals of Enzymology*. 2nd Edition, Oxford Press, **Chapter 6**, 253-315.

48. Tsao, M. U., & Madley, T. I., *Biochim. Biophys. Acta.*, **258**, 99-105.

49. Heinisch, J., Ritzel, RG. & Van Borstel, RC., (1989) *Gene*, **78**, 309-321.

50. Alves, AMCR., Euverink, GJW., Bibb, MJ. & Dijkhuizen, L., (1997) *Appl. Environ. Microbiol*, **63**, 956-961.

51. Evans, P. R., Rarrants G. W., & Hudson P. J., (1981) *Phil. Trans. R. Sco. Lond.*, **B, 293**, 53-62.

52. Evans, P. R. & Hudson P. J., (1979) *Nature*, **Vol. 279**, 500-504.

53. Dunaway, G. A., (1983) *Mole. Cell. Biochem.* **Vol. 52**, 75-91.

54. Goldhammer, Alan R. & Paradies, Hasko H., (1979) *Current Topics in Cellular Regulation*, **Vol. 15**, 109-142.

55. Evans, P. R., Rarrants, G. W. & Lawrence, M. C., (1986) *J. Mol. Biol.* **191**, 713-720.

56. Stryer, L., (1995) *Biochemistry 4th ed.*, New York. **Chapter 19**, 483-529.

57. Byrnes, M., Zhu, XM., Younathan, Ezzat S. & Chang, S. H., (1994)

Biochemistry, **33**, 3424-3431.

58. Otto, M., Heinrich, R., Kuhn, B., & Jacobasch, G., (1974) *Eur. J. Biochem.*, **49**, 169-178.

59. Bette L. Braxton, Valarie L. Tlapak-Simmons, & Gregory D. R., (1994) *J. Biol. Chem.*, **Vol. 269**, 47-50.

60. Dominique, D. B., Florence B., & Garel, J. R., (1991) *Biochemistry*, **30**, 5750-5754.

61. Frieden, C., Gilbert, H. R., & Bock, P. E., (1976) *J. Biol. Chem.*, **Vol. 251**, 5644.

62. Tornheim, K., & Lowenstein, J. M., (1976) *J. Biol. Chem.*, **Vol. 251**, 7322-28.

63. Rose, I. A., & Warms, J. V. B., (1974) *Biochem. Biophys. Res. Commun.*, **Vol. 59**, 1333-40.

64. Passonneau, J. V., & Lowry, O. H., (1963) *Biochem. Biophys. Res. Commun.*, **Vol. 13**, 372-9.

65. Colombo, G., Tate, P. W., & Kem, R. G., (1975) *J. Biol. Chem.*, **Vol. 250**, 940-12.

66. Hill, D. E., & Hammes, G. C., (1975) *Biochemistry*, **Vol. 14**, 203-13.

67. Rundle, P. J., Denton, R. M., & England, P. J., (1968) *Biochem. Soc. Symp.*, **Vol. 27**, 87-103.

68. Pogson, C. I., & Randle, P. J., (1966) *Biochem. J.*, **Vol. 100**, 683-93.

69. Lad, P. M., & Hammes, G. C., (1973) *Biochemistry*, **Vol. 12**, 4303-09.

70. Shirakihara, Y., & Evans, P. R., (1988) *J. Mol. Biol.*, **Vol. 204**, 973-994.

71. French, B. F., & Chang, S. H., (1987) *Gene*, **Vol. 54**, 65-71.

72. Audrey, S. P., & Gregory, D. R., (2001) *Biochemistry*, **Vol. 40**, 4150-58.

73. Johnson, J. L., & Reinhart, G. D., (1997) *Biochemistry*, **Vol. 36**, 12814-22. 8in72

74. Van Schaftingen, E., & Hers, H. G., (1980) *Biochem Biophys Res Commun.*, **Vol. 96 (4)**, 1524-31.

75. Pilkis, S. J., El-Maghrabi, M. R., & Cumming, D. A., (1981) *J. Biol. Chem.*, **Vol. 256**, 3171-74.

76. Schliselfeld, L. H., & Danon, M. J., (1996) *Clinical Biochemistry*, **Vol. 29, No.1**, 79-83.

77. Hussey, C. R. & Kellet, G. L., (1972) *Eur. J. Biochem.*, **80**, 497-506.

78. Uyeda, K. M. & Luby, L. J., (1978) *J. Biol. Chem.*, **253**, 8319-27.
79. Furuya, E. & Uyeda, K., (1980) *J. Biol. Chem.*, **255**, 11656-59.
80. Sakakibara, R. & Uyeda, K., (1983) *J. Biol. Chem.*, **258**, 8656-62.
81. Foe, L. G. & Kemp, R. G., (1982) *J. Biol. Chem.*, **257**, 6368-72.
82. Kemp, R. G., Foe, L. G. & Latshaw, S. P., (1981) *J. Biol. Chem.*, **256**, 7282-86.
83. Pettigrew, D. W. & Frieden, C., (1979) *J. Biol. Chem.*, **254**, 1887-95.
84. Kitajima, S., Sakakibara, R. & Uyeda, K., (1983) *J. Biol. Chem.*, **258**, 13292-98.
85. Fletterick, R. J. & Sprang, S. R., (1982) *Accts, Chem. Rev.*, **15**, 361-69.
86. Sprang, S. R. & Fletterick, R. J., (1980) *Biophys. J.*, **32**, 174-192.
87. Higashi, T. & Richards, C. S., (1979) *J. Biol. Chem.*, **254**, 9542-50.
88. Karadsheh, N. S. & Uyeda, K., (1977) *J. Biol. Chem.*, **252**, 7418-20.
89. Jenkins, J. D. & Kezdy, F. J., (1985) *J. Biol. Chem.*, **260**, 10426-33.
90. Sotgia, F., Bonuccelli, G., Minetti, C. & Woodman, S. E., (2003) *American J. Pathology*, Vol. **163**, 2619-34.
91. Su, Ya, Zhou, Aiwu. & Kare, E. F., (2003) *J. Biol. Chem.*, **278**, 20013-18.
92. Low, P. S., Rathinavelu, P. & Harrison, M. L., (1993) *J. Biol. Chem.*, **268**, 14627-31.
93. Harris, S. J., & Winzor, D. J., (1990) *Biochim. Biophys. Acta.*, **1038**, 306-314.
94. Tsai, I., Murthy, S. N. P., & Steck, T. L., (1982) *J. Biol. Chem.*, **257**, 1438-42.
95. Harrison, M. L., Rathinavelu, P. & Low, P. S., (1991) *J. Biol. Chem.*, **266**, 4106-11.
96. Strapazon, E., & Steck, T. L., (1977) *Biochemistry*, **16**, 2966-71.
97. Scherer, P. E., Lisanti, M. P., Corley-Mastick C, Lodish, H. F., (1994) *J. Cell. Biol.*, **127**, 1233-43.
98. Karlsson, M., Thorn, H., Parpal, S., Stralfors, P., & Gustavsson, J., (2002) *EMBO J.*, **16**, 249-251.
99. Lehotzky, A., Telegdi, M., Liliom, K., Ovadi, J., (1993) *J. Biol. Chem.*, **268**, 10888-94.
100. Kurzchalia, T.V., & Parton, R.G., (1999) *Curr. Opin. Cell Biol.* **11**, 424-431.
101. Smart, E.J., Graf, G.A., McNiven, M.A., Sessa, W.C., Engelman, J.A.,

Scherer, P.E., Okamoto, T., and Lisanti, M.P., (1999) *Mol. Cell. Biol.*, **19**, 7289–7304.

102. Hazen, S. L., Gross, R. W., (1993) *J. Biol. Chem.*, **268**, 9892–9900.

References in Chapter Three:

103. Bergey, D. H., (c1974) *Bergey's Manual of determinative bacteriology*, 8th ed., Baltimore : Williams & Wilkins Co.

104. Nicklin J. Jane, Graeme-Cook, K. & Killington, R., (2002) *Instant notes microbiology*, 2nd ed., Oxford : BIOS Scientific, pp5.

105. Kimmel, J. L. & Reinhart, G. D., (2000) *Proc. Natl. Acad. Sci.*, **97**, No. **8**, 3844-49.

106. Valdez, B. C., French, B. A., Younathan, E. S., & Chang, S. H., (1989) *J. Biol. Chem.*, **264**, 131-135.

107. Kimmel, J. L. & Reinhart, G. D., (2001) *Biochemistry*, **40**, 11623-29.

108. Tlapak-Simmons, V. L. & Reinhart, G. D., (1994) Vol. 308, No. 1, 226-230.

109. Poorman, R. A., Randolph, A., Kemp, R. G. & Heinrikson, R. L., (1984) *Nature*, Vol. **309**, 467-469.

110. Zhu, X., Byrnes, M., Nelson, J. W. & Chang, S. H., (1995) *Biochemistry*, **34**, 2560-65.

111. Uyeda, K., (1979) *Adv. Enzymol. Relat. Areas Mol. Biol.*, **48**, 193-244.

112. Gebhard, S., Ronimus, R. S., & Morgan, H. W., (2001) *FEMS Microbiol. Letts.*, **197**, 105-109.

113. Braxton, B. L., V. L., and Reinhart, G. D., (1994) *J. Biol. Chem.*, **269**, No. **1**, 47-50.

114. Schirmer, T., & Evans, P. G., (1990) *Nature*, **343**, 140-145.

115. Hellinga, H. W., & Evans, P. R., (1985) *Eur. J. Biochem.*, **149**, 363-73.

116. Riley-Lovingshimer, M. R. & Reinhart, G. D., (2001) *Biochemistry*, **40**, 3002-08.

117. Carpenter, J. F., Crowe, L. M. & Crowe, J. H., (1987) *Biochim. Biophys. Acta.*, **923**, 109-115.

118. Bonne, D. D., Bowgain, F., & Garel, J. R., (1991) *Biochemistry*, 30, 5750-54.
119. Schleif, R., & Wensink, P. C., (1982) *Practical Methods in Molecular Biology*, Springer-Verlag, New York, NY.
120. Wu L-F, Reizer, A., & Cai, B., (1991) *J. Bacteriol.*, **173**, 3117-27.

References in Chapter Four, Five and Six:

121. Kruger, N. J., (1994) *Phytochemistry*, **Vol. 38, No. 5**, 1065-1071.
122. Knowles, V. L., Greyson, M. F., & Dennis, D. T., (1990) *Plant Physiol.*, **92**, 155-59.
123. Kundrot, C. E., & Evans, P. R., (1991) *Biochemistry*, **30**, 1478-84.
124. Thomas, S., & Kruger, N. J., (1994) *Plant Sci.*, **95**, 133.
125. Toribio, F., Alhama, J., & Lopez-Barea, (1996) *J. Chromatogr. B.*, **684** 1-23.
126. , K. P., (1970) *Analytic. Biochem.*, **38 (2)**, 383-388.
127. Sola-Penna, M., Santos, A. C., Alves, G. G., & El-Bacha, T., (2002) *J. Biochem. Biophys. Methods*, **50**, 129-140.
128. Grubmeyer, C., & Penefsky, HS., (1981) *J. Biol. Chem.*, **256**, 3718-27.
129. Kirchner, Justus G., (1978) *Thin-Layer Chromatography*. 2nd ed., (Techniques of chemistry; Vol. 14), Wiley-Interscience publication.
130. Joseph, C. Touchstone, & Murrell, F. Dobbins, (1978) *Practic of thin layer chromatography*, Wiley-Interscience publication.
131. Randerath, K., (1963) *Biochim. Biophys. Atca.*, **76**, 622.
132. Roster, J. M., Abbott, H., & Terry, M. L., (1966) *Anal. Biochem.*, **16**, 149.
133. Randerath, K., (1962) *Nature*, **194**, 768.
134. Randerath, K., (1962) *Angew. Chem. Int. Ed. Engl.*, **1**, 435.
135. Bolliger, H. R., & Brenner, M., (1965) *Thin-layer chromatography*, A laboratory handbook. Academic Press Inc..
136. Wimmer, J. & Reichmann, M. E., (1969) *Nature*, **221**, 1122.
137. Hawrylshyn, K., & Struck, H., (1966) *J. Chromatogr.*, **6**, 365.
138. Scheit, K. H., (1967) *Biochim. Biophys. Atca.*, **134**, 218.
139. Figueira, M. A., & Ribeiro, J. A., (1985) *J. Chromatogr.*, **325**, 317-322.

140. Hansen, Thomas., Musfeldt, Meike., & Schönheit, P., (2002) *Arch Microbiol* **177**, 401–409.
141. Hansen, Thomas., & Schönheit, P., (2000) *Arch Microbiol* **173**, 103–109.
142. Zuleski, F. R., & McGuinness, E. T., (1973) *Analytic. Biochem.*, **54**, 406-12.

Appendix 1 Glossary and Abbreviation

ADP	Adenosine diphosphate
AMP	Adenosine monophosphate
AMPPCP	2,3-methyleneadenosine 5-triphosphate
ATP	Adenosine triphosphate
BsPFK	Phosphofructokinase from <i>Bacillus stearothermophilus</i>
CCT	phosphocholine cytidyltransferase
CDP	Cytidine diphosphate
CMC	Critical micelle concentration
CTP	Cytidine triphosphate
cAMP	cyclic Adenosine monophosphate
cpm	count per minute
DOG	1,2-dioleoyl-sn-glycerol
DOPA	1,2-dioleoyl-sn-glycero-3-phosphatidic acid
DOPC	1,2-dioleoyl-sn-glycero-3-phosphocholine
DOPE	1,2-dioleoyl-sn-glycero-3-phosphoethanolamine
DOPS	1,2-dioleoyl-sn-glycero-3-phosphoserine
EcBSPFK	Phosphofructokinase from <i>Escherichia coli</i>
F1,6-BP	Fructose 1,6-bisphosphate
F2,6-BP	Fructose 2,6-bisphosphate
F6P	Fructose 6-phosphate
G1,6-BP	Glucose 1,6-bisphosphate
G6P	Glucose 6-phosphate
H ₁	Normal topology hexagonal phase
HII	Inverse topology hexagonal phase
ITP	Inosine triphosphate
L _α	Fluid lamellar phase
lyso-OPA	1-oleoyl-2-hydroxy-sn-glycero-3-phosphatidic acid
NAD	Nicotinamide adenine dinucleotide

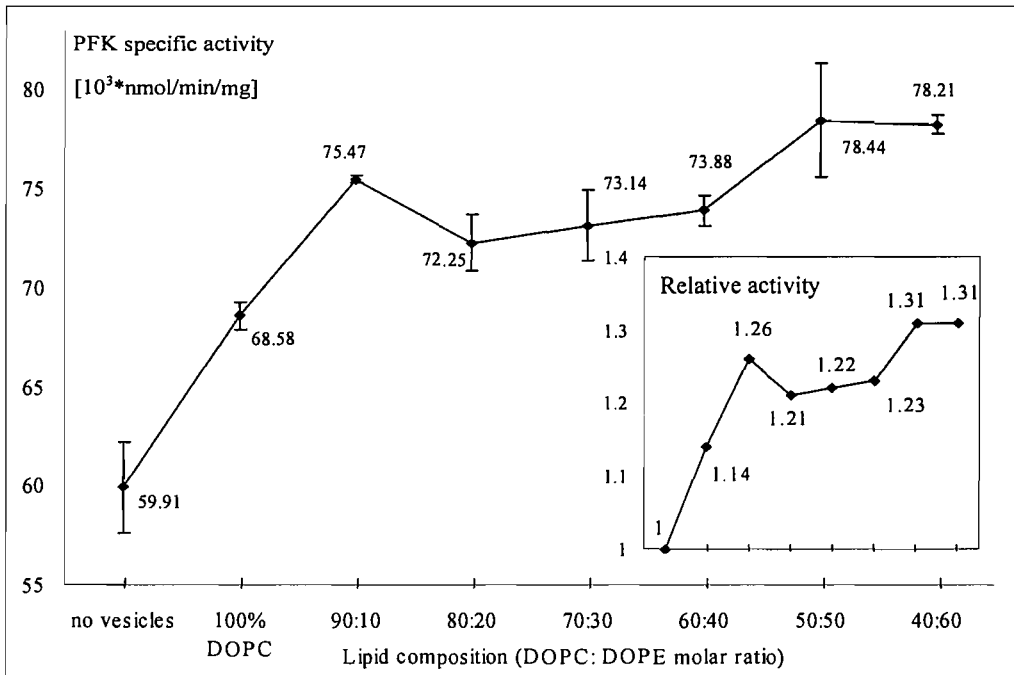
NADH	Nicotinamide adenine dinucleotide
NTP	Nucleoside triphosphate
OA	Olaic acid
PC	Phosphatidylcholine
PE	Phosphatidylethanolamine
PEP	Phosphoenolpyruvate
PFK	Phosphofructokinase or Fructose-6-phosphate-1 kinase
PFK2	Fructose-6-phosphate-2 kinase
PI	Phosphatidylinositol
PKC	Protein kinase C
PLA2	Phospholipase A2
PPi	Pyrophosphate
PS	Phosphatidylserine
RMPFK	PFK from rabbit muscle
TLC	Thin layer chromatography
UTP	Uridine triphosphate
UV	Ultraviolet

Appendix 2 Lipid vesicles composition and preparation

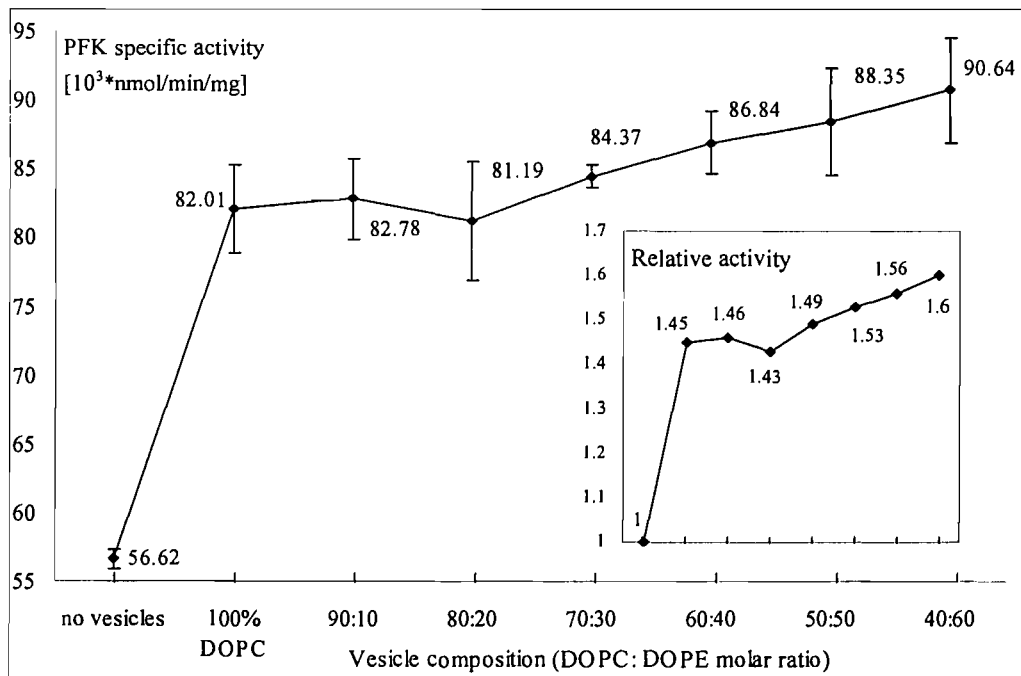
Vesicle systems	Composition (molar fraction% of DOPC) and μ l of each lipid solvent in preparation.						
	100	90	80	70	60	50	40
DOPC/DOPE	100/0	90/18.9	80/37.8	70/56.7	60/75.6	50/94.5	40/113
	100	90	80	70	60	50	40
DOPC/OA	100/0	90/3.6	80/7.2	70/10.8	60/14.4	50/18	40/21.6
	100	90	80	70	60	50	40
DOPC/DOPA	100/0	97.5/2.3	95/4.6	92.5/6.9	90/9.2	80/18.4	70/27.6
	100	97.5	95	92.5	90	80	70
DOPC/lyso-OPA	100/0	97.5/1.2	95/2.3	92.5/3.5	90/4.7	80/9.4	70/14
	100	97.5	95	92.5	90	80	70
DOPC/DOG	99/1.6	98/3.2	97/4.7	96/6.3	95/7.9	94/9.5	93/11.1
	99	98	97	96	95	94	93

Note: Compositions refer to the molar fraction of DOPC. All lipids were chloroform solvents. The concentration of the lipid solvent was 10 mg/ml for DOPE and DOG, and 20 mg/ml for other lipids.

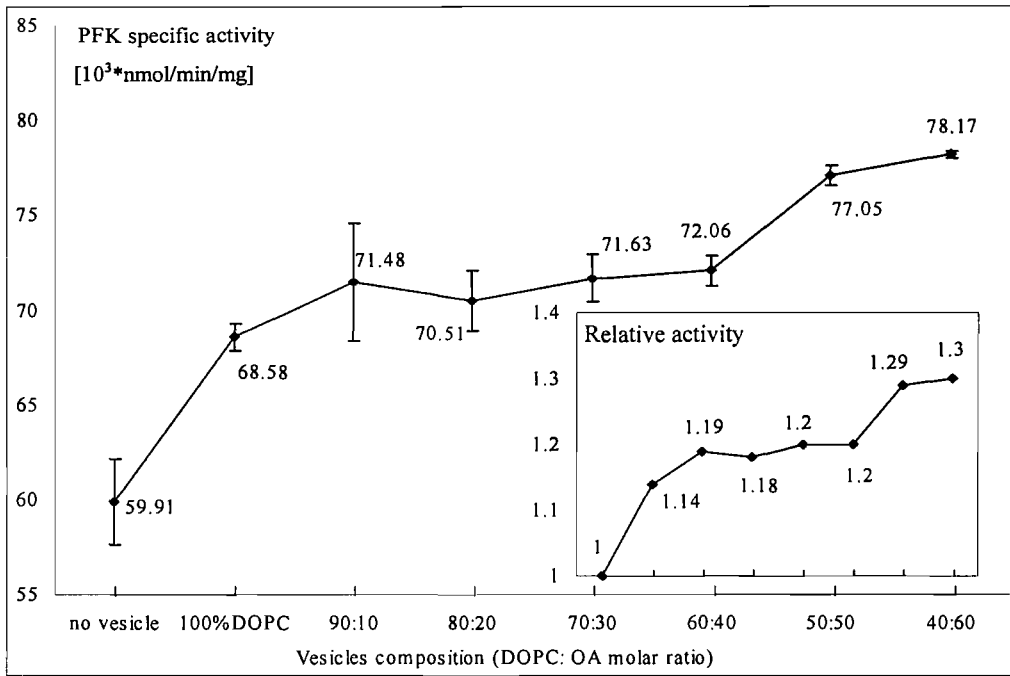
Appendix 3 Specific BsPFK activity in vesicle systems



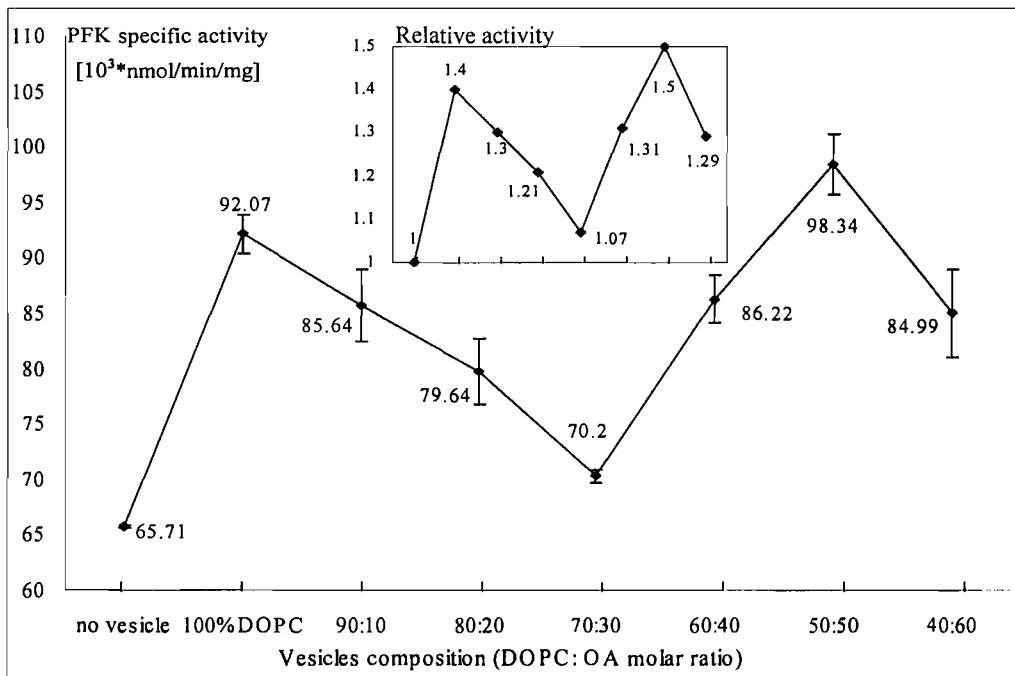
BsPFK activity in DOPC/DOPE vesicles



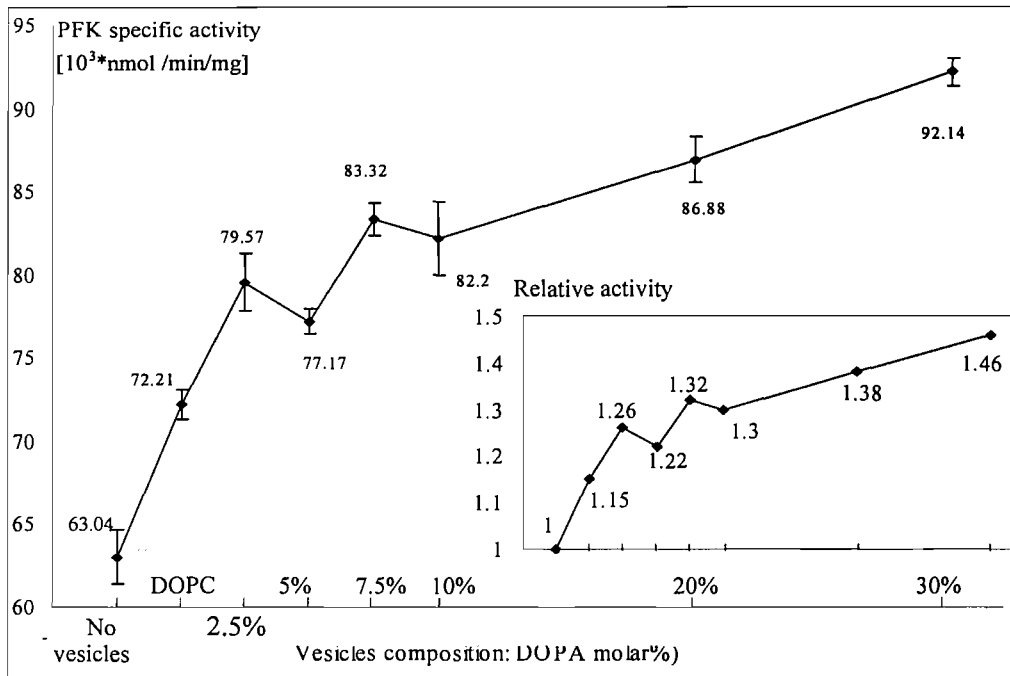
2nd BsPFK activity in DOPC/DOPE vesicles



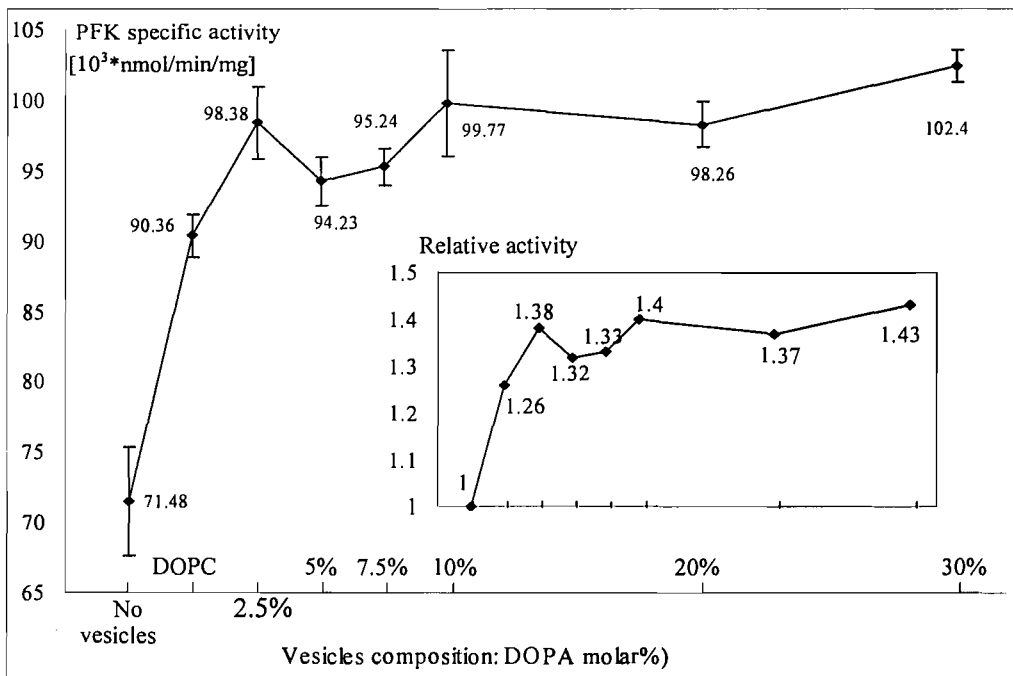
BsPFK activity in DOPC/OA vesicles



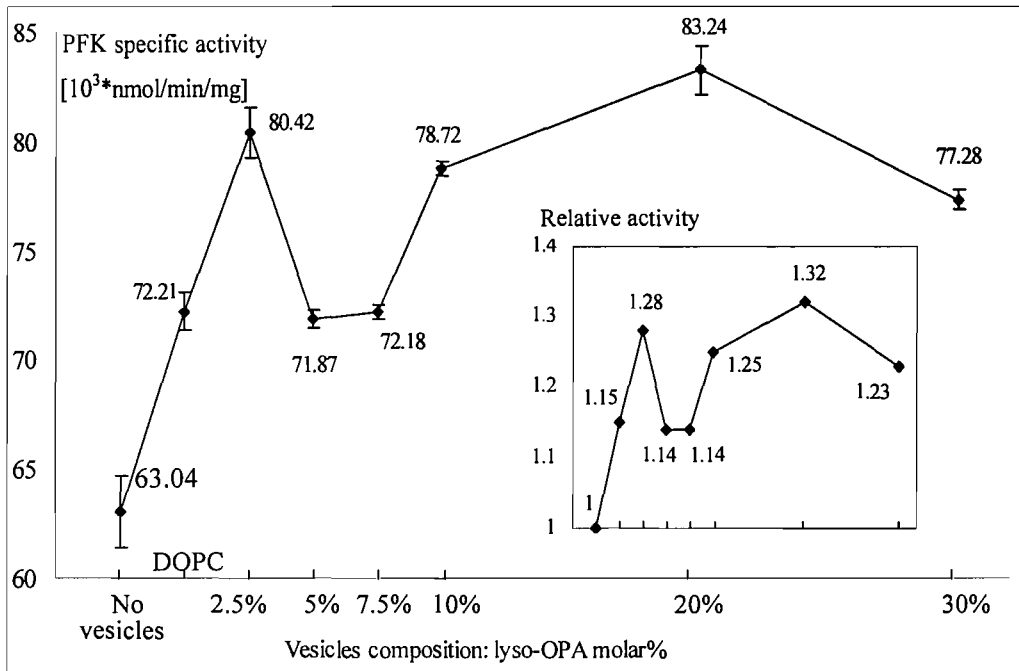
2nd BsPFK activity in DOPC/OA vesicles



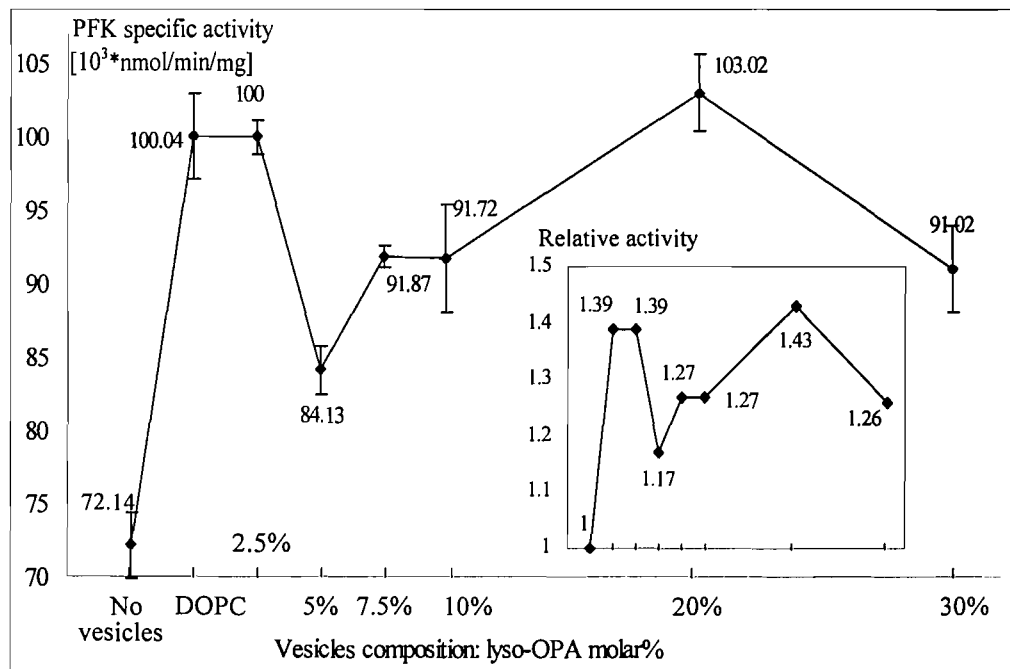
BsPFK activity in DOPC/DOPA vesicles



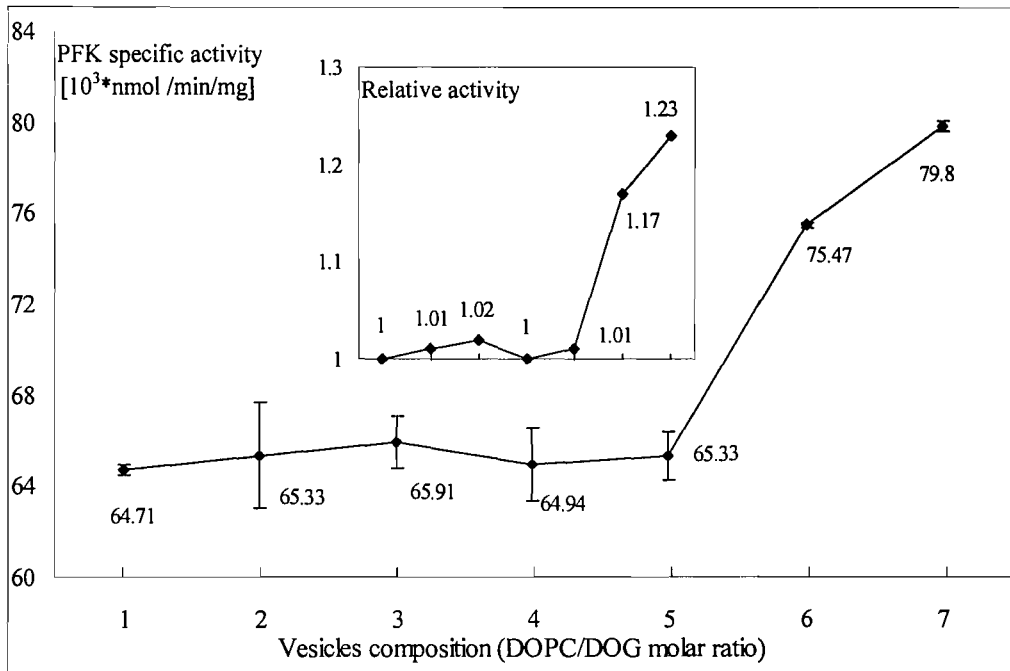
2nd BsPFK activity in DOPC/DOPA vesicles



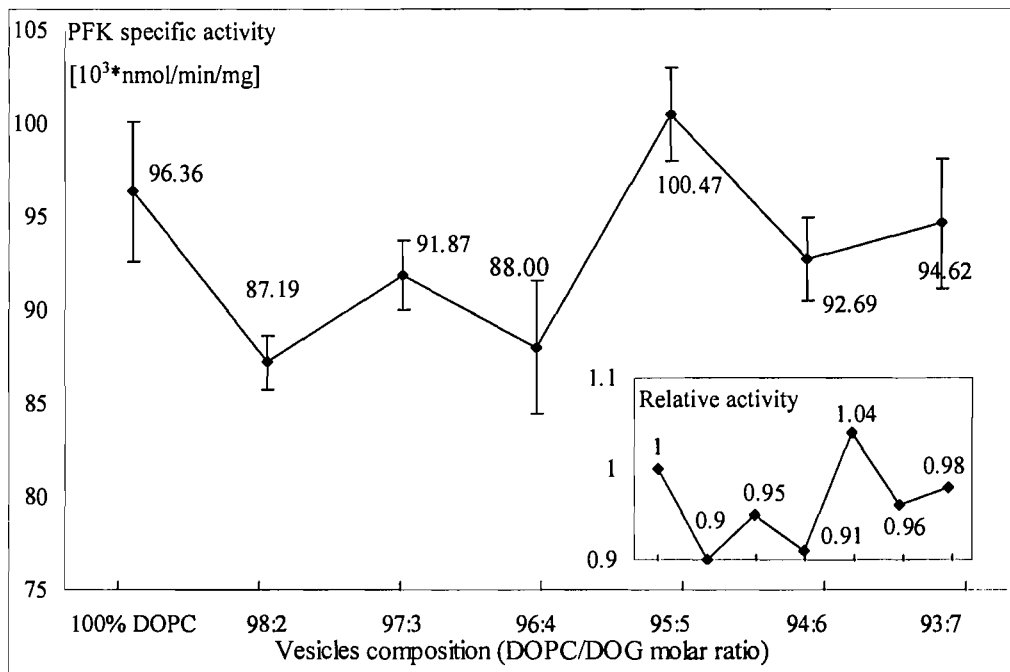
BsPFK activity in DOPC/lyso-OPA vesicles



2nd BsPFK activity in DOPC/lyso-OPA vesicles



BsPFK activity in DOPC/DOG vesicles



2nd BsPFK activity in DOPC/DOG vesicles

Appendix 4 Amino acid sequence of EcPFK and RM-PFK

Sequence No.	10	20	30	40
Amino acids	MILLIGVLTS	GGDAPGMNAA	IRGVVRSALT	EGLEVMMGIYD
50	60	70	80	90
GYOGLYEDRM	VQLDRYSVSD	MINRGGRFLG	SARCPEFRDE	NIRAVAIENL
100	110	120	130	140
KKRGIDALVV	IGGDGSYMGA	MRLTEMGFPC	IGLPGTIDND	IKGTDYTIGF
150	160	170	180	190
FTALSTVVEA	IDRLRDTSSS	HQRISVVEVM	GRYCGDLTLA	AAIAGGCEFV
200	210	220	230	240
VVPEVEFSRE	DLVNEIKAGI	AKGKKHAIVA	ITEHMCVDEL	AHFIEKETGR
250	260	270	280	290
ETRATVLGHI	QRGGSPVPYD	RILASRMGAY	AIDLLLAGYG	GRCVGIQNEQ
300	310	319		
LVHHDIIIDAI	ENMKRPFKGD	WLDCAEKMY		

Amino acids of EcPFK

Amino acids of RM-PFK

N-Half:

THEEHAARTLGVGKAI AVL TSGGDAQGMNA AVRAVVRVGIFTGARVFFVH
 EGYQGLVDGGDHIREATWESVSMMLQLGGTVIGSARCKDRREREGRLRTR
 SSYLNIVGLVGSIDNDFDGTDMTIGTDSALHRITEIVDAITTTAQSHQRT
 FVLEVMGRHCGYLA V TSLSCGADWYFIPECPPDDN WEDHLCRRLSETRTR
 GSRLNIIIVAEGAIDSNGKPITSEGVKDLVVRRLGYDTRVTVLGHVQRGG
 TPSAFDRILGSRMGVEAVMALLEGTPDTPACVVSLSGNQAVRLPLMECVQ
 VTKDVTKAMDEKRFDEAMKLRGRSFMNNWEVYKLLAHIRPPAPKSGSYTV

C-Half:

A VMN V G A P A A G M N A A V R S T V R I G L I Q E N R V L V V H D G F E G L A K G Q I E E A G W
S Y V G G W T G Q G G S K L G S K R T L P K K S F E M E G R K Q F D E L C I P F V V I P A T V S N N
V P G S D F S V G A D T A L N T I C T T C D R I K Q I A A G T K R V F I I E T M G G Y D G Y L A T M
A G L A A G A D A A Y I F E E P F T I R D L Q A N V E H L V Q K M K T T V K R G L V L R N E K C N E
N Y T T D F I F N L Y S E E G K G I F D S R K N V L G H M Q Q G G S P T P F D R N F A T K M G A K A
M N W M A G K I K E S Y R N G R I F A N T P D S G C V L G M R K R A L V F Q P V T E L Q N Q T D F E
H R I P K E Q W W L K L R P I L K I L A K Y E I D L D T S E H A H L E H I S R K R S G E A T V

Appendix 5 Sc intillation counting results and data processing

Table 1 BsPFK assay: activity tested in DOPC/DOPE vesicles

Vesicles systems	Scintillation counting results (count/minute)			Data processing			
	FBP	ATP	Total radio-activity	Conversion%	Average conversion% & S.D.	Specific activity & S.D.	Relative activity
No vesicles	71880	14133	86013	16.0004	15.48 & 0.59	59.91 & 2.29	1
	75256	13562	88818	14.8379			
	73615	14056	87671	15.6050			
100:0	71550	15775	87325	17.6610	17.72 0.18	68.58 0.71	1.14
	70415	15799	86214	17.9197			
	73371	16064	89435	17.5664			
90:10	67478	16709	84187	19.4520	19.5 0.04	75.47 0.15	1.26
	73069	18135	91204	19.5197			
	70920	17617	88537	19.5227			
80:20	72372	16589	88961	18.2586	18.67 0.36	72.25 1.42	1.21
	70898	16990	87888	18.9463			
	72380	17197	89577	18.8186			
70:30	70892	17323	88215	19.2574	18.9 0.46	73.14 1.80	1.22
	70227	16232	86459	18.3755			
	69777	16858	86635	19.0695			
60:40	68248	18413	86661	20.8809	19.09 0.20	73.88 0.79	1.23
	73698	17638	91336	18.9405			
	71416	17418	88834	19.2298			
50:50	70568	18479	89047	20.3895	20.27 0.74	78.44 2.87	1.31
	70433	19057	89490	20.9412			
	71457	17695	89152	19.4749			
40:60	66845	17191	84036	20.0685	20.21 0.12	78.21 0.47	1.31
	67723	17605	85328	20.2521			
	70335	18319	88654	20.2983			
The second experiment of the same vesicle system							
No vesicles	81822	14673	96495	14.8084	14.63 0.19	56.62 0.73	1
	85000	15057	100057	14.6635			
	85288	14839	100127	14.4330			
100:0	76307	19883	96190	20.3344	21.19 0.82	82.01 3.19	1.45
	80110	22023	102133	21.2560			
	81102	23239	104341	21.9794			

90:10	79287	20859	100146	20.5076	21.39 0.76	82.78 2.95	1.46
	78355	22333	100688	21.8759			
	78220	22163	100383	21.7719			
80:20	78402	19677	98079	19.7260	20.98 1.1	81.19 4.31	1.43
	77498	21466	98964	21.3754			
	78198	22250	100448	21.8452			
70:30	75542	21233	96775	21.6209	21.8 0.22	84.37 0.83	1.49
	77411	21895	99306	21.7378			
	77440	22282	99722	22.0385			
60:40	78118	22004	100122	21.6688	22.44 0.60	86.84 2.30	1.53
	79947	22963	102910	22.0173			
	78642	23688	102330	22.8595			
50:50	72495	22983	95478	23.7721	22.83 0.99	88.35 3.84	1.56
	74636	22575	97211	22.9190			
	81776	23182	104958	21.7940			
40:60	72567	21482	94049	22.5228	23.42 0.99	90.64 3.84	1.60
	75538	23252	98790	23.2416			
	75485	24844	100329	24.4853			

Table 2 BsPFK assay: activity tested in DOPC/OA vesicles

Vesicles systems	Scintillation counting results (count/minute)			Data processing				
	DOPC: OA mol ratio	FBP	ATP	Total radio-activity	Conversion%	Average conversion% & S.D.	Specific activity & S.D.	Relative activity
No vesicles		71880	14133	86013	16.0004	15.48 0.59	59.91 2.29	1
		75256	13562	88818	14.8379			
		73615	14056	87671	15.6050			
100:0		71550	15775	87325	17.6610	17.72 0.18	68.58 0.71	1.14
		70415	15799	86214	17.9197			
		73371	16064	89435	17.5664			
90:10		64452	14482	78934	17.9038	18.47 0.80	71.48 3.08	1.19
		67878	17189	85067	19.8197			
		65078	15711	80789	19.0291			
80:20		63700	15068	78768	18.6964	18.22 0.41	70.51 1.59	1.18
		66987	15069	82056	17.9384			
		66714	15109	81823	18.0397			
70:30		64080	14622	78702	18.1377	18.51 0.32	71.63 1.25	1.20
		65637	15503	81140	18.6858			
		66830	15802	82632	18.7106			

60:40	65115	15151	80266	18.4475	18.62 0.20	72.06 0.79	1.20
	67278	16040	83318	18.8439			
	67425	15793	83218	18.5661			
50:50	67858	17375	85233	20.0017	19.91 0.14	77.05 0.53	1.29
	68700	17556	86256	19.9739			
	69080	17414	86494	19.7520			
40:60	67605	17452	85057	20.1353	20.2 0.05	78.17 0.21	1.30
	68405	17751	86156	20.2266			
	69320	17985	87305	20.2285			
The second experiment of the same vesicle system							
No vesicles	86800	18242	105042	17.0242	16.98 0.04	65.71 0.15	1
	80716	16919	97635	16.9600			
	82162	17209	99371	16.9555			
100:0	77789	23966	101755	23.2663	23.79 0.46	92.07 1.77	1.40
	78700	25352	104052	24.0934			
	71653	23017	94670	24.0137			
90:10	75364	22534	97898	22.7140	22.13 0.83	85.64 3.22	1.30
	77162	21509	98671	21.4837			
	76484	21388	97872	21.5360			
80:20	77875	20108	97983	20.1903	20.58 0.77	79.64 2.99	1.21
	79865	20483	100348	20.0870			
	78473	21857	100330	21.4752			
70:30	82466	18476	100942	17.9576	18.14 0.16	70.20 0.61	1.07
	86892	19786	106678	18.2227			
	87020	19834	106854	18.2378			
60:40	75045	21515	96560	21.9650	22.28 0.55	86.22 2.12	1.31
	77642	22234	99876	21.9555			
	76422	23093	99515	22.9088			
50:50	75624	27103	102727	26.1302	25.41 0.72	98.34 2.77	1.50
	76316	26343	102659	25.3995			
	76622	25496	102118	24.6971			
40:60	77653	23664	101317	23.0666	21.96 1.0194	84.99 3.95	1.29
	78104	21241	99345	21.0636			
	77185	21830	99015	21.7360			

Table 3 BsPFK assay: activity tested in DOPC/DOPA vesicles

Vesicles systems	Scintillation counting results (count/minute)			Data processing				
	DOPC: DOPA mol ratio	FBP	ATP	Total radio-activity	Conversion%	Average conversion% & S.D.	Specific activity & S.D.	Relative activity
No vesicles		69625	14384	84009	16.6898	16.29 0.42	63.04 1.61	1
		69470	13998	83468	16.3308			
		70627	13755	84382	15.8599			
100:0		67953	15751	83704	18.4061	18.66 0.22	72.21 0.86	1.15
		66837	15911	82748	18.8175			
		68352	16206	84558	18.7629			
97.5:2.5		67133	17348	84481	20.1497	20.56 0.44	79.57 1.72	1.26
		69852	18415	88267	20.4985			
		68580	18663	87243	21.0300			
95:5		66065	17045	83110	20.1170	19.94 0.19	77.17 0.74	1.22
		66953	16873	83826	19.7351			
		67512	17245	84757	19.9601			
92.5:7.5		65052	18001	83053	21.2974	21.53 0.24	83.32 0.95	1.32
		66137	18530	84667	21.5191			
		64389	18330	82719	21.7876			
90:10		65746	18425	84171	21.5212	21.24 0.58	82.20 2.23	1.30
		66840	18833	85673	21.6214			
		66817	17716	84533	20.5781			
80:20		64925	18780	83705	22.0723	22.45 0.35	86.88 1.36	1.38
		65703	19490	85193	22.5260			
		66531	19992	86523	22.7629			
70:30		65585	21105	86690	24.0187	23.81 0.22	92.14 0.84	1.46
		65746	20668	86414	23.5842			
		64448	20533	84981	23.8262			
The second experiment of the same vesicle system								
No vesicles		77244	16609	93853	17.3172	18.47 1.0	71.48 3.86	1
		76600	18428	95028	19.0370			
		77435	18641	96076	19.0512			
100:0		73769	22336	96105	22.9343	23.35 0.40	90.36 1.52	1.26
		72931	22647	95578	23.3913			
		73325	23175	96500	23.7187			
97.5:2.5		73807	25814	99621	25.6457	25.42 0.67	98.38 2.59	1.38
		72403	24069	96472	24.6629			
		71655	25456	97111	25.9433			

95:5	71537	25113	96650	25.7095	24.35 0.45	94.23 1.73	1.32
	71812	23095	94907	24.0362			
	74849	24878	99727	24.6692			
92.5:7.5	74262	24647	98909	24.6394	24.61 0.35	95.24 1.34	1.33
	73009	24627	97636	24.9436			
	73491	23898	97389	24.2505			
90:10	71678	24368	96046	25.0885	25.78 0.96	99.77 3.73	1.40
	72497	24655	97152	25.0984			
	72038	26268	98306	26.4596			
80:20	69588	24609	94197	25.8455	25.39 0.42	98.26 1.63	1.37
	72540	24955	97495	25.3203			
	72587	24576	97163	25.0133			
70:30	73378	27090	100468	26.7111	26.46 0.30	102.4 1.18	1.43
	75020	26878	101898	26.1219			
	74773	27389	102162	26.5593			

Table 4 BsPFK assay: activity tested in DOPC/lyso-OPA vesicles

Vesicles systems	Scintillation counting results (count/minute)			Data processing			
	FBP	ATP	Total radio-activity	Conversion%	Average conversion% & S.D.	Specific activity & S.D.	Relative activity
No vesicles	69625	14384	84009	16.6898	16.29 0.42	63.04 1.61	1
	69470	13998	83468	16.3308			
	70627	13755	84382	15.8599			
100:0	67953	15751	83704	18.4061	18.66 0.22	72.21 0.86	1.15
	66837	15911	82748	18.8175			
	68352	16206	84558	18.7629			
97.5:2.5	64349	17529	81878	21.0229	20.78 0.29649	80.42 1.15	1.28
	67313	18152	85465	20.8676			
	67952	17873	85825	20.4496			
95:5	68570	14383	82953	16.9039	18.57 0.11	71.87 0.41	1.14
	67682	15778	83460	18.4934			
	68053	16016	84069	18.6445			
92.5:7.5	69508	16342	85850	18.6373	18.65 0.09	72.18 0.35	1.14
	69388	16427	85815	18.7454			
	70598	16517	87115	18.5667			
90:10	67988	16299	84287	18.9358	20.34 0.08	78.72 0.33	1.25
	66437	17309	83746	20.2816			
	66574	17470	84044	20.4029			

80:20	66868	19007	85875	21.7751	21.51 0.28	83.24 1.09	1.32
	66551	18668	85219	21.5419			
	66715	18363	85078	21.2149			
70:30	74124	19048	93172	20.0940	19.97 0.12	77.28 0.46	1.23
	66269	16831	83100	19.8586			
	67547	17266	84813	19.9718			
The second experiment of the same vesicle system							
No vesicles	76424	18707	95131	19.3129	18.64 0.59	72.14 2.29	1
	79160	18045	97205	18.2074			
	77945	17992	95937	18.3949			
100:0	72098	24704	96802	25.2413	25.85 0.76	100.0 2.94	1.39
	72677	25373	98050	25.6064			
	71683	26458	98141	26.7004			
97.5:2.5	71985	25589	97574	25.9566	25.84 0.29	100.0 1.14	1.39
	71223	25455	96678	26.0598			
	71122	24710	95832	25.5061			
95:5	74258	20756	95014	21.5185	21.74 0.42	84.13 1.63	1.17
	76487	21319	97806	21.4794			
	76638	22293	98931	22.2279			
92.5:7.5	73144	23078	96222	23.6860	23.74 0.19	91.87 0.74	1.27
	73533	23539	97072	23.9566			
	74942	23507	98449	23.5849			
90:10	72911	21843	94754	22.7387	23.7 0.94	91.72 3.63	1.27
	73435	24341	97776	24.6116			
	74515	23580	98095	23.7462			
80:20	69700	26414	96114	27.2236	26.62 0.68	103.0 2.64	1.43
	70998	26281	97279	26.7557			
	70752	25059	95811	25.8802			
70:30	77840	25006	102846	24.0389	23.52 0.76	91.02 2.93	1.26
	76140	22688	98828	22.6555			
	74182	23642	97824	23.8768			

Table 5 BsPFK assay: activity tested in DOPC/DOG vesicles

Vesicles systems	Scintillation counting results (count/minute)			Data processing			
	FBP	ATP	Total radio-activity	Conversion%	Average conversion% & S.D.	Specific activity & S.D.	Relative activity
100:0	22299	4474	26773	16.7109	16.72 0.06	64.71 0.25	1
	22629	4524	27153	16.6611			
	22733	4587	27320	16.7899			
98:2	67795	14520	82315	17.2053	16.88 0.60	65.33 2.32	1.01
	66140	14218	80358	17.2491			
	67342	13448	80790	16.1895			
97:3	69673	14431	84104	16.7273	17.03 0.30	65.91 1.14	1.02
	67987	14410	82397	17.0527			
	68192	14713	82905	17.3171			
96:4	69647	14824	84471	17.1250	16.78 0.41	64.94 1.59	1.00
	70333	14727	85060	16.8894			
	69860	14069	83929	16.3256			
95:5	68547	14253	82800	16.7764	16.88 0.28	65.33 1.08	1.01
	68805	14199	83004	16.6687			
	68703	14699	83402	17.1955			
94:6	65414	16255	81669	19.4964	19.5 0.03	75.47 0.12	1.17
	65565	16264	81829	19.4689			
	65142	16222	81364	19.5294			
93:7	64286	17040	81326	20.5581	20.62 0.06	79.8 0.22	1.23
	63133	16845	79978	20.6622			
	63508	16925	80433	20.6445			
The second experiment of the same vesicle system							
100:0	70343	22096	92439	23.9033	24.9 0.97	96.36 3.76	1
	70830	23550	94380	24.9523			
	68375	23829	92204	25.8438			
98:2	72192	20942	93134	22.1601	22.53 0.37	87.19 1.41	0.90
	72840	21596	94436	22.5516			
	74433	22479	96912	22.8904			
97:3	73024	22506	95530	23.2539	23.74 0.48	91.87 1.88	0.95
	72412	22907	95319	23.7315			
	72228	23462	95690	24.2252			
96:4	70522	19910	90432	21.6751	22.74 0.93	88.00 3.59	0.91
	70822	21823	92645	23.2407			
	72098	22303	94401	23.3177			

95:5	69703	23985	93688	25.3137	25.96 0.65	100.5 2.53	1.04
	70918	25208	96126	25.9512			
	69422	25534	94956	26.6220			
94:6	72262	23464	95726	24.2181	23.95 0.58	92.69 2.25	0.96
	71392	23354	94746	24.3540			
	74387	22957	97344	23.2842			
93:7	71485	22436	93921	23.5816	24.45 0.90	94.62 3.47	0.98
	73956	24231	98187	24.3942			
	73560	25366	98926	25.3700			

Notes:

1.) For a better comparison, the data of one vesicle system studied at two parallel experiments are put in one table.

2.) The conversion of each PFK reaction was calculated by:

$$\text{Conversion \%} = \frac{\text{radioactivity of FBP} - \text{background}}{\text{total radioactivity} - 2 \times \text{background}} \times 100\%$$

There backgrounds were tested for every set of experiment, the average was then taken as background in final calculation. That is, background of the first experiment (five vesicle systems) was 545 (average of 824, 447 and 367) and the second 537 (average of 229, 642 and 741).

3.) The specific activity of PFK activity (how much of FBP yielded per min per mg PFK), was calculated by:

$$\begin{aligned} \text{Specific activity} &= \frac{\text{Reaction conversion\%} \times \text{Reaction volume} \times \text{ATP concentration}}{\text{Reaction time} \times \text{PFK amount}} \\ &= 3.867 \times 10^3 \times \text{Conversion\%} \text{ [nmol/min/mg]} \end{aligned}$$

and the standard deviation of PFK specific activity was calculated by:

$$\text{Standard deviation of specific activity} = 3.867 \times \text{Standard deviation of Conversion\%} .$$

4.) In above tables, bad data were shown with shadow and neglected in further calculation.